



UNIVERSIDADE ESTADUAL DE CAMPINAS  
FACULDADE DE ENGENHARIA QUÍMICA  
ÁREA DE CONCENTRAÇÃO: DESENVOLVIMENTO DE  
PROCESSOS BIOTECNOLÓGICOS

**Tiago Albertini Balbino**

**DESENVOLVIMENTO DE PROCESSO MICROFLUÍDICO PARA  
INCORPORAÇÃO DE DNA EM LIPOSSOMAS CATIÔNICOS  
DESTINADOS A TERAPIA E VACINAÇÃO GÊNICA**

***DEVELOPMENT OF MICROFLUIDIC PROCESS FOR DNA  
INCORPORATION INTO CATIONIC LIPOSOMES FOR GENE  
THERAPY AND VACCINATION***

CAMPINAS, 2012





UNIVERSIDADE ESTADUAL DE CAMPINAS

FACULDADE DE ENGENHARIA QUÍMICA

ÁREA DE CONCENTRAÇÃO: DESENVOLVIMENTO DE  
PROCESSOS BIOTECNOLÓGICOS

DEPARTAMENTO DE ENGENHARIA DE MATERIAIS E BIOPROCESSOS

**Tiago Albertini Balbino**

*Autor*

**DESENVOLVIMENTO DE PROCESSO MICROFLUÍDICO PARA  
INCORPORAÇÃO DE DNA EM LIPOSSOMAS CATIÔNICOS  
DESTINADOS A TERAPIA E VACINAÇÃO GÊNICA**

***DEVELOPMENT OF MICROFLUIDIC PROCESS FOR DNA  
INCORPORATION INTO CATIONIC LIPOSOMES FOR GENE  
THERAPY AND VACCINATION***

Este exemplar corresponde à versão final da dissertação de mestrado defendida por Tiago Albertini Balbino e orientada pela Profa. Dra. Lucimara Gaziola de La Torre.

A handwritten signature in black ink, appearing to read "Lucimara Gaziola de La Torre".

Assinatura da orientadora

Dissertação de Mestrado apresentada à Faculdade de Engenharia Química para obtenção do título de Mestre em Engenharia Química, na área de concentração Desenvolvimento de Processos Biotecnológicos.

*Orientadora:* Profa. Dra. Lucimara Gaziola de La Torre

*Co-orientador:* Prof. Dr. Adriano Rodrigues Azzoni

CAMPINAS, 2012

FICHA CATALOGRÁFICA ELABORADA PELA  
BIBLIOTECA DA ÁREA DE ENGENHARIA E ARQUITETURA - BAE - UNICAMP

B185d      Balbino, Tiago Albertini  
Desenvolvimento de processo microfluídico para  
incorporação de DNA em lipossomas catiônicos  
destinados a terapia e vacinação gênica / Tiago Albertini  
Balbino. --Campinas, SP: [s.n.], 2012.

Orientador: Lucimara Gaziola de La Torre  
Co-orientador: Adriano Rodrigues Azzoni.  
Dissertação de Mestrado - Universidade Estadual de  
Campinas, Faculdade de Engenharia Química.

1. Lipossomas. 2. Transfecção. 3. Microfluídica. 4.  
Nanotecnologia. I. Torre, Lucimara Gaziola de La, 1971-.  
II. Azzoni, Adriano Rodrigues. III. Universidade Estadual  
de Campinas. Faculdade de Engenharia Química. IV.  
Título.

Título em Inglês: Development of microfluidic process for DNA incorporation into  
cationic liposomes for gene therapy and vaccination

Palavras-chave em Inglês: Liposomes, Transfection, Microfluidics,  
Nanotechnology

Área de concentração: Desenvolvimento de Processos Biotecnológicos

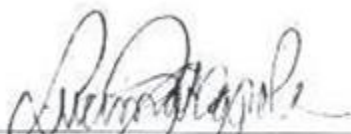
Titulação: Mestre em Engenharia Química

Banca examinadora: Maria Helena de Andrade Santana, Leide Passos  
Cavalcanti

Data da defesa: 22-07-2012

Programa de Pós Graduação: Engenharia Química

Dissertação de mestrado defendida por Tiago Albertini Balbino e aprovada no dia 22 de junho de 2012 pela banca examinadora constituída pelos seguintes doutores:



---

Prof. Dr. Luçimara Gaziola De La Torre  
Presidente da Comissão Julgadora  
Orientadora



---

Prof. Dr. Maria Helena Andrade Santana  
Membro



---

Dr. Leide Passes Cavalcanti  
Membro



*Aos meus pais: aqueles que  
mais contribuíram com esta pesquisa,  
muito embora dificilmente possam  
compreendê-la.*



## AGRADECIMENTOS

Que toda pesquisa acadêmica é motivada por algum desafio ou alguma curiosidade científico-tecnológica é sabido desde os primeiros cientistas. Porém, mais motivadores que os desafios encontrados durante o percurso desta pesquisa, foram as pessoas que, de alguma forma, me motivavam a superá-los e a me superar. Pessoas que me marcaram durante esse meu trajeto, ou que já haviam me marcado antes mesmo do seu início.

Primeiramente, agradeço imensamente à minha família, já que, nas rápidas folgas, muitas vezes o voltar para casa realmente fazia sentido. Esperar minha mãe perguntar o que eu queria que ela cozinhasse, apesar de ela já saber o que seria... Dar uma volta com meu pai e vê-lo orgulhoso enquanto conto das coisas de Campinas... Conversar amenidades com as minhas irmãs, Danúbia e Marcela, só para, no fundo, não perder o costume... Era nessas minhas voltas para casa que realmente conseguia me desligar do que sou em Campinas e ser filho e irmão de verdade. O amor tão forte que tenho por vocês é a matéria-prima de todo meu sucesso profissional e, acima de tudo, dos valores que me constituem humano antes de cientista.

Aos amigos que conheci em Campinas e que me fizeram amadurecer pessoalmente numa fase tão importante e marcante da minha vida. Também aos amigos de Umuarama e Maringá, que hoje já não são mais tão presentes ou próximos pelo contato cotidiano, mas que de alguma forma participaram da minha formação como pessoa.

Aos tios, tias, primos e primas, por sempre me acolherem tão ternamente nos encontros familiares. Especialmente à Lu e ao Zito, por serem minha família em Maringá durante minha graduação. E à Lu, minha segunda mãe, pelas horas de conversa, pelo apoio incondicional e pelo amor quase materno que recebo em cada abraço.

Aos amigos do laboratório: Carol, Zômpero, Amanda, Gabi, Mica, Nayla, Rafa, Andréia, Gilson, Mari, Pati, Fer, Aline, Felipe e Leandra. O passar do tempo dentro e, algumas vezes, fora da FEQ só me fizeram admirá-los ainda mais como pessoas e profissionais que são. Àqueles com mais proximidade pessoal, agradeço carinhosamente por toda a atenção essencial nos momentos mais difíceis.

À professora Anete, pelo uso do laboratório, e aos colegas do CBMEG, pelo modo como me acolheram e também pelas grandes ajudas com as bactérias e HeLas.

Ao CNPq, à FAPESP e à FUNCAMP, pelo financiamento.

Ao Instituto Butantã, especialmente Sylvia e Simone, pelo suporte técnico nas análises de microscopia eletrônica de transmissão.

Ao Laboratório Nacional de Luz Síncrotron (LNLS), pelas medidas de SAXS, e ao Laboratório de Microfabricação/LNLS, pelo auxílio técnico no *design* e confecção dos dispositivos microfluídicos.

Ao professor Mário Gongora Rubio e à Juliana Schianti, do Instituto de Pesquisas Tecnológicas de São Paulo, pelas sugestões dadas no exame de qualificação e pelas grandes contribuições referentes aos processos microfluídicos.

À Leide, por quem tenho grande admiração, pelas agradáveis e, muitas vezes, intermináveis horas nas linhas de SAXS madrugada adentro. Pela paciência com as cobranças dos prazos e por ter de explicar mais de uma vez sobre *cailles*, *fittings*, distâncias interlamelares etc. Também pela disposição ao aceitar compor a banca avaliadora. Também agradeço ao Antônio e ao Cristiano pelo vasto enriquecimento deste trabalho ao torná-lo tão interdisciplinar.

Agradeço gentilmente à professora Maria Helena, por ter disponibilizado o uso de seu laboratório, pelo conhecimento compartilhado dentro e fora da sala de aula, e pela participação como membro da banca avaliadora.

Ao meu co-orientador, professor Adriano. Por ter me ensinado meticulosamente toda a parte biológica, que foi fundamental para esta pesquisa. Por sempre se dispor a resolvermos juntos qualquer empecilho.

À minha orientadora e professora, Lucimara, por quem tenho admiração e respeito imensos. Por tudo o que fez e tem feito por mim, por acreditar sempre em meu trabalho e em meu potencial. Por nunca impor, mas sempre sugerir direções. Por me incitar à investigação tecnológica e também me ensinar que, mais que com planejamentos experimentais, uma boa pesquisa também pode ser resolvida à base do “truco”.

E ao meu companheiro, Jefferson, por estar ao meu lado durante a escrita de cada página deste texto. Agradeço pela compreensão, pelo amor, pelo incentivo, pela companhia... E, especialmente, pela beleza e poesia de uma vida a dois.

A todos vocês, agradeço humildemente por estarem presentes de alguma forma durante essa etapa tão importante na minha vida.

*La utopía está en el horizonte. Me acerco  
dos pasos, ella se aleja dos pasos. Camino  
diez pasos y el horizonte se desplaza diez  
pasos más allá. Por mucho que camine,  
nunca la alcanzaré. Entonces ¿para qué  
sirve la utopía? Para eso: sirve para  
caminar.*

*Eduardo Galeano*



## RESUMO

Esta pesquisa teve como objetivo o desenvolvimento tecnológico de processo microfluídico para a obtenção de vetores não virais, baseados na complexação eletrostática entre lipossomas catiônicos (LC) e DNA plasmideal (pDNA) destinados à terapia e vacinação gênica. O desenvolvimento desse processo foi comparado ao processo convencional “bulk”, que, a partir da simples mistura manual entre as soluções ou em sistema de vórtice, gera dificuldade no controle do tamanho destas estruturas e pode produzir variações nos resultados biológicos e na estabilidade coloidal. Já o processo microfluídico, que utiliza dispositivos que processam pequenas quantidades de fluidos ( $10^{-9}$  a  $10^{-18}$  litros), permite a complexação eletrostática em regime contínuo, com o controle das condições difusionais, o que também permite melhor controle do tamanho destes complexos. Metodologicamente, o trabalho foi dividido em três principais etapas: na primeira parte, foi realizado o estudo físico-químico, estrutural e biológico dos complexos pDNA/LC obtidos por processo “bulk”. Nessa etapa, verificou-se a correlação das propriedades físico-químicas e estruturais dos complexos com o processo de transfecção *in vitro* em células HeLa. A segunda parte do trabalho visou à otimização da produção de lipossomas catiônicos em dois dispositivos microfluídicos, com uma única e com dupla focalização hidrodinâmica, de modo a se obter lipossomas similares aos estudados na primeira parte do trabalho. Na utilização do segundo dispositivo, foi possível operar em vazões volumétricas mais altas quando comparadas ao primeiro. Por fim, na terceira parte, foi realizado o estudo da complexação entre LC e pDNA por processo microfluídico também em dois diferentes dispositivos, um similar ao utilizado na segunda parte do trabalho, com focalização hidrodinâmica única, e outro com blocos regulares nas paredes do microcanal, o que aumenta a área de contato entre os fluidos. Os complexos formados no primeiro dispositivo apresentaram melhores respostas biológicas *in vitro*, as quais foram similares às do processo “bulk”. No segundo dispositivo, ensaios de acessibilidade de sonda de fluorescência ao DNA indicaram alteração na associação entre LC e DNA. Dessa forma, a partir dos resultados, conclui-se que os dispositivos microfluídicos estudados são uma alternativa promissora para a formação de LC e também sua complexão com pDNA em modo contínuo, tanto pela potencialidade tecnológica quanto biológica, o que contribui para o desenvolvimento de produtos farmacêuticos que veiculam DNA e que são destinados à terapia e vacinação gênica.

**Palavras chave:** Lipossomas; Transfecção; Microfluídica; Nanotecnologia.



## ABSTRACT

This research aimed at the technological development of microfluidic process for nonviral carriers production based on the electrostatic complexation between cationic liposomes (CL) and plasmid DNA (pDNA) for gene and vaccine therapy applications. The development of this process was compared to the conventional bulk process, in which the solutions are mixed followed by the simple hand shaking or brief vortexing, what generates difficulties on the particles sizes control and can affect the biological functionality and colloidal stability of the formulations. In contrast, microfluidic process, which uses devices that manipulate small amounts of fluids ( $10^{-9}$  to  $10^{-18}$  liters), allows the electrostatic complexation in continuous mode, controlling diffusion conditions, which also allows the colloidal control of the obtained formulations. Furthermore, microfluidic devices have minimum dimensions and operate with low energy consumption. Methodologically, the present work was carried out in three main steps: in the first step, the physicochemical, structural and biological characteristics of the pDNA/CL complexes obtained by the bulk process were studied. In this step, it was possible to verify the correlation of physicochemical and structural properties with the transfection phenomenon *in vitro* of HeLa cells. The second part of this work focused the optimization of the production of CL through two microfluidic devices, with single and double hydrodynamic focusing, to obtain similar CL to those of the first step of this work. By employing the second device, it was possible to operate at higher volumetric flow rates than the first one. Finally, in the third step, it was explored the complexation between CL and pDNA via microfluidic process also in two different microfluidic devices; the first was similar to that employed in the second part of this work, with a single hydrodynamic focusing, and a second one with patterned microchannel walls, which increase the surface contact area between the fluids. The complexes formed in the first device showed better biological results *in vitro*, which were similar to the complexes formed in the bulk complexation method. In the patterned device, the experiments of the DNA accessibility to fluorescent probe pointed out modifications between the pDNA and CL association in the complexes. In conclusion, we showed that the studied microfluidic devices are a promising alternative for the production of CL and the complexation with pDNA in continuous mode, because of the technological and biological potentialities, which contributes to the development of feasible processes, for the production of new pharmaceutical products for gene and vaccine therapies.

**Keywords:** Liposomes; Transfection; Microfluidics; Nanotechnology.



## SUMÁRIO

<b>Agradecimentos .....</b>	<b>ix</b>
<b>Resumo .....</b>	<b>xiii</b>
<b>Abstract.....</b>	<b>xv</b>
<b>Sumário.....</b>	<b>xvii</b>
<b>Lista de Figuras.....</b>	<b>xxi</b>
<b>Lista de Tabelas .....</b>	<b>xxv</b>
<b>Nomenclatura .....</b>	<b>xxvi</b>
<b>Capítulo 1 – Introdução Geral .....</b>	<b>29</b>
1. Introdução .....	29
2. Objetivos .....	31
3. Organização da Dissertação em Capítulos .....	32
4. Referências .....	34
<b>Capítulo 2 – Revisão Bibliográfica.....</b>	<b>35</b>
1. Lipossomas .....	35
1.1. Veiculação de DNA em lipossomas catiônicos.....	35
1.2. Produção de lipossomas catiônicos .....	38
2. Microfluídica .....	40
3. Produção de Lipossomas em Microcanais .....	42
4. Sistemas Microfluídicos para a complexação eletrostática entre lipossomas catiônicos e DNA.....	46
5. Referências .....	49
<b>Capítulo 3 – Correlation between Physicochemical and Structural Properties with <i>In Vitro</i> Transfection of pDNA/Cationic Liposomes Complexes .....</b>	<b>53</b>
Abstract .....	53
1. Introduction.....	54

2. Materials and Methods .....	57
2.1. Materials.....	57
2.2. Plasmid DNA purification.....	57
2.3. Preparation of pVAX-Luc/cationic liposome complexes (pDNA/CL) .....	57
2.4. Physicochemical Characterization.....	58
2.4.1. Average Hydrodynamic Diameter and Polydispersity.....	58
2.4.2. Measurement of Zeta Potential .....	58
2.4.3. Gel retardation assay for determining the molar charge ratio for complete DNA complexation with CL.....	58
2.4.4. Morphology.....	59
2.5. <i>In Vitro</i> Cytotoxicity.....	59
2.6. Culture and transfection of mammalian cells.....	60
2.7. Structural characterization of the pDNA/CL complexes using Synchrotron SAXS.....	60
3. Results .....	61
3.1. Physicochemical characterization of pDNA/CL complexes .....	61
3.2. <i>In vitro</i> transfection of HeLa cells .....	65
3.3. <i>In vitro</i> cytotoxicity .....	66
3.4. Structural characterization of the pDNA/CL complexes using Synchrotron SAXS.....	67
4. Discussion.....	72
5. Conclusions.....	77
6. Acknowledgements .....	78
7. References.....	78

**Capítulo 4 – Continuous Flow Production of Cationic Liposomes at High Lipid Content in Microfluidic Devices for Gene and Vaccine Therapy ..... 83**

Abstract .....	83
1. Introduction.....	84
2. Materials and Methods .....	86

2.1. Materials.....	86
2.2. Cationic Liposome Production.....	87
2.3. Physicochemical and structural characterization.....	89
2.3.1. Average hydrodynamic diameter and Polydispersity .....	89
2.3.2. Zeta Potential Measurement .....	89
2.3.3. Morphology.....	89
2.3.4. Structural characterization using Synchrotron SAXS .....	90
2.4. Process productivity .....	90
2.5. Culture and transfection of mammalian cells.....	91
2.6. Experimental design for response surface methodology.....	92
3. Results and Discussion .....	92
3.1 Cationic liposome production using the single hydrodynamic focusing (SHF) microfluidic device .....	93
3.2 Cationic liposome production using the double hydrodynamic focusing (DHF) microfluidic device .....	98
3.3. Comparison of the effect of flow velocities on the particle size of the liposomes produced using the SHF and DHF microfluidic devices .....	100
3.4. Flow properties and mixing time.....	101
3.4. Analysis of the Productivity and Physicochemical and Structural characterization of the Cationic Liposomes Produced by the SHF and DHF Devices .....	104
3.5. Biological evaluation of the Cationic Liposomes Produced by the SHF and DHF Devices .....	107
4. Conclusions.....	109
5. References.....	109

**Capítulo 5 – Microfluidic Devices for Continuous production of DNA/Cationic Liposomes Complexes for Gene Delivery and Vaccine Therapy ..... 113**

Abstract .....	113
1. Introduction.....	114

2. Materials and Methods .....	116
2.1. Materials.....	116
2.2. Microfluidic Devices Fabrication .....	117
2.3. Plasmid DNA purification.....	118
2.4. Cationic Liposome Production.....	118
2.5. Preparation of DNA/CL complexes.....	119
2.7. Physicochemical characterization .....	120
2.7.1. Average hydrodynamic diameter and Polydispersity .....	120
2.7.2. Zeta Potential Measurement .....	120
2.7.3. Morphology.....	120
2.7.4. Gel retardation assay .....	121
2.7.5. Plasmid DNA accessibility .....	121
2.8. Culture and transfection of mammalian cells.....	121
2.9. Statistical analysis .....	122
3. Results and Discussion .....	122
3.1. Effect of temperature control on complexation process between CLs and plasmid DNA in microfluidic devices.....	123
3.2. Effect of Average Fluid Flow Velocity ( $V_f$ ) on Complexes Size Distribution ..	126
3.3. Physicochemical properties and Morphology of DNA/CL complexes .....	128
3.6. <i>In vitro</i> HeLa transfection.....	131
4. Conclusion.....	132
5. Acknowledgements .....	133
6. References .....	133
<b>Capítulo 6 – Conclusões Gerais.....</b>	<b>139</b>
<b>Capítulo 7 – Sugestões para Trabalhos Futuros .....</b>	<b>141</b>

## LISTA DE FIGURAS

### Capítulo 2

Figura 1. (A) Ilustração da construção do filme lipídico. Água, óleo com lipídios e água são seqüencialmente injetados no canal principal do dispositivo microfluídico, que contém microcâmaras em sua parede. (B) Bombas pneumáticas são acionadas formando vesículas lipídicas, que saem pelo canal principal (Fonte: KURAKAZU *et al.*, 2010). ..... **43**

Figura 2. (A) Diagrama esquemático do processo de formação de lipossomas em canal microfluídico. A relação de cores representa as razões de concentração de álcool isopropílico e tampão aquoso. (B) Mapa 3-D de intensidade de fluorescência durante formação de lipossomas (adaptado de JAHN *et al.*, 2004). **44**

Figura 3. Representação esquemática do sistema microfluídico de focalização hidrodinâmica para a formação do sistema auto-agregado lipossoma catiônico-DNA (Fonte: KOH *et al.* 2005). ..... **47**

### Capítulo 3

Figure 1. Number-weighted hydrodynamic mean diameter (A), polydispersity index (B) and zeta potential (C) profiles of pDNA/CL complexes at different molar charge ratios ( $R_{+/-}$ ). The solid lines are a visual guide to better demonstrate the trend of the variations. The error bars represent the standard error of independent triplicates. **62**

Figure 2. Number (A) and volume-weighted (B) size distribution of pDNA/CL complexes at  $R_{+/-}$  values of 1.8, 3, 6 and 9. “Empty” cationic liposomes are presented for comparison. The lines in each size distribution represent the profile of three independent pDNA/CL complexes. .... **63**

Figure 3. Gel retardation assay. One microgram of pDNA was complexed with CL at different positive/negative molar charge ratios ( $R_{+/-}$ ) in PBS. .... **64**

Figure 4. Negative staining electron micrographs of “empty” cationic liposomes (CL) (A and B) and pDNA/CL complexes at a molar charge ratio of  $R_{+/-}=3$  (C and D). Scale bars indicate 100 nm in (A, B and C) and 200 nm in (D). .... **65**

Figure 5. In vitro efficacy of HeLa cell transfection using pDNA/CL complexes at different molar charge ratios ( $R_{+/-}$ ); the plasmid pVAXLUC contains a luciferase reporter gene under the control of the CMV promoter. Luciferase activity was expressed in RLU/mg protein. “Naked” pDNA and Lipofectamine (negative and positive controls) are shown in the inset graph. The error bars represent the

standard error of triplicates. \*  $p < 0.05$  was considered statistically different compared to other samples, except at  $R_{+/-}=6$ . NS, not significant. .... **66**

Figure 6. Cell viability assay of pDNA/CL complexes in HeLa cells. Lipofectamine and pDNA were used as controls. Data are presented as the mean  $\pm$  SD of six experiments. \*  $p < 0.05$  was considered statistically different. .... **67**

Figure 7. Small angle x-ray scattering intensity for “empty” liposomes and pDNA/CL complexes at four different molar charge ratios ( $R_{+/-}$ ) with the respective fitting curves. .... **68**

Figure 8. Electronic density profile across the lipid membrane for three different phases resulting from modeling and fitting of SAXS data..... **70**

Figure 9. Phase partitioning for all of the studied systems. The largest amount of pDNA added to the system generates a ternary phase system with single, double and multiple bilayers..... **72**

#### **Capítulo 4**

Figure 1. Microfluidic devices with single (A) and double (B) hydrodynamic focusing with a Total Lipid Concentration of 25 mM dispersed in ethanol, a Fluid Flow Velocity of 143 mm/s and a Flow Rate Ratio of 10..... **88**

Figure 2. Response surfaces of the particle size of cationic liposomes produced by the single hydrodynamic focusing (SHF) microfluidic device as a function of the Lipid Concentration of the dispersion in ethanol ( $C_{lip}$ ), the Average Flow Velocity ( $V_f$ ) and the Flow Rate Ratio (FRR)..... **95**

Figure 3. Schematic diagram of the hypothesized mechanism for liposome formation in a microfluidic hydrodynamic focusing device. The central stream is composed of the lipid dispersion in ethanol, which is hydrodynamic compressed by the two adjacent aqueous streams. The mixing of the water and ethanol through the main channel forms phospholipid bilayer fragments (PBF) that grow into vesicles to stabilize their hydrophobic PBF edges. The decrease in ethanol concentration destabilizes the PBFs, influencing then to close into vesicles and thus form liposomes. .... **97**

Figure 4. Effect of average flow velocity ( $V_f$ ) on particle size (intensity-weighted) for the production of cationic liposomes using the Single (SHF) and Double (DHF) Hydrodynamic Focusing devices. Production conditions: FRR of 10 and  $C_{lip}$  of 25 mM. The error bars represent the standard deviation of three independent experiments..... **100**

Figure 5. (A) Particle size distributions (intensity weighted) obtained by DLS and (B) Transmission electron micrographs of cationic liposomes produced by the Single Hydrodynamic Focusing microfluidic device at a  $C_{lip}$  of 25 mM, FRR of 10 and  $V_f$  of 143 mm/s. The bars represent 100 nm. .... **106**

Figure 6. (A) Particle size distributions (intensity weighted) obtained by DLS and (B) Transmission electron micrographs of cationic liposomes produced by the Double Hydrodynamic Focusing microfluidic device at a  $C_{lip}$  of 25 mM, FRR of 10 and  $V_f$  of 285 mm/s. The bars represent 100 nm. .... **106**

Figure 7. Small Angle X-ray Scattering intensity of cationic liposomes produced by the Single (SHF) and Double (DHF) Hydrodynamic Focusing devices with respective fitting curves. Production conditions:  $C_{lip}$  of 75 mM, FRR of 10 and  $V_f$  of 143 mm/s..... **107**

## Capítulo 5

Figure 1. Schematic diagram of (A) simple microfluidic hydrodynamic focusing device with inset illustrating the hydrodynamic focusing (SMD). (B) Patterned microfluidic device and the inset illustrating the geometry and dimensions of the barriers (PMD). The microchannels are 140  $\mu\text{m}$  wide and 100  $\mu\text{m}$  deep. .... **118**

Figure 2. Effect of temperature on (A) Particle size and (B) Polydispersity Index of the complexation process between CLs and plasmid DNA for different methods. Average fluid flow velocity of the microfluidic devices of 140 mm/s. The flow rate ratio was maintained at 5. Error bars correspond to SD of three independent experiments. \*Statistically different ( $p < 0.05$ ) when compared between the pairs. \*\*Statistically different ( $p < 0.05$ ) when compared to the bulk mixing method at 4 or 25°C. .... **124**

Figure 3. Particle size and polydispersity index of the complexes formed in simple and patterned microfluidic devices as function of mean fluid flow velocity in the center outlet channel (the combined flow velocities of all inlets) at 4°C. The flow rate ratio was maintained at 5. The error bars represent the standard error of independent triplicates. .... **126**

Figure 4. TEM images of DNA/cationic liposomes complexes produced by (A) simple microfluidic device and (B) patterned microfluidic device at flow rate ratio of 5, at 4 °C and  $V_f$  of 140 mm/s. Scale bars indicate 500 nm..... **129**

Figure 5. Electrophoretic mobility retardation assay of DNA complexed with cationic liposomes in different methods. Lanes: (1) free DNA; complexation processes: (2) bulk mixing; (3) simple microfluidic device; and (4) patterned

microfluidic device. Average fluid flow velocity of the microfluidic devices of 140 mm/s, at 4°C and FRR 5. .... **130**

Figure 6. Relative fluorescence obtained by the probe in ultra pure water. Results with free DNA used as control for complexes DNA/cationic liposomes formed by three different methods: bulk, in the simple and in the patterned microfluidic devices. The operational conditions of the microfluidic process were average fluid flow velocity of 140 mm/s at 4°C and FRR 5. Error bars correspond to SD of three independent experiments (n = 3). \* p < 0.05 was considered statistically different when compared to other samples. .... **131**

Figure 7. *In vitro* efficacy on HeLa cells transfection of DNA/CL complexes formed by bulk mixing and microfluidic methods. Activity was expressed in RLU/mg protein. The DNA/CL complexes were obtained applying average fluid flow velocity of the microfluidic devices of 140 mm/s at 4°C and FRR of 5. Each data represents SD of three experiments, \* p < 0.05 was considered statistically different. NS, no significant (p < 0.05). .... **132**

## LISTA DE TABELAS

### Capítulo 3

Table 1. Parameters obtained from simultaneous fitting of all scattering curves. .. 71

### Capítulo 4

Table 1. CCRD matrix with the real and coded values (in parenthesis) for the factors (Average Flow Velocity ( $V_f$ ), Lipid Concentration dispersed in ethanol ( $C_{lip}$ ), and Flow Rate Ratio (FRR)) tested and the responses (Particle Size and Polydispersity (Pdl)) obtained using the SHF device in the production of cationic liposomes. .... 94

Table 2. ANOVA for the Cationic Liposomes produced by the Single Hydrodynamic Focusing (SHF) device. .... 94

Table 3. CCRD matrix with the real and coded values (in parenthesis) for the factors (Average Flow Velocity ( $V_f$ ), Lipid Concentration of the dispersion in ethanol ( $C_{lip}$ ) and Flow Rate Ratio (FRR)) tested and the responses (Particle Size and Polydispersity (Pdl)) obtained using the DHF device in the production of cationic liposomes. .... 99

Table 4. ANOVA for the Cationic Liposomes produced by the Double Hydrodynamic Focusing (DHF) device. .... 99

Table 5. Physicochemical properties of cationic liposomes produced by the single and double hydrodynamic focusing microfluidic devices (SHF and DHF, respectively). Operating parameters: FRR of 10,  $C_{lip}$  of 25 mM and  $V_f$  of 165 and 285 mm/s for the SHF and DHF, respectively. .... 104

### Capítulo 5

Table 1. Flow properties of continuous formation of DNA/CL complexes in simple and patterned microfluidic devices at  $V_f$  of 140 mm/s and temperature control. The maximum and minimum for the patterned microfluidic device indicates the flow through compression regions (in the blocks) and expansion regions. .... 128

Table 2. Physicochemical properties of DNA/CL complexes obtained by the bulk mixing and microfluidic methods with  $V_f$  of 140 mm/s and at 4 °C. .... 128

## NOMENCLATURA

$\rho$ :	Densidade do fluido;
$\mu$ :	Viscosidade dinâmica;
CL:	<i>Cationic Liposomes</i>
$C_{lip}$ :	Concentração lipídica na dispersão em etanol;
D:	Coeficiente de difusão das partículas;
DC-Chol:	<i>3<math>\beta</math>-[N-(N',N'-dimethylaminoethane)-carbamoyl]cholesterol hydrochloride</i> ;
DCCR:	Delineamento Composto Central Rotacional;
$D_h$ :	Diâmetro hidráulico;
DHF:	<i>Double Hydrodynamic Focusing</i> ;
DHF:	<i>Double hydrodynamic focusing</i> ;
DLS:	<i>Dynamic Light Scattering</i> ;
DMPC:	<i>1,2-Dihexanoyl-sn-Glycero-3-Phosphocholine</i> ;
DNA:	Ácido desoxirribonucleico;
DOPC:	1,2-dioleoil- <i>sn</i> -glicero- <i>sn</i> -3-fosfatidilcolina;
DOPE:	L- $\alpha$ -dioleoil fosfatidiletanolamina;
DOSPA:	2,3 Dioleoiloxi-N-[(esperminacarboxamino)etil]-N,N-dimetil-1-propanamínio;
DOTAP:	1,2-dioleoil -3-trimetilamônio-propano;
DOTMA:	Cloreto de dioleoxi propil trimetil amônio;
DRV:	<i>Dehydrated-hydrated vesicles</i> ;
DRV:	Dehydrated-rehydrated vesicles;
EDP:	Electronic Density Profile;
EPC:	L-a-fosfatidilcolina de ovo;
EtBr:	Brometo de etídio;
FRR:	<i>Flow Rate Ratio</i> ;

H <sup>C</sup> <sub>II</sub> :	Fase hexagonal inversa;
HeLa:	<i>Human epithelial carcinoma</i> ;
LC:	Lipossomas Catiônicos;
Luc:	Luciferase;
MCT:	<i>Modified Caillé Theory</i> ;
MET:	Microscopia eletrônica de transmissão;
N:	Número de bicamadas;
P:	Produtividade molar de lipossomas;
PdI:	<i>Polydispersity Index</i> ;
PDMS:	Polidimetilsiloxano;
pDNA:	DNA plasmideal
Pe:	Peclet, número adimensional;
PMD:	<i>Patterned Microfluidic Device</i> ;
Q <sub>T</sub> :	Vazão Volumétrica Total;
R <sub>+/-</sub> :	Razão molar de cargas, relação entre moles de cargas positivas de lipídios catiônicos e cargas negativas do DNA;
Re:	Reynolds, número adimensional;
RLU:	<i>Relative Light Units</i> ;
SAXS:	<i>Small Angle X-ray Scattering</i> ;
SD:	<i>Standard Deviation</i> ;
SD:	<i>Standard Deviation</i> ;
SHF:	<i>Single Hydrodynamic Focusing</i> ;
SMD:	<i>Simple Microfluidic Device</i> ;
TEM:	Microscopy Electron Transmission;
V <sub>f</sub> :	Velocidade Superficial de Escoamento;
ζ:	Potencial Zeta.



---

## CAPÍTULO 1 – INTRODUÇÃO GERAL

---

### 1. Introdução

A terapia gênica é uma técnica promissora destinada à terapia preventiva e ao tratamento de inúmeras doenças, baseada na introdução de material genético em células específicas (CORSI *et al.*, 2003). Visa a correção dos genes responsáveis por uma *determinada* doença ou a produção de determinada proteína pela própria célula. Esta terapia pode ser utilizada em diversos tipos de doenças, tais como câncer, AIDS e doenças cardiovasculares (TURAN *et al.* 2003). A partir da década de 90, este conceito foi também estendido à profilaxia e tratamento de doenças infecciosas, tais como a tuberculose (Rosada *et al.* 2008 e TORRE *et al.*, 2009) e Leishmaniose (GOMES *et al.*, 2007).

Uma grande dificuldade na utilização deste material genético em aplicações *in vitro* e *in vivo* é que o DNA é quimicamente instável quando em contato com vários componentes corpóreos e, considerando sua natureza química (carga negativa) e seu tamanho elevado, o processo de transfecção (entrada nas células e no núcleo) é dificultado (LASIC, 1997, ROPERT, 1999).

Nesse sentido, os efeitos de veiculadores têm sido investigados por vários grupos de pesquisa, a fim de se obter proteção para o DNA em contato com os fluidos corpóreos/extracelulares e aumentar sua eficiência de transfecção *in vitro* e *in vivo*. Dentre os vetores não virais para entrega de material genético, os Lipossomas Catiônicos (LC) se apresentam promissores, pois permitem a proteção do DNA e o acoplamento, na sua superfície, de compostos que aumentam a eficiência de transfecção. Além disso, a facilidade de interação com as células é uma característica intrínseca dessas estruturas lipídicas, devido à sua semelhança com a membrana celular (LABAS *et al.*, 2010, DE ROSA & LA ROTONDA, 2009).

Lipossomas são estruturas aproximadamente esféricas de dimensões coloidais com cerne aquoso circundado por uma ou mais bicamadas lamelares lipídicas. São formados principalmente por fosfolipídios que se auto-agregam espontaneamente em vesículas em meio aquoso, incorporando parte desse meio em que se encontram.

Apesar da grande quantidade de estudos na área e de demonstrar sucesso em suas aplicações, o número de produtos lipossomais aprovados em aplicação humana é pequeno. Dentre outras razões, isso se deve ao fato de não haver métodos de produção de lipossomas eficientes de baixo-custo. Em muitos dos métodos, a auto-agregação não é completamente controlada, levando à necessidade de utilização de operações unitárias subsequentes para a redução do tamanho (MOZAFARI, 2005). Assim, a produção desses vetores em larga escala nas condições requeridas para sua aplicação é uma etapa limitante das formulações lipossomais destinadas à terapia e à vacinação gênica. Para isto, fazem-se necessários estudos de processos capazes de reproduzirem as propriedades físico-químicas e biológicas dos lipossomas funcionais, anteriormente obtidos por processos laboratoriais, sem alterar a estabilidade coloidal dos mesmos.

Uma alternativa para contornar estas dificuldades de processo é a realização da produção de LC e sua complexação eletrostática com DNA em sistemas microfluídicos, permitindo um melhor controle dos processos difusionais e, conseqüentemente, melhorando o controle do tamanho e polidispersidade das partículas e sua estabilidade. Além disso, os sistemas microfluídicos possuem tamanho mínimo e operam com baixo consumo de energia.

Essa perspectiva, chamada de Intensificação de Processo, tem recebido muita atenção na Engenharia Química moderna. Ela concerne a inovações que reduzem o tamanho da planta e consumo de energia em várias ordens de grandeza para um determinado objetivo e consiste no desenvolvimento de novas tecnologias que tragam melhorias na produção e processamento. Essas inovações diminuem substancialmente a razão tamanho de equipamento/capacidade de produção e são mais eficientes energeticamente,

resultando em tecnologias sustentáveis de menor custo (STANKIEWICZ *et al.*, 2009; SPOORTHI *et al.*, 2010). Neste contexto, a microfluídica se apresenta como uma forma de alcançar a intensificação de processo, integrando, em uma única etapa, determinados processos e etapas subsequentes de produção.

No cerne dessa perspectiva de desenvolvimento de processos microfluídicos, esse trabalho visa a contribuir para o desenvolvimento de novos processos de obtenção de vetores não virais baseados em LC, destinados à terapia e à vacinação gênica utilizando a microfluídica como estratégia para o controle na formação dos lipossomas e seus complexos com DNA.

Em última instância, esse trabalho contribuirá para o desenvolvimento tecnológico de novos processos que viabilizem produtos farmacêuticos que veiculem DNA destinados à terapia e vacinação gênica.

## 2. Objetivos

O objetivo deste trabalho foi o de contribuir na área da nanobiotecnologia, mais especificamente para o desenvolvimento de novos processos de obtenção de vetores não virais baseados em lipossomas catiônicos destinados à terapia e vacinação gênica. Para tal, a partir de LC obtidos por processo microfluídico, estudou-se o processo de complexação eletrostática entre LC e DNA, em sistema microfluídico, empregando dispositivos de focalização hidrodinâmica e comparou-os ao processo de complexação convencional “bulk”.

A pesquisa foi estruturada a partir dos três principais objetivos:

- Caracterização dos complexos DNA/lipossomas catiônicos obtidos pelo método convencional “bulk”: determinação das condições de complexação “bulk” entre LC e DNA que foram utilizadas como referência para o desenvolvimento do processo microfluídico.
- Estudo do processo microfluídico para a produção de lipossomas catiônicos: produção de LC através de dispositivos microfluídicos de focalização hidrodinâmica (simples e dupla) em maiores concentrações lipídicas, a fim de produzir essas nanopartículas com níveis de polidispersidade e tamanho similares aos LC produzidos pelo método “bulk”.

- Desenvolvimento de processo microfluídico para a complexação eletrostática entre lipossomas catiônicos e DNA: desenvolvimento de processos que permitam a complexação eletrostática entre LC e DNA em dispositivos microfluídicos de focalização hidrodinâmica única, similar ao estudado na segunda parte, com e sem blocos regulares nas paredes do microcanal, de modo a aumentar a área de contato entre os fluidos.

### 3. Organização da Dissertação em Capítulos

A presente dissertação está organizada em capítulos, conforme descrito a seguir. Os resultados estão divididos na forma de artigos que serão submetidos a periódicos internacionais, selecionados de acordo com a afinidade do conteúdo abordado. Dessa forma, os itens introdução, metodologia, resultados e discussão e conclusões de cada etapa constam nos artigos em seus respectivos capítulos.

No Capítulo 2, *Revisão Bibliográfica*, são abordados os aspectos teóricos quanto ao Estado da Arte no âmbito em que essa pesquisa se insere.

No Capítulo 3, intitulado *Correlation between Physicochemical and Structural Properties with In Vitro Transfection of pDNA/Cationic Liposomes Complexes*, a caracterização físico-química aliada à estrutural pôde ser correlacionada com ensaios biológicos. Uma vez que a caracterização físico-química dos complexos não foi suficiente para elucidar os diferentes níveis de transfecção obtidos para diferentes razões molares de cargas, foram conduzidas investigações de espalhamento de raios-x a baixo ângulo (SAXS - Small angle X-ray scattering) a fim de avaliar as modificações estruturais, já evidenciadas por estudos de DLS por volume. As análises de SAXS mostraram que a população de vesículas com dupla bicamada cresce gradativamente com o aumento da razão molar de cargas, assim como observado na transfecção *in vitro* em células HeLa. Próxima à região de isoneutralidade de cargas, a queda nos níveis de transfecção foi explicada pelo aparecimento de outra população de partículas, com uma média de 5 bicamadas lipídicas, o que, provavelmente, interferiu na liberação do DNA às células.

Já no Capítulo 4, *Continuous Flow Production of Cationic Liposomes at High Lipid Content in Microfluidic Devices for Gene and Vaccine Therapy*, foi estudada a produção de lipossomas catiônicos em sistema contínuo em altas concentrações com o emprego de dois dispositivos microfluídicos. O primeiro com única focalização hidrodinâmica e o segundo com dupla, objetivando o aumento da área de contato entre os fluxos aquosos e orgânicos, e assim a área de difusão. Verificou-se que o dispositivo com dupla focalização hidrodinâmica é capaz de operar a vazões mais altas que o de focalização única. Os estudos de SAXS revelaram a predominância de lipossomas unilamelares em ambos os dispositivos. Estudos biológicos *in vitro* mostraram a potencialidade do processo para produzir essas estruturas lipossomais carreadoras de DNA.

O Capítulo 5, por sua vez, sob o título de *Continuous Formation of DNA/Cationic Liposomes Complexes using Microfluidic Hydrodynamic Focusing Devices for Gene Delivery and Vaccine Therapy*, investiga a utilização de sistemas microfluídicos para a formação de complexos DNA/lipossomas catiônicos em modo contínuo. Com o emprego de dois dispositivos e tendo o método de complexação convencional “bulk” como referência, os complexos obtidos através de os ambos dispositivos estudados – um de paredes dos microcanais com blocos padronizados e outro de parede simples – foram capazes de transfectar *in vitro* células humanas do tipo HeLa. O dispositivo simples atingiu níveis de transfecção similares ao alcançados pelos complexos obtidos pelo método “bulk”, enquanto o dispositivo com blocos nos microcanais apresentou menores níveis de transfecção. Isso provavelmente ocorreu devido à diferença de acomodação do DNA nas estruturas lipossomais, conforme mostrado nos ensaios de sonda de fluorescência. De modo geral, ambos os dispositivos foram capazes de produzir complexos de tamanho e polidispersidade controlados para aplicações em terapia e vacinação gênicas.

Por fim, a dissertação é fechada com dois outros capítulos: *Conclusões Gerais e Sugestões para Trabalhos Futuros*, em que são listadas as conclusões que os estudos desenvolvidos permitiram e em que também se sugere rumos para pesquisas futuras.

#### 4. Referências

- CORSI, K., CHELLAT, F., YAHIA, L., & FERNANDES, J. C. Mesenchymal stem cells, MG63 and HEK293 transfection using chitosan–DNA nanoparticles. *Biomaterials*, v. 24, p. 1255-1264, 2003.
- DE ROSA, G.; LA ROTONDA, M. I., Nano and Microtechnologies for the Delivery of Oligonucleotides with Gene Silencing Properties. *Molecules*, v. 14, p. 2801-2823, 2009.
- GOMES, D. C. O.; PINTO, E. F.; MELO, L. D. B.; LIMA, W.P.; LARRAGA, V.; LOPES, U.G.; ROSSI-BERGMANN, B. Intranasal delivery of naked DNA encoding the LACK antigen leads to protective immunity against visceral leishmaniasis in mice. *Vaccine*, v. 25, p. 2168-2172, 2007.
- LABAS, R.; BEILVERT, F.; BARTEAU, B.; DAVID, S.; CHE`VRE, R.; PITARD, B. Nature as a source of inspiration for cationic lipid synthesis. *Genetica*, v.138, p. 153-168, 2010.
- LASIC, D.D. *Liposomes in Gene Delivery*. Boca Raton-Florida: CRC Press, p. 295. 1997.
- ROPERT, C. Liposomes as a gene delivery system. *Brazilian Journal of Medical and Biological Research*, v. 32, p. 163-169, 1999.
- ROSADA, R. S., TORRE, L. G.; FRANTZ, F. G. *et al.* Protection Against Tuberculosis by a Single Intranasal Administration of DNA-hsp65 Vaccine Complexed with Cationic Liposomes. *BMC Immunology*, 9:38, 2008.
- SPOORTHY, G., THAKUR, R. S., KAISTHA, N., RAO, D. P., Process intensification in PSA processes for upgrading synthetic landfill and lean natural gases. *Adsorption-Journal of the International Adsorption Society*, v. 17, p. 121-133, 2011.
- STANKIEWICZ, A. I., MOULIJN, J. A., Process intensification: Transforming chemical engineering. *Chemical Engineering Progress*, v. 96, p. 22-34, 2000.
- TORRE, L. G.; ROSADA, R. S.; TROMBONE, A.P.F., FRANTZ, F.G.; COELHO-CASTELO, A.A.M., SILVA, C.L.; SANTANA, M.H.A. Synergy between structural stability and dna-binding controls the antibody production in EPC/DOTAP/DOPE vesicles and DOTAP/DOPE lipoplexes. *Colloids and Surfaces*, v. 73, p. 175-184, 2009.
- TURAN, S., ARAL, C., KABASAKAL, L., & UYSAL, M. K. Coencapsulation of two plasmids in chitosan microspheres as a nonviral gene delivery vehicle. *Journal of Pharmacy and Pharmaceutical Sciences*, 1, 27–32, 2003.

---

## CAPÍTULO 2 – REVISÃO BIBLIOGRÁFICA

---

### 1. Lipossomas

Lipossomas são estruturas aproximadamente esféricas de dimensões coloidais com cerne aquoso circundado por uma ou mais bicamadas lamelares lipídicas. São formados quando fosfolipídios se autoagregam espontaneamente em vesículas na presença de água, incorporando parte do meio em que se encontram. Pelo fato das lamelas mimetizarem membranas celulares, os lipossomas possuem diversas características biológicas, que incluem interações com biomembranas e com diversas células (LASIC, 1995).

Pela sua degradabilidade e não-toxicidade (que depende da sua composição), uma das principais vantagens da utilização de lipossomas é sua aplicação como transportadores de fármacos de qualquer natureza, como hidrofílicos, que se posicionam nos domínios aquosos internos, lipofílicos, que se localizam nas bicamadas, e anfifílicos, que se localizam entre ambos os domínios. As lamelas protegem os compostos carregados das agressões do meio biológico e promovem sua liberação sustentada (BATISTA, 2008).

#### 1.1. Veiculação de DNA em lipossomas catiônicos

Os lipossomas catiônicos apresentam-se promissores para a veiculação de DNA, pois permitem a sua proteção contra a degradação por fluidos corpóreos e complexação eletrostática. Além disso, a facilidade de interação com as células é uma característica intrínseca das estruturas lipídicas, devido à sua semelhança com a membrana celular (LABAS *et al.*, 2010, DE ROSA & LA ROTONDA, 2009 e LASIC, 1993).

O transporte efetivo de nucleotídeos para o interior das células foi conseguido com a utilização de lipídios catiônicos, como reportado por Felgner

(1987), em mecanismo denominado lipofecção. Desta forma, lipídios catiônicos foram usados para carrear nucleotídeos por meio de simples complexação eletrostática e para facilitar o seu transporte para o interior das células, por possuírem cargas opostas. Vários lipídios catiônicos sintéticos têm sido usados, dentre os quais os sais quaternários de amônio, tais como o brometo de dimetildioctadecil amônio (DDAB) e o 1,2-dioleoil -3-trimetilamônio-propano (DOTAP), são os mais conhecidos como carreadores de nucleotídeos (Labas *et al.* 2010).

No processo de transporte para o interior das células, os nucleotídeos associados a lipossomas catiônicos são inicialmente internalizados preferencialmente através do mecanismo de endocitose. Em uma segunda etapa é necessário que os nucleotídeos sejam liberados da membrana endossomal para o citoplasma, possivelmente por ruptura da membrana que se desestabiliza devido a interações entre os lipídios catiônicos e suas moléculas aniônicas (Wattiaux *et al.*, 1997). Dentro desse mecanismo, a presença de fosfatidiletanolaminas (PEs), também designadas como auxiliares (do inglês, *helpers*), intensifica o processo de liberação por possuírem características fusogênicas, que facilitam a desestabilização da membrana endossomal (FELGNER *et al.*, 1994). Porém, a fusão dos lipídios associados ao DNA com a membrana endossomal provocada pelas PEs não ocorre diretamente com a membrana citoplasmática, sendo necessária a etapa inicial da endocitose (Wrobel & Collins, 1995). Por essa razão as PEs são também designadas na literatura como co-lipídios em relação aos lipídios catiônicos.

Dentre as PEs, é mais conhecida a ação fusogênica do 1,2 dioleoil- sn-glicero-3-fosfo etanolamina (DOPE). Sua importância nos estudos de potencialização da liberação dos nucleotídeos *in vitro* com lipídios catiônicos, deve-se à sua capacidade de passar para a fase hexagonal H<sub>II</sub>, facilitando a desestabilização da membrana endossomal e promovendo a liberação dos nucleotídeos no citoplasma através da troca de lipídios do endossoma com a membrana lipossomal.

Em geral, a geometria molecular dos anfifílicos catiônicos e do DOPE, por si só não favorece a agregação em bicamadas lamelares nas condições fisiológicas. Os agregados formados são instáveis, havendo co-existência entre as fases lamelar e hexagonal tal como reportado por Rädler *et al.* (1997), com o DNA intercalado nas estruturas. A associação de lipídios catiônicos e DOPE com fosfolipídios estruturais tais como fosfatidilcolinas (PCs) é imprescindível para a formação de lipossomas, os quais são constituídos de bicamadas regulares ou lamelas, que se agregam intercalando domínios aquosos e gerando partículas coloidais aproximadamente esféricas.

Devido à correlação direta entre a fluidez da bicamada e a capacidade de transfeção (DUZGUNES *et al.*, 1989), idealmente, a temperatura de transição de fases das PCs deve ser baixa, o que é encontrado na fosfatidilcolina natural de ovo (EPC). Isso faz com que, a temperatura corpórea, os lipídios que constituem as estruturas lipossomais estejam no estado líquido-cristalino, o que lhes confere a fluidez necessária para facilitar a ação do DOPE e do lipídeo catiônico (DOTAP) no processo de internalização nas células. Além disso, a inclusão de EPC nas formulações demonstrou que a citotoxicidade *in vitro* é drasticamente reduzida (DE LA TORRE *et al.*, 2009).

O desenvolvimento da nanoestrutura lipossomal incorporando o DNA-hsp65 foi inicialmente realizado por de La Torre *et al.* (2006). A composição lipídica apresenta os três lipídios DOTAP/DOPE/EPC, com funcionalidades de incorporação do DNA e ligação eletrostática com a superfície das células, intensificação da liberação do DNA no citoplasma celular e estruturação em nanopartículas, utilizando a composição lipídica otimizada por Perrie *et al.* (2001). Os lipossomas foram preparados pelo método da desidratação-rehidratação com duas configurações referentes à localização do DNA nas nanoestruturas lipossomais: uniformemente distribuído no interior ou preferencialmente na superfície (TORRE *et al.*, 2009 e ROSADA *et al.*, 2008).

Os resultados mostraram que ambas as configurações foram capazes de incorporar o DNAhsp65 com eficiência elevada e capacidade de incorporar 50 µg de DNA em 100 µL de preparação lipídica (ROSADA *et al.*, 2008, TORRE *et al.*,

2009, TORRE, 2006). Além disso, as preparações foram reprodutíveis e estáveis durante a estocagem, apresentando níveis de citotoxicidade semelhantes ao do DNA nu (TORRE *et al.* 2009). A avaliação do efeito profilático mostrou a potencialidade da nanoestrutura lipossomal incorporando o DNA-hsp65 preferencialmente na sua superfície (ROSADA *et al.*, 2008). Além da sua eficácia profilática, esta vacina possui a vantagem adicional de ser mais efetiva pela via intranasal, que é uma via não invasiva, desejável para a administração de fármacos, com a redução da dose de 400 µg de DNA nu para 25 µg de DNA veiculado na nanoestrutura lipossomal (ROSADA *et al.*, 2008). Desta forma, as nanoestruturas lipossomais complexando DNAhsp65 apresentaram-se promissoras para a produção de vacina para a tuberculose tanto do ponto de vista físico-químico quanto tecnológico (TORRE *et al.*, 2006).

Uma vez que as pesquisas para a obtenção dos lipossomas “vazios” estão em andamento, a busca de novas estratégias para avaliação da complexação eletrostática entre os lipossomas catiônicos e o DNA vem sendo a próxima etapa de investigação, visando processos menos suscetíveis a variações de processo, além de garantir maior estabilidade durante a estocagem.

Uma alternativa para contornar estas dificuldades de processo é a realização da complexação eletrostática entre os lipossomas catiônicos e DNA em sistema microfluídico, permitindo um melhor controle dos processos difusionais e conseqüentemente, melhorando o controle do tamanho das partículas e sua estabilidade.

## **1.2. Produção de lipossomas catiônicos**

Apesar da grande quantidade de estudos na área e de demonstrar sucesso em suas aplicações, o número de produtos lipossomais aprovados em aplicação humana é pequeno. Dentre outras razões, isso se deve ao fato de não haver métodos de produção de lipossomas eficientes de baixo-custo (MOZAFARI, 2005). Em muitos dos métodos, a agregação coloidal não é completamente controlada levando a necessidade de utilização de operações unitárias subsequentes para a redução do tamanho.

Há diversas técnicas de produção em escala laboratorial e algumas em larga escala (MOZAFARI, 2005). Dentre os métodos tradicionais de produção laboratorial de lipossomas, o proposto por Bangham é, provavelmente, um dos mais utilizados (LESOIN *et al.*, 2011). O método consiste na dispersão dos lipídios em uma fase orgânica e sua posterior remoção, formando um filme seco de lipídios, que é então hidratado com uma solução aquosa. Outros métodos tradicionais, como o método de injeção de etanol, de evaporação da fase reversa e emulsão, também se baseiam na produção de uma solução lipídica com um solvente orgânico antes da dispersão em uma fase aquosa. Todos esses métodos necessitam de uma operação unitária posterior à produção dos lipossomas para atender tamanhos e polidispersidade de tamanhos requeridos. Os métodos mais comuns de redução/uniformização do tamanho dos lipossomas são sonicação, extrusão e homogeneização a alta pressão (MEURE *et al.*, 2008).

Os métodos mais recentes desenvolvidos para a produção de lipossomas abordam técnicas que utilizam altas temperaturas, liofilização de soluções monofásicas, fluidos supercríticos e microcanais (MEURE *et al.*, 2008). Os processos que utilizam gás denso e fluidos supercríticos utilizam apenas uma pequena quantidade de solvente orgânico, além de possibilitarem a esterilização *in situ* (LESOIN *et al.*, 2011). Todos os novos métodos exploram técnicas que visam a intensificação do processo, para que sejam em uma única etapa, atendam às especificações de Boas Práticas de Fabricação, eliminem a utilização de solventes, diminuam a complexidade e o tempo de produção (MEURE *et al.*, 2008). Apesar de alguns serem passíveis de escalonamento, nenhum desses métodos opera em regime contínuo, exceto a produção de lipossomas em microcanais a baixa pressão.

Em geral, os métodos para produção de nanopartículas podem ser divididos em duas abordagens: “top-down” e “bottom up”. A abordagem top-down é a forma mais usada de obtenção de nanopartículas. Primeiramente, as partículas são obtidas em grande tamanho, e com a aplicação de forças de alta energia, o tamanho é reduzido para escalas nanométricas. Na abordagem bottom up, as

nanopartículas são formadas diretamente no tamanho desejado, pela auto-organização das moléculas (TREVISAN, 2010).

A busca por processos que forneçam lipossomas com tamanhos menores e com menor polidispersidade vem da necessidade de melhorar a aparência macroscópica da preparação e sua possível esterilização, e melhorar a estabilidade física em termos de sedimentação e flotação. Adicionalmente, quanto menor o tamanho dos lipossomas, o processo de remoção da corrente sanguínea é prolongado, elevando o tempo de circulação na corrente sanguínea, viabilizando aplicações intravenosas (TORCHILIN & WEISSIG, 2007).

Além disso, para aplicações dos lipossomas catiônicos em transfecções *in vitro*, o tamanho e a polidispersidade da dispersão é fundamental para garantir a condição ideal para a entrada dos complexos lipossomas-DNA nas células. Uma alternativa promissora para o controle do tamanho é a área de microfluídica.

## 2. Microfluídica

Microfluídica é um campo multidisciplinar que estuda fluidos em volumes milhares de vezes menores que uma gota ( $10^{-9}$  a  $10^{-18}$  litros). Além de pequenas dimensões e quantidade de fluidos, a microfluídica explora características hidrodinâmicas para organizar no espaço e no tempo fluxos de fluidos como reagentes químicos, células, lipídios, ácidos nucleicos (DRAGHICIU *et al.*, 2010; BAEK *et al.*, 2011; YAMASHITA *et al.*, 2011; REINER *et al.*, 2010; KURITA *et al.*, 2010). Esta ciência está entre as áreas que mais têm crescido na pesquisa científica e no desenvolvimento tecnológico (LI, 2008).

Os dispositivos micrométricos projetados para realizar tarefas específicas têm demonstrado superioridade sobre seus análogos em macroescala (LUTZ, 2002). As especificidades destes sistemas conferem diversas vantagens em relação aos sistemas fluídicos convencionais: tamanho mínimo de dispositivos; menor consumo de amostra e reagente; controle preciso de fenômenos de transferência térmico e mássico; escoamento estritamente laminar; reações muito mais rápidas; baixo consumo e dissipação de energia; baixo custo relativo de produção por dispositivo.

A estratégia de aumento de produção (“scale-up”) se dá de forma diferente dos processos fluídicos, uma vez que estes últimos requerem aumento do tamanho dos equipamentos e das vazões de processo. O aumento de produção dos processos microfluídicos ocorre em termos de amplificação de processos, isto é, os dispositivos não são alterados em suas dimensões, mas sim, montados em paralelo de forma a se elevar a produção por réplica. Assim, os dispositivos são portáteis, possuem elevada superfície de contato entre os fluidos em relação ao volume e possibilitam a fácil amplificação da produção, utilizando sistemas em paralelo e, em algumas vezes, até mesmo dispositivos descartáveis (JAHN *et al.*, 2010; LUTZ *et al.*, 2002; TERRAY *et al.*, 2002; SEKHON *et al.*, 2010; TIAN *et al.*, 2009).

Uma nova perspectiva que tem recebido muita atenção na engenharia química moderna, que concerne a inovações que reduzem o tamanho da planta e consumo de energia em várias ordens de grandeza para um determinado objetivo, é a Intensificação de Processo. Esta perspectiva consiste no desenvolvimento de novas tecnologias que tragam melhorias na produção e processamento, reduzindo substancialmente a produção de resíduos e a razão tamanho de equipamento/capacidade de produção, que sejam mais eficientes energeticamente, resultando em tecnologias sustentáveis mais baratas (STANKIEWICZ *et al.*, 2000 e 2009; SPOORTHI *et al.*, 2010). Neste contexto, a microfluídica se apresenta como uma forma de alcançar a intensificação de processo, integrando em uma única etapa determinados processos e etapas subsequentes de produção, além de minimizar efeitos de transferência de calor e massa, pela própria dimensão dos dispositivos.

As técnicas utilizadas para a fabricação dos dispositivos dependem do material a ser empregado, que deve se adequar a aplicação preterida de acordo com as características físicas e químicas desse material. A utilização de vidro e polímeros para a produção de microdispositivos é amplamente utilizada, pois tais materiais unem boas propriedades químicas e físicas a baixo custo, além de permitirem a fácil estruturação do sistema que constituem o dispositivo, isto é, canais, orifícios, colunas, bombas, válvulas etc (LI *et al.*, 2010; BECKER *et al.*, 2001). Atualmente, diversas tecnologias para a fabricação de dispositivos

microfluídicos são empregadas: impressão e estampagem a quente, moldagem por injeção, litografia macia, fotoablação a laser, litografia de raio-x, dentre outros (BECKER, 2001).

As aplicações da microfluídica na biotecnologia são uma interessante área que começou a revolucionar a forma como pesquisadores estudam e manipulam macromoléculas (BELTHIER, 2006). Os avanços na microfabricação permitem que tais sistemas operem com diversos biomateriais com investigações nas diversas áreas desde o desenvolvimento de biorreatores, processos de separação e também para a obtenção de nanopartículas para diversas aplicações (BETTINGER, 2010).

A obtenção de nanopartículas em microcanais é uma das aplicações que tem se mostrado uma alternativa promissora para superar obstáculos existentes nos métodos convencionais de produção, como o controle da polidispersidade, do tamanho de partícula e do potencial zeta. Devido à flexibilidade desses dispositivos para operar com uma variedade de diferentes materiais, vários tipos de nanopartículas obtidas por síntese, formação ou auto-agregação em microcanais são reportadas na literatura, como niosomas, emulsões, nanocristais, partículas de PLGA e lipossomas (LO *et al.*, 2010; PERRO *et al.*, 2010; ZHAO *et al.*, 2010; SHAN *et al.*, 2003).

### **3. Produção de Lipossomas em Microcanais**

O escoamento em multicanais que utilizam os princípios da microfluídica vêm sendo uma das alternativas mais estudadas para a produção de lipossomas pré-formados produzidos sem a necessidade de etapas subsequentes ao processo para redução do tamanho e da polidispersidade, além de operarem em regime contínuo (JAHN *et al.*, 2003 e 2007). Esta é uma abordagem *bottom up*, pois visa à produção dos lipossomas já no tamanho e polidispersidade apropriados para a aplicação biológica.

A formação dos lipossomas nos microcanais que utilizam o princípio da focalização hidrodinâmica ocorre através do contato de duas fases de fluidos solúveis entre si, uma aquosa e outra orgânica. A fase orgânica é aquela na qual

os lipídeos estão dispersos em um solvente, como etanol ou isopropanol. Dessa forma, ocorre a difusão entre essas fases. Conforme ocorre essa difusão na interface entre as fases, os lipídeos se tornam cada vez menos solúveis no meio aquoso, e começam a se agregar, formando discos de bicamadas lipídicas planares. À medida que essas bicamadas lipídicas planares crescem, elas começam a se ligar a fim de diminuir a área superficial das cadeias hidrofóbicas dos lipídeos expostas pelas extremidades ao meio aquoso. Dessa forma, os discos se fecham em vesículas esféricas com uma bicamada separando um meio aquoso no cerne do meio externo (ZOOK *et al.*, 2010).

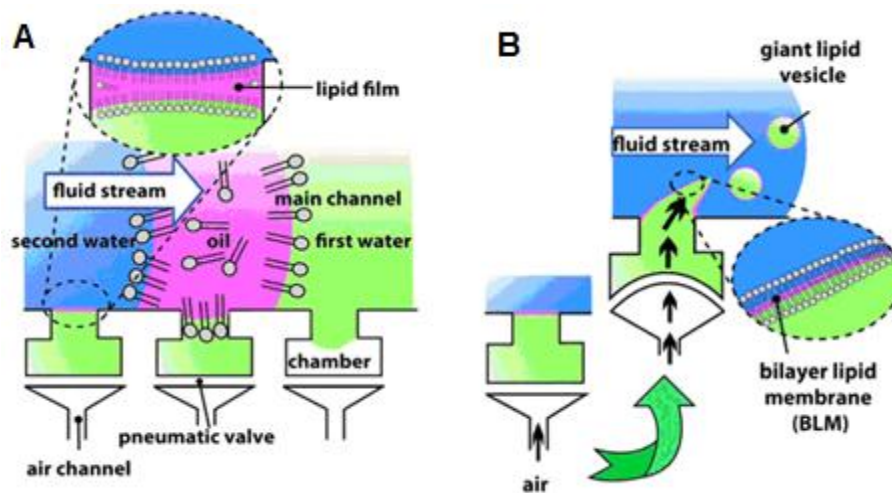


**Figura 1.** (A) Ilustração da construção do filme lipídico. Água, óleo com lipídios e água são sequencialmente injetados no canal principal do dispositivo microfluídico, que contém microcâmaras em sua parede. (B) Bombas pneumáticas são acionadas formando vesículas lipídicas, que saem pelo canal principal (fonte: KURAKAZU *et al.*, 2010).

Dentre os trabalhos que focam a formação de lipossomas em dispositivos microfluídicos, Kurakazu *et al.* (2010) estudaram a formação de lipossomas gigantes utilizando um sistema microfluídico de junção T com válvulas pneumáticas. A operação do aparato se dava com a passagem sequencial de água, solução de óleo contendo os lipídios e água novamente, por um canal com microcâmaras distribuídas ao longo de sua parede, como mostra a Figura 1A. A água da primeira passagem preenchia as microcâmaras, que posteriormente eram seladas com a membrana de bicamada lipídica formada na interface dos líquidos. Válvulas pneumáticas empurravam a água de dentro das câmaras para fora,

fazendo com que os lipossomas fossem formados encapsulando a água da primeira passagem (Figura 1B). Com esse sistema, é factível a produção de lipossomas monodispersos e unilamelares de forma contínua. Um dispositivo com operação similar, foi elaborado por Ota *et al.* (2009), que formaram lipossomas de tamanho de diâmetro entre 18 e 31  $\mu\text{m}$ . Os lipossomas eram formados encapsulando calceína, que estava em solução na primeira fase aquosa a passar pelo canal.

Utilizando injeção cruzada de lipídios dispersos em etanol, Wagner *et al.* (2002) produziram uma população homogênea de lipossomas. Este processo, denominado também de focalização hidrodinâmica, representa um melhoramento em relação ao método tradicional de injeção de etanol, em que a mistura lipídio-etanol é lentamente injetada em um tanque agitado contendo solução aquosa tamponada. O processo de injeção cruzada mostrou maior facilidade de controle do tamanho das partículas, sendo mais reprodutível que o processo convencional. As partículas geradas apresentaram diâmetros na faixa de 200 a 500nm.

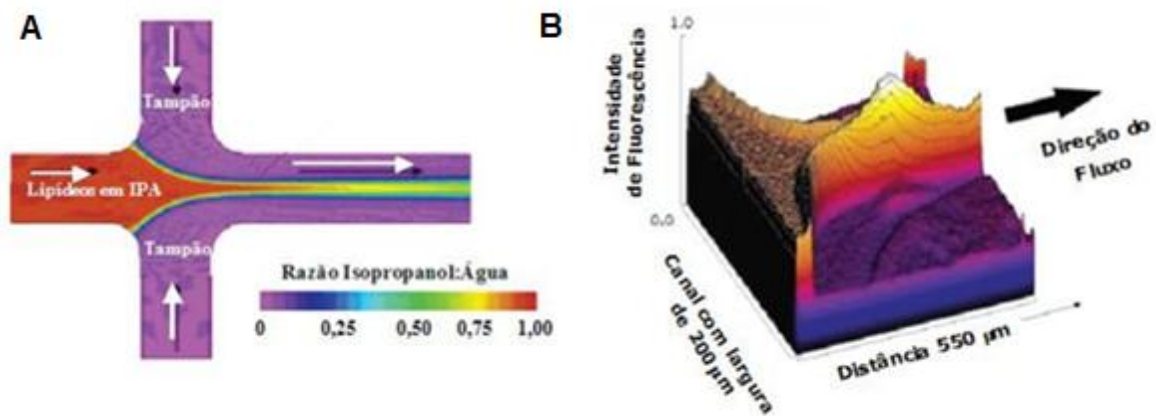


**Figura 2.** (A) Diagrama esquemático do processo de formação de lipossomas em canal microfluídico. A relação de cores representa as razões de concentração de álcool isopropílico e tampão aquoso. (B) Mapa 3-D de intensidade de fluorescência durante formação de lipossomas (adaptado de JAHN *et al.*, 2004).

Jahn *et al.* (2004 e 2007) descreveram a formação de lipossomas em uma rede de microcanais, conforme ilustrado na Figura 2. Os lipossomas foram formados por um processo controlado pela difusividade, quando uma corrente de lipídios dispersos em solvente orgânico é hidrodinamicamente comprimido por duas correntes aquosas tamponadas. Os lipossomas formados apresentaram

tamanhos de 50 a 150nm, com distribuição de tamanhos menor e maior reprodutibilidade quando comparados aos produzidos pelo processo convencional de injeção de etanol (“bulk”). Este processo é sensível à geometria do canal e à razão entre as vazões volumétricas de álcool e água, sendo essa última razão, a variável controladora do processo. A formação dos lipossomas foi também mais fortemente dependente da corrente de solvente orgânico e da sua difusividade na corrente aquosa, do que das forças de cisalhamento na interface solvente-solução tampão.

Utilizando um dispositivo microfluídico imerso em um banho de ultra-som, Huang *et al.* (2010) obtiveram lipossomas monodispersos com tamanho médio de partícula entre 50 e 150 nm. Com a sonicação, o tamanho de partícula foi reduzido significativamente quando comparado com os lipossomas produzidos sem sonicação. Segundo os autores, isso se deve provavelmente ao fato de que, com o processo de sonicação, pode haver cavitação no sistema, melhorando a dispersão das moléculas de lipídio e conseqüentemente, reduzindo o tamanho dos lipossomas. Os autores também observaram que o tamanho dos lipossomas obtidos nos microcanais diminuiu com o aumento da razão entre as taxas de fluxo aquosa e alcoólica/lipídica (do inglês, Flow Rate Ratio – FRR). O aumento de FRR promove a formação de lipossomas em concentração lipídica menor.

Trevisan *et al.* (2011), empregando a mesma composição lipídica do presente trabalho, produziu lipossomas catiônicos em altas concentrações em dispositivos microfluídicos de vidro. A concentração lipídica da dispersão etanólica utilizada foi muito acima àquelas reportadas na literatura, variando entre 100 e 400 mM. Entretanto, provavelmente devido às altas concentrações empregadas não se adequarem a produção de LC em sistemas microfluídicos, os lipossomas obtidos não apresentaram bom controle de tamanho e polidispersidade.

A produção de niossomas também é factível em microcanais (LO *et al.*, 2010). Niossomas são e são formadas pela auto-agregação de tensoativos não-iônicos. Os niossomas são comumente usados como transportadores de agentes de tratamento para aplicações farmacêuticas e cosméticas. Comparada com o método tradicional, a produção em microcanais se mostrou mais eficiente tanto no

controle do tamanho das partículas, quanto na sua polidispersidade. Pelo fato dos sistemas microfluídicos apresentarem uma mistura rápida e controlada dos dois fluidos miscíveis (álcool e água) foi possível a obtenção de niossomas com distribuição de tamanho 40% menor em comparação com o método tradicional, sugerindo a factibilidade do desenvolvimento e otimização de sistemas coloidais em dispositivos microfluidicos para a aplicação em nanomedicina.

#### **4. Sistemas Microfluídicos para a complexação eletrostática entre lipossomas catiônicos e DNA**

A formação de vetores não virais depende do empacotamento apropriado do DNA em sua estrutura. As interações eletrostáticas entre os lipídeos catiônicos e o DNA produzem estruturas auto-agregadas em partículas de tamanho e morfologia diversas (MANNISTO *et al.*, 2002 e OBERLE *et al.*, 2000), que dependem de fatores tais como a razão molar de cargas positivas/negativas, força iônica do tampão, ordem de mistura, condições de reações, tipo de lipídeo (TORRE, 2006, MOUNT *et al.*, 2003 e ZELPHATI *et al.*, 1998).

A variação dos resultados de transfecção reflete muitas vezes a dificuldade de controle do processo de auto-agregação e tem como consequência a produção de partículas de elevado grau de polidispersidade, levando a formação grandes frações das populações fora da faixa de tamanho correta para a transfecção da célula alvo do estudo (HSIEH *et al.*, 2009). Vários autores reportaram que o tamanho dos complexos lipossoma-DNA é um parâmetro que influencia diretamente a transfecção gênica (MA *et al.*, 2007, REJMAN *et al.*, 2004, WIEWRODT *et al.* 2002, ROSS & HUI, 1999, OGRIS *et al.*, 1998). Neste contexto, o desenvolvimento de processos que promovam o controle da complexação eletrostática entre os lipossomas catiônicos e o DNA, que permitam a formação de partículas uniformes e de forma reprodutiva, resultará consequentemente em transfecções uniformes. Estes resultados são fundamentais para o desenvolvimento de produtos farmacêuticos que veiculam tanto DNA como também RNA.

Uma abordagem recente no estudo do controle do tamanho destas partículas é a utilização de processos microfluídicos. Estes sistemas permitem a realização da complexação eletrostática em fluxo contínuo, com o controle do cisalhamento e das condições difusionais, permitindo a orientação de macromoléculas. O método da focalização hidrodinâmica também têm sido utilizado em estudos de complexação eletrostática entre DNA e lipossomas catiônicos (OTTEN *et al.*, 2005; JELLEMA *et al.*, 2010), dendrímeros (DOOTZ *et al.*, 2006) e polietilenoimina (KOH *et al.*, 2009), bem como lipossomas catiônicos e RNA, visando a caracterização físico-química destas partículas.

Adicionalmente, a focalização hidrodinâmica leva a formação de estruturas mais organizadas. O regime de escoamento laminar também permite que a compactação do DNA seja controlada pelo processo difusional, contribuindo para a maior organização estrutural (DOOTZ *et al.*, 2006). Este processo permite que agregados formados em microcanais sejam mais compactos, porém dependentes principalmente das velocidades superficiais dos fluidos (DOOTZ *et al.*, 2006).

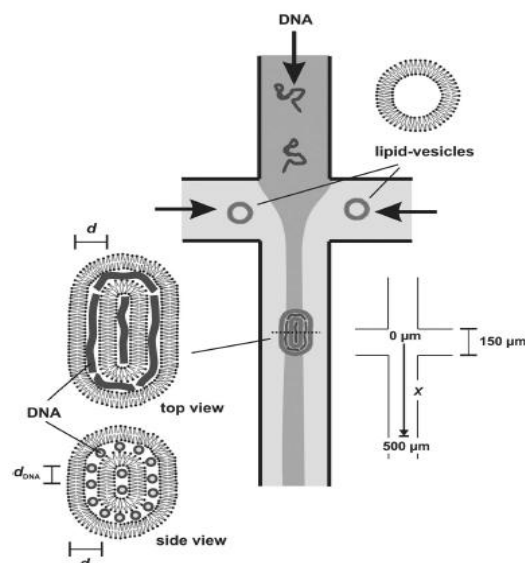


**Figura 3:** Representação esquemática do sistema microfluídico de focalização hidrodinâmica para a formação do sistema auto-agregado lipossoma catiônico-DNA (Fonte: KOH *et al.* 2005).

Otten *et al.* (2005) elaboraram um aparato microfluídico, baseado na focalização hidrodinâmica, conforme apresentado na Figura 3, objetivando a investigação do comportamento dinâmico na formação de complexos lipossoma

catinônico-DNA. O DNA é inserido na posição central da focalização hidrodinâmica e os lipossomas catiônicos pré-formados têm seu fluxo dividido em duas entradas laterais, comprimindo hidrodinamicamente a corrente de DNA. Este esquema é similar ao realizado experimentalmente em nosso grupo de pesquisa para a obtenção dos lipossomas “vazios” (ou pré-formados) (TREVISAN *et al.*, 2011).

A largura da corrente líquida focalizada pode ser ajustada de acordo com as taxas de escoamento entre as fases. De acordo com o regime laminar, a mistura é controlada somente pelo processo difusivo. Reduzindo a largura da corrente líquida focalizada, ocorre a diminuição do comprimento no qual o processo difusivo ocorre e conseqüentemente a mistura ocorre mais rapidamente (KNIGHT *et al.*, 1998). Em seus estudos, Otten *et al.* (2005), utilizaram uma solução de DNA (calf thymus DNA) em  $5 \text{ mg.mL}^{-1}$ , com velocidade superficial de  $100 \text{ mm.s}^{-1}$ . A dispersão aquosa dos lipossomas catiônicos (diâmetro médio hidrodinâmico inferior a 200 nm), formados por DOTAP e DOPC (dioleoyl-phosphatidylcholine) (1:1) (concentração lipídica de  $25 \text{ mg.mL}^{-1}$ ), com velocidade superficial de  $v_{\text{Lipossomas}} = 13v_{\text{DNA}}$  e  $v_{\text{Lipossomas}} = 130v_{\text{DNA}}$ . Neste estudo os autores verificaram que o processo de auto-agregação ocorre em duas etapas: a primeira, na qual ocorre a formação do complexo multilamelar e uma segunda, na qual ocorre um rearranjo do DNA dentro das lamelas.

Outro aparato microfluídico também é reportado em uma patente internacional (LEE *et al.* 2009), que descreve a obtenção de nanopartículas formadas por lipídeos e oligonucleotídeos para a liberação de DNA ou RNA para células de câncer. Neste caso os lipídeos são dispersos em uma fase orgânica (miscível em água) e os oligonucleotídeos (DNA ou RNA) são solubilizados em água. A mistura destas duas correntes em sistema microfluídico permite a formação do sistema nanoparticulado de entrega de genes. De acordo com os autores, o sistema microfluídico permite a formação de nanopartículas de tamanho bem definido, bem como estrutura e função farmacológica (Patente internacional WO2009120247-A2, 2009).

Jellema *et al.* (2010) utilizaram um sistema de fluxo contínuo para a complexação eletrostática entre lipossomas catiônicos formados com os lipídios DOPE/DOTAP e DNA. Um micromisturador com 12 estágios foi empregado para preparar os complexos lipossomas-DNA na razão de cargas apropriada. Lipoplexos com uma estreita distribuição de tamanhos foram eficientemente obtidos utilizando essa técnica.

Um dispositivo multi-entradas de focalização hidrodinâmica foi estudado para a formação complexos contendo mRNA por Koh *et al.* (2010). Os melhores resultados foram obtidos utilizando uma configuração de 3 canais: no canal, a solução de mRNA era injetada, enquanto nas entradas laterais eram injetadas as correntes lipídicas. O diâmetro hidrodinâmico das partículas variou entre 100 e 300 nm. Comparado com o método bulk, as nanopartículas obtidas pelo sistema microfluídico apresentaram menores tamanho e polidispersidade, além de propiciar a produção de estruturas mais uniformes. Esses complexos também se mostraram eficientes em aplicações biológicas *in vitro*.

Neste contexto, o desenvolvimento de processos que promovam o controle da complexação eletrostática entre os lipossomas catiônicos e o DNA, que permitam a formação de partículas uniformes e de forma reprodutiva, resultará conseqüentemente em transfecções mais eficientes. Estes resultados são fundamentais para o desenvolvimento de produtos farmacêuticos que veiculam tanto DNA como também RNA para aplicação em vacinação e terapia gênica.

## 5. Referências

- DE ROSA, G.; LA ROTONDA, M. I. Nano and Microtechnologies for the Delivery of Oligonucleotides with Gene Silencing Properties. *Molecules*, v.14, p.2801-2823, 2009.
- DUZGUNES, N.; GOLDSTEIN, J.A.; FRIEND, D.S.; FELGNER, P.L. Fusion of liposomes containing a novel cationic lipid, N[2,3-(dioleoyl-oxy)propyl]-N,N,N-trimethylammonium: induction by multivalent anions and asymmetric fusion with acidic phospholipid vesicles. *Biochemistry*, v. 28, p. 9179-9184, 1989.
- FELGNER, J.H.; KUMAR, R.; SRIDHAR, C.N.; WHEELER, C.J.; TSAI, Y.J.; BORDER, R.; MARTIN, M.; FELGNER, P.L. Enhanced gene delivery and mechanism studies with a novel series of cationic formulations. *Journal of Biological Chemistry*, v. 269, p. 2550-2561, 1994.

- FELGNER, P.L.; GADEK, T.R.; HOLM, M.; ROMAN, R.; CHAM, H.W.; WENZ, M.; NORTHROP, J.P.; RINGOLD, G.M.; DANIELSEN, M. Lipofection: a highly efficient, lipid-mediated DNA-transfection procedure. *Proceedings of the National Academy of Sciences of the United States of America*, v. 84, p. 7413-7417, 1987.
- HSIEH, A. T-H.; HORI, N.; MASSOUDI, R.; PAN, P. J-H.; SASAKI, H.; LIN, Y. A.; LEE, A. P. Nonviral gene vector formation in monodispersed picolitre incubator for consistent gene delivery. *Lab Chip*, v. 9, p. 2638–2643, 2009
- JAHN, A.; REINER, J.E.; VREELAND, E.W.N.; DEVOE, E.D.L.; LOCASCIO, E.L.E.; GAITAN, E.M., Preparation of nanoparticles by continuous-flow microfluidics, *J Nanopart. Res* 10:925–934, 2008.
- JAHN, A.; VREELAND, E.W.N.; DEVOE, E.D.L .; LOCASCIO, L.E; GAITAN, M., Microfluidic directed formation of liposomes of controlled size, *Langmuir* 23: 6289-6293, 2007.
- JAHN, A.; VREELAND, W.; GAITAN, M.; LOCASCIO, L.E., Controlled Vesicle Self-Assembly in Microfluidic Channels with Hydrodynamic Focusing, *J. Am. Chem. Soc.* 126, 2674-2675, 2004.
- KNIGHT, J. B.; VISHWANATH, A.; BRODY, J. P.; AUSTIN, R. H. Hydrodynamic focusing on a silicon chip: Mixing nanoliters in microseconds. *Phys. Rev. Lett.* , v. 80, p. 3863–3866, 1998.
- KOH, C. G.; KANG, X. ; XIE, Y.; FEI, Z.; GUAN, J.; YU, B.; ZHANG, X.; LEE L. J. Delivery of Polyethylenimine/DNA Complexes Assembled in a Microfluidics Device. *Molecular Pharmaceutics* , v. 6, p.1333–1342 , 2009.
- LABAS, R.; BEILVERT, F.; BARTEAU, B.; DAVID, S.; CHE`VRE, R.; PITARD, B. Nature as a source of inspiration for cationic lipid synthesis. *Genetica*, v.138, p. 153–168, 2010.
- LASIC, D.D. *Liposomes in Gene Delivery*. Boca Raton-Florida:CRC Press, p. 295. 1997.
- LUTZ, B. R.; CHEN, J.; DANIEL T. SCHWARTZ, D. T. Microfluidics without microfabrication. *PNAS*. v. 100, p. 4395–4398, 2003.
- MA, B. C.; ZHANG, S. B. ; JIANG, H. M.; ZHAO, B. D.; LV, H. T. Cationic lipids and polymers mediated vectors for delivery of siRNA. *Journal of Controlled Release*, 2007, 123, 184–194.
- MANNISTO, M; VANDERKERKEN, S.; TONCHEVA, V.; ELOMAA, M.; RUPONEN, M.; SCHACHT, E.; URTTI, A. Structure–activity relationships of poly(L-lysines): effects of pegylation and molecular shape on physicochemical and biological properties in gene delivery. *Journal of Controlled Release*, v.83, p. 169–182, 2002.

- MOUNT, C. N.; LEE, L. K.; YASIN, A.; SCOTT, A.; FEARN, T.; SHAMLOU, P. A. The influence of physico-chemical and process conditions on the physical stability of plasmid DNA complexes using response surface methodology. *Biotechnology and Applied Biochemistry*, 37, 225–234, 2003.
- OGRIS, M.; STEINLEIN, P. ; KURSA, M.; MECHTLER, K.; KIRCHEIS, R.; WAGNER, E. The size of DNA/transferrin-PEI complexes is an important factor for gene expression in cultured cells . *Gene Therapy*, 5, 1425–1433, 1998.
- OTTEN, A.; KOSTER, S.; STRUTH, B.; SNIGIREV, A.; PFOHL, T. Microfluidics of soft matter investigated by small-angle X-ray scattering. *J. Synchrotron Radiat.* , v. 12, p.745–750, 2005.
- PERRIE, Y.; FREDERIK, P.M.; GREGORIADIS, G. Liposome-mediated DNA vaccination: the effect of vesicle composition. *Vaccine*, v. 19, p. 3301-3310, 2001.
- REJMAN, J.; OBERLE, V.; ZUHORN, I. S.; HOEKSTRA, D. Size-dependent internalization of particles via the pathways of clathrin-and caveolae-mediated endocytosis. *Biochemical Journal*, 2004, 377, 159–169.
- ROSADA, R. S., TORRE, L. G.; FRANTZ, F. G. *et al.* Protection Against Tuberculosis by a Single Intranasal Administration of DNA-hsp65 Vaccine Complexed with Cationic Liposomes. *BMC Immunology*, 9:38, 2008.
- ROSS, P. C.; HUI, S. W. Lipoplex size is a major determinant of *in vitro* lipofection efficiency *Gene Therapy*, 6, 651–659, 1999.
- TORRE, L. G., Desenvolvimento de vacina gênica veiculada em adjuvantes lipídicos para tratamento da tuberculose. Tese de Doutorado apresentada na Faculdade de Engenharia Química da Universidade Estadual de Campinas. 2006.
- TORRE, L. G.; ROSADA, R.S.; TROMBONE, A.P.F., FRANTZ, F.G.; COELHO-CASTELO, A.A.M., SILVA, C.L.; SANTANA, M.H.A. Synergy between structural stability and dna-binding controls the antibody production in EPC/DOTAP/DOPE vesicles and DOTAP/DOPE lipoplexes. *Colloids and Surfaces*, v. 73, p. 175-184, 2009.
- TREVISAN, J. E., CAVALCANTI, L. P., OLIVEIRA, C. L. P., TORRE, L. G., SANTANA, M. H. A. Technological Aspects of Scalable Processes for the Production of Functional Liposomes for Gene Therapy. *InTech*. Capítulo 18, 2011.
- WAGNER, A.; VORAUER-UHL, k.; KREISMAYR, G.; KATINGE, H., The cross-flow injection technique: an improvement of the etanol injection method. *Journal of Liposome Research*. v. 12, p. 259-270, 2002.

- WATTIAUX, R.; JADOT, M.; WARNIER-PIRROTTE, M.T.; WATTIAUX-DE CONINCK, S. Cationic lipids destabilize lysosomal membrane *in vitro*. FEBS Letters, v. 417, p. 199-202, 1997.
- WHITESIDES, G. The origins and the future of microfluidics. Nature, v. 442, p. 368, 2006.
- WIEWRODT, R.; THOMAS, A. P. ; CIPELLETTI, L.; CHRISTOFIDOU-SOLOMIDOU, M.; WEITZ, D. A. ; FEINSTEIN, S. I.; SCHAFFER, D.; ALBELDA, S. M.; KOVAL, M.; MUZYKANTOV, V. R. Size-dependent intracellular immunotargeting of therapeutic cargoes into endothelial cells . Blood, 2002, 99, 912–922.
- WROBEL, I.; COLLINS, D. Fusion of cationic liposomes with mammalian cells occurs after endocytosis. Biochimica et Biophysica Acta, v. 1235, p. 296-304, 1995.
- ZELPHATI, O.; NGUYEN, C.; FERRARI, M.; FELGNER, J.; TSAI AND, Y.; FELGNER, P. L. Stable and monodisperse lipoplex formulations for gene delivery. Gene Therapy, v. 5, 1272–1282, 1998.

---

## CAPÍTULO 3 – CORRELATION BETWEEN PHYSICOCHEMICAL AND STRUCTURAL PROPERTIES WITH *IN VITRO* TRANSFECTION OF pDNA/CATIONIC LIPOSOMES COMPLEXES

---

Tiago A. Balbino<sup>1</sup>, Antônio Gasperini<sup>2</sup>, Cristiano L. P. Oliveira<sup>3</sup>, Leide P. Cavalcati<sup>2</sup>, Adriano R. Azzoni<sup>1,3</sup>, Lucimara G. de La Torre<sup>1\*</sup>

<sup>1</sup>University of Campinas, Brazil;

<sup>2</sup>Synchrotron Light National Lab, Brazil;

<sup>3</sup>University of São Paulo, Brazil.

\*Corresponding author: [latorre@feq.unicamp.br](mailto:latorre@feq.unicamp.br)

Accepted for publication in *Langmuir*.

### Abstract

In this study, we characterized the conventional physicochemical properties of the complexes formed by pDNA (pDNA) and cationic liposomes (CL) composed of egg phosphatidylcholine (EPC), 1,2-dioleoyl-sn-glycero-3-phosphoethanolamine (DOPE) and 1,2-dioleoyl-3-trimethylammonium-propane (DOTAP) (50/25/25% molar ratio). We found that these properties are nearly unaffected at the studied ranges when the molar charge ratio ( $R_{+/-}$ ) between the positive charge from the CL and negative charge from pDNA is not close to the isoneutrality region ( $R_{+/-}=1$ ). However, the results from *in vitro* transfection of HeLa cells showed important differences when  $R_{+/-}$  is varied, indicating that the relationships between the physicochemical and biological characteristics were not completely elucidated. To obtain information regarding possible liposome structural modifications, small angle x-ray scattering (SAXS) experiments were performed as a function of  $R_{+/-}$  to obtain correlations between structural, physicochemical and transfection properties. The SAXS results revealed that pDNA/CL complexes can be described as being composed of single bilayers, double bilayers and multiple bilayers, depending on the  $R_{+/-}$  value. Interestingly, for  $R_{+/-}=9, 6$  and  $3$ , the system is composed of

single and double bilayers, and the fraction of the latter increases with the amount of DNA (or a decreasing  $R_{+/-}$ ) in the system. This information is used to explain the transfection differences observed at an  $R_{+/-}=9$  compared to  $R_{+/-}=3$  and 6. Close to the isoneutrality region ( $R_{+/-}=1.8$ ), there was an excess of pDNA, which induced the formation of a fraction of aggregates with multiple bilayers. These aggregates likely provide additional resistance against the release of pDNA during the transfection phenomenon, reflected as a decrease in the transfection level. In conclusion, the obtained results permitted proper correlation of the physicochemical and structural properties of pDNA/CL complexes with the *in vitro* transfection of HeLa cells by these complexes, contributing to a better understanding of the gene delivery process.

## 1. Introduction

Gene delivery is a promising strategy for the treatment of different diseases, including gene-related disorders, infectious diseases and cancer [1-3]. However, the success of gene delivery depends on the efficiency of the transfection process, which is based on the introduction of engineered DNA encoding a functional/therapeutic protein into the cell nucleus to modulate cellular functions and responses [4, 5]. However, because efficient delivery requires protection of DNA against nucleases and interstitial fluids, a wide variety of carriers are employed to efficiently deliver nucleic acids to target cells with high transfection efficiencies [6]. Viral gene delivery is an alternative method that promotes transfection at a high level. However, oncogenic effects are a major drawback of viral gene delivery [7, 8].

Another important strategy is the use of nonviral systems, such as cationic polymers or lipids. These systems present lower transfection efficiencies compared to viral carriers but are safer [9]. In the field of nonviral gene delivery systems, different factors may influence transfection efficiency, such as the nature and cytotoxicity of the carrier, DNA entrapment in carrier structures, the zeta potential of the structures, the culture conditions in the case of *in vitro* transfections, and the cell line employed [10, 11]. In addition to the factors that influence transfection efficiency, the particle size of the complexes is also relevant, as it has an important impact on the efficiency of cellular

uptake and the subsequent intracellular processing [12]. Among many nonviral carriers, the cationic liposomes (CLs) have long been investigated.

Liposomes are self-assembled phospholipid aggregates that mimic the cell membrane. The use of cationic lipids allows the formation of cationic liposomes that can form complexes with pDNA through electrostatic interactions. Since the first utilization of pDNA/CL complexes as nonviral vectors by Felgner and co-workers [13], many cationic liposomal formulations have been extensively applied in gene delivery studies, employing different lipid compositions [14-17]. The transfection process using CLs is simple and is tolerated by cells. Basically, the pDNA/CL complexes associate with the cell membrane, which allows DNA internalization and release into the cell cytoplasm [11].

Liposomes have been successfully applied in *in vitro* and *in vivo* gene delivery studies. A liposomal formulation was optimized for tumor-targeting delivery of an anticancer small-molecule and significantly improved the anticancer effect in human melanoma and prostate cancer cells [18]. *In vivo* experiments also showed the feasibility of using CL for delivering genes, resulting in the induction of effective immune responses [19, 20].

Despite the promising results regarding gene delivery using CLs, the physicochemical and structural characteristics of CLs and their relationship with biological results remain unclear. Several research groups have struggled in attempts to correlate the physicochemical properties observed in *in vitro* transfection experiments and structural properties, but the results obtained thus far do not completely elucidate the differences in transfection efficiency found *in vitro* and *in vivo* [21]. It has been reported that the structures of pDNA/CL complexes do not show any influence on transfection efficiency, suggesting that they are not correlated [22]. In contrast, Savva and co-workers [23] correlated the efficiency of the transfection of pDNA/CL complexes with their structural properties by means of membrane elasticity analyses.

A similar conclusion was obtained from fluorescence anisotropy results, which indicated that the fluidity of liposome and lipoplex membranes is also related to better transfection results [24]. This clear disagreement between the reported results is difficult to address, principally because the studied systems involved different lipid compositions,

DNA sequences and cell types, impairing the possibility of establishing a pattern or any general conclusion. One possible way to obtain important structural information about pDNA/CL complexation is through the use of the small angle x-ray scattering (SAXS) technique, which is a powerful tool for structural characterization of amphiphilic systems providing information on the electronic contrast of bilayers and several other structural parameters, such as membrane periodicity, size and fluidity. Despite all of the information that can be obtained from scattering experiments, only a few publications have reported the use of this technique to its full potential, particularly for drug delivery systems. In this work, we propose a modeling procedure that allowed DNA complexation to be described. As shown below, analysis of scattering data permitted the description of systems with different liposome membrane formulations, relating the cationic lipid content to the transfection results [15].

In previous work, we demonstrated the *in vivo* efficacy of CL composed of egg phosphatidylcholine (EPC), 1,2-dioleoyl-sn-glycero-3-phosphoethanolamine (DOPE) and 1,2-dioleoyl-3-trimethylammonium-propane (DOTAP) (50/25/25% molar) in dehydrated-hydrated vesicles (DRVs) for vaccination against tuberculosis [25, 26] and hepatitis B [27]. Using this lipid composition, in *in vivo* analyses of tuberculosis vaccination using a unique dose administered *via* the intranasal route, a 16-fold reduction was achieved in the amount of plasmid DNA employed [25, 26]. This formulation was also viable for producing multifunctional nanoparticles with different domains when associated with a synthetic peptide. This pseudo-ternary complex (peptide/pDNA/CL) presented therapeutic effects against tuberculosis [2]. In this work, the same lipid composition of DRVs was employed for tuberculosis vaccination, but with extruded cationic liposomes and the plasmid DNA vector pVAX-Luc encoding a luciferase reporter gene being used to produce pDNA/CL complexes. The electrostatic effects of complexation between CLs and pDNA on physicochemical and structural properties were evaluated in SAXS experiments, permitting correlation with the results of *in vitro* transfection of HeLa cells.

## 2. Materials and Methods

### 2.1. Materials

The plasmid pVAX1 encoding luciferase was used as a modified version of pVAX1-GFP, following the description of Toledo *et al.* [28]. Basically, the sequence encoding Luciferase protein was removed from the pGL3-Luc Control vector using the XbaI and EcoRI restriction endonucleases. A similar procedure was carried out to insert *LUC* in the vector pVAX1, replacing the *GFP* gene. Therefore, the vector used here has the same pVAX backbone, but luciferase is used as the reporter gene. This vector was designated pVAX-Luc. The performance of pVAX-Luc was assessed *via* transfection assays based on correct luciferase expression.

Egg phosphatidylcholine (EPC) (96% of purity), 1,2-dioleoyl-sn-glycero-3-phosphoethanolamine (DOPE) (99.8% of purity) and 1,2-dioleoyl-3-trimethylammonium-propane (DOTAP) (98% of purity) were purchased from Lipoid and used without further purification. Other materials were of analytical grade.

### 2.2. Plasmid DNA purification

PVAX-Luc was amplified *in Escherichia coli* bacteria and purified using the PureLink™ HiPure Plasmid DNA Purification Kit-Maxiprep K2100-07 (Invitrogen, Maryland, USA). The plasmid concentration and purity were determined spectrophotometrically at 260 nm (A<sub>260</sub>) using a Nanodrop UV spectrophotometer ND-1000 (PeqLab, Erlangen, Germany). An A<sub>260</sub> nm/A<sub>280</sub> nm ratio higher than 1.8 was used as the criterion for purity.

### 2.3. Preparation of pVAX-Luc/cationic liposome complexes (pDNA/CL)

pDNA/CL complexes were obtained as described previously by adding the appropriate amount of pDNA to CL under intense vortexing at 4°C for at least 40 s [26]. pDNA/CL complexes were prepared at different cationic lipid:DNA molar charge rates (R<sub>+/-</sub>) [29].

Cationic liposomes were prepared *via* the thin film method [30]. Briefly, a mixture of EPC, DOPE and DOTAP (50/25/25% molar) [26] was solubilized in chloroform, and

the solvent was subsequently removed in a rotary evaporator under a vacuum of 650 mmHg for 1 h. The dried lipid film was hydrated with PBS buffer to a final lipid concentration of 16 mM. The hydrated liposomes were extruded through double polycarbonate membranes (100 nm nominal diameter) 15 times under nitrogen (12 kgf/cm<sup>2</sup>).

## **2.4. Physicochemical Characterization**

### **2.4.1. Average Hydrodynamic Diameter and Polydispersity**

The average hydrodynamic diameter and size distribution were measured *via* the dynamic light scattering (DLS) technique using a Malvern Zetasizer Nano ZS with a backscattering configuration with detection at a scattering angle of 173° using a He/Ne laser emitting at 633 nm and a 4.0 mW power source. Each measurement was repeated in triplicate, and the obtained values were averaged to obtain the mean particle size weighted by number and volume.

The polydispersity index was calculated from cumulant analysis of the measured DLS intensity autocorrelation function. The polydispersity index varied from 0 to 1 (higher values indicate a less homogeneous nanoparticle size distribution). The mean diameter and polydispersity index of particle sizes were estimated *via* CONTIN algorithm analysis through inverse Laplace Transformation of the autocorrelation function.

### **2.4.2. Measurement of Zeta Potential**

The zeta potential ( $\zeta$ ) was measured by applying an electric field across the samples, and the value of the zeta potential was obtained by measuring the velocity of the electrophoretic mobility of the particles using the laser Doppler anemometry technique. The measurements were performed three times for each sample at 25°C using a Malvern Zetasizer 3000 in water.

### **2.4.3. Gel retardation assay for determining the molar charge ratio for complete DNA complexation with CL**

Agarose gel electrophoresis was used to determine the molar charge ratio for complete pDNA complexation with CL. pDNA/CL complexes at different cationic:anionic

molar charge ratios (R+/-) (containing 1 µg of pDNA) were run in 0.8% agarose gels in 40 mM TRIS-acetate buffer solution and 1 mM EDTA (TAE 1X) at 60 V for 3 h, followed by staining for 30 min in a 0.5 µg/mL ethidium bromide solution. The EtBr-stained DNA bands were then visualized and photographed using an ultraviolet image acquisition system.

#### **2.4.4. Morphology**

We employed transmission electron microscopy and the negative staining method to study the morphology of CL and pDNA/CL complexes. For this analysis, a LEO 906E electron microscopic (Zeiss, Germany) was used at 80 kV, together with a MEGA VIEW III /Olympus camera and ITEM E 23082007/ Olympus Soft Imaging Solutions GmbH software. Briefly, 5 µL of CL or pDNA/CL complexes was added to a carbon-coated grid for 5 min, and the excess liquid was then blotted, leaving a thin aqueous film on the grid. Negative staining was performed with a 2% solution of ammonium molybdate for 10 s, followed by blotting the samples dry.

#### **2.5. *In Vitro* Cytotoxicity**

We evaluated the *in vitro* cytotoxicity of the pDNA:CL complexes in HeLa cells employing the cell proliferation reagent WST-1 from Roche Molecular Biochemicals (Mannheim, Germany). The commercial transfection reagent Lipofectamine® and “naked” pVAX-LUC were used as reference. The cells were seeded into 96-well microplates in 100 µL of culture medium (7,000 cells per well), and after incubation for 48 h (37 °C, 5% CO<sub>2</sub>), the complexes were added. At the end of the treatment, 10 µL of the cell proliferation reagent WST-1 was added to each well. The cells were incubated under the prior conditions for 2 h. Absorption was measured with a scanning multiwell spectrophotometer following gentle agitation (1 min) (ELISA-Reader MRX, Dynex Technologies, Chantilly, USA) at detection wavelength of 440 nm, and a reference wavelength of 650 nm was used to subtract nonspecific signals.

Viable cells converted WST-1 to a yellow-orange water-soluble formazan dye that was detectable at 420 – 480 nm. The absorbance was directly correlated with the cell numbers present. The experiments were performed in hexaplicate. The percentage of

viable cells in comparison to the control (untreated cells) was calculated using the following equation: % viable cells =  $[(OD_{440}^{\text{treated}} - OD_{650}^{\text{treated}}) / (OD_{440}^{\text{control}} - OD_{650}^{\text{control}})] \times 100$ .

## 2.6. Culture and transfection of mammalian cells

The complexes were tested *in vitro* using the plasmid pVAX-Luc in human epithelial carcinoma cells (HeLa cells) according to Toledo *et al.* [28]. The cells were first cultured in 75 cm<sup>2</sup> flasks using the F-12 (Ham) nutrient mixture (Gibco, UK) containing 10% (v/v) fetal bovine serum (FBS) (Gibco, UK) and supplemented with non-essential amino acids (Gibco, UK), gentamicin (Gibco, UK), sodium pyruvate (Gibco, UK), and an antibiotic–antimycotic solution (Gibco, UK). The cultures were incubated in 5% CO<sub>2</sub> humidified environment at 37°C. The cells were trypsinized after reaching confluence and then seeded into 24-well culture plates (5×10<sup>4</sup> cells per well). Next, the cells were incubated for 48 h and transfected using the pDNA/CL complexes at different R<sub>+/-</sub> with statistically equals amounts of pVAX-LUC per well. Finally, the medium was replaced 6 h after transfection to remove plasmids that were not internalized by the cells. The commercial transfection reagent Lipofectamine® was used as a positive control following the manufacturer’s protocol, and naked plasmid DNA was employed as a negative control.

Subsequently, the medium was removed; the cells were washed using PBS and lysed; and luciferase activity was determined according to the Promega Luciferase Assay protocol. The Relative Light Units (RLUs) were measured with a chemiluminometer (Lumat LB9507, EG&G Berthold, Germany). The total protein was measured according to a BCA protein assay kit (Pierce), and the luciferase activity was expressed as RLU/mg protein.

## 2.7. Structural characterization of the pDNA/CL complexes using Synchrotron SAXS

Structural information, such as the bilayer electronic density profile (EDP) and bilayer-bilayer distance, was obtained via small angle x-ray scattering (SAXS) analysis. The SAXS experiments were performed at the SAXS1 beamline at the Brazilian

Synchrotron Light National Lab (LNLS) using a beam energy of 8 keV ( $\lambda=1.55 \text{ \AA}$ ) and sample-to-detector distance of 561 mm. The measured intensity is displayed as a function of the reciprocal space momentum transfer modulus  $q=4\pi \sin(\theta) / \lambda$ , where  $2\theta$  is the scattering angle, and  $\lambda$  is the radiation wavelength. The typical  $q$  range was from  $0.017 \text{ \AA}^{-1}$  to  $0.45 \text{ \AA}^{-1}$ .

The dispersion of the liposomes exhibits a liquid-crystalline character and can be considered as presenting a form factor,  $P(q)$ , related to the electronic density profile (EDP) across the lipid bilayer and a structure factor,  $S(q)$ , related to the periodicity of the lipid bilayer. Therefore, the scattering intensity  $I(q)$  can be expressed as follows:

$$I(q) = P(q)S(q) \quad (\text{Equation 1})$$

This procedure is known as the decoupling method and assumes that in the intensity formulation, the form factor and the structure factor can be treated separately. The model used for the form factor and the optimization method are described elsewhere [32, 33]. For the structure factor, a model based on the Modified Caillé Theory (MCT) was used, permitting a proper description of the structure factor for lamellar systems.

### 3. Results

#### 3.1. Physicochemical characterization of pDNA/CL complexes

pDNA/CL complexes were obtained at different molar charge ratios ( $R_{+/-}$ ) and their number-weighted mean diameter, polydispersity index and zeta potential profiles as a function of  $R_{+/-}$  are presented in Figure 1. Similar profiles can be observed for the number-weighted mean diameter and polydispersity index (Figures 1A and 1B, respectively). The greatest mean diameter was approximately 500 nm, and the highest polydispersity index was 0.5. These high values correspond to the isoneutrality region, where the  $R_{+/-}$  values are close to 1. With increasing  $R_{+/-}$  values (decreasing the proportion of DNA and increasing the lipid content), the mean diameter and polydispersity index decrease until the liposome properties are achieved (diameter of 100 nm and a polydispersity index of 0.1). The zeta potential profile has a sigmoidal shape, as expected based on previously reported results for other lipid complexes [15,

34, 35] (Figure 1 C). This trend shows three different zeta potential regions: (i) a region where the negative net charge of the complex is close to the plasmid DNA net charge ( $\zeta = -52.2 \pm 6.1$  mV); (ii) an isoneutrality region, where inversion of the zeta potential sign takes place (approx.  $R_{+/-} = 1$ ); and (iii) a region where the net charge of the complexes is positive, tending toward the value of empty liposomes ( $\zeta = +60.8 \pm 1.7$  mV).

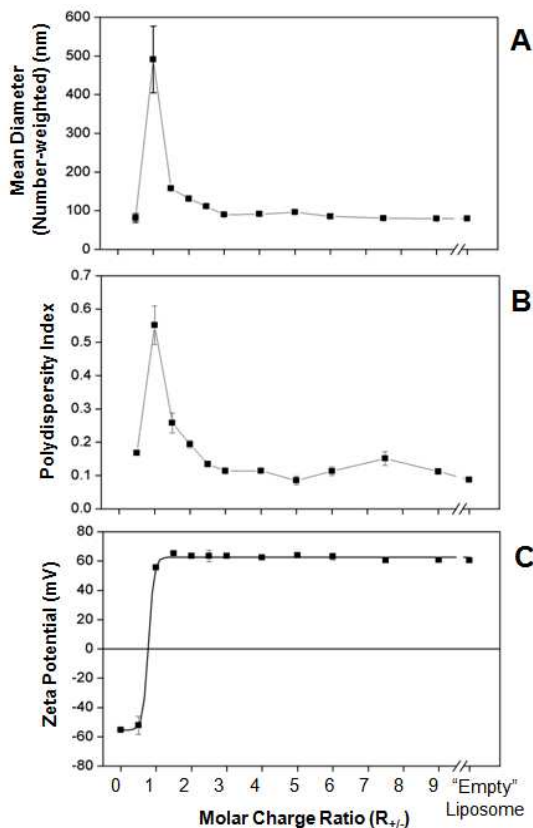


**Figure 1.** Number-weighted hydrodynamic mean diameter (A), polydispersity index (B) and zeta potential (C) profiles of pDNA/CL complexes at different molar charge ratios ( $R_{+/-}$ ). The solid lines are a visual guide to better demonstrate the trend of the variations. The error bars represent the standard error of independent triplicates.

From the profiles shown in Figure 1, four different  $R_{+/-}$  values (1.8, 3, 6 and 9) were selected for further investigation based on the number and volume-weighted size distributions (Figure 2). The selection of  $R_{+/-}$  values was based on pDNA/CL complexes with a positive zeta potential, which is the minimal condition for transfection experiments in the absence of any specific mechanism for transfection [36]. Both size distributions were investigated because the volume-weighted size is more sensitive to the presence of small fractions of a population with larger sizes. Additionally, the intensity of scattered

light is proportional to the diameter raised to the sixth power, and number-weighted mean diameter presents the distribution profile in terms of most numerous (relevant) population (the intensity of scattered light is proportional to the number of particles) [37].

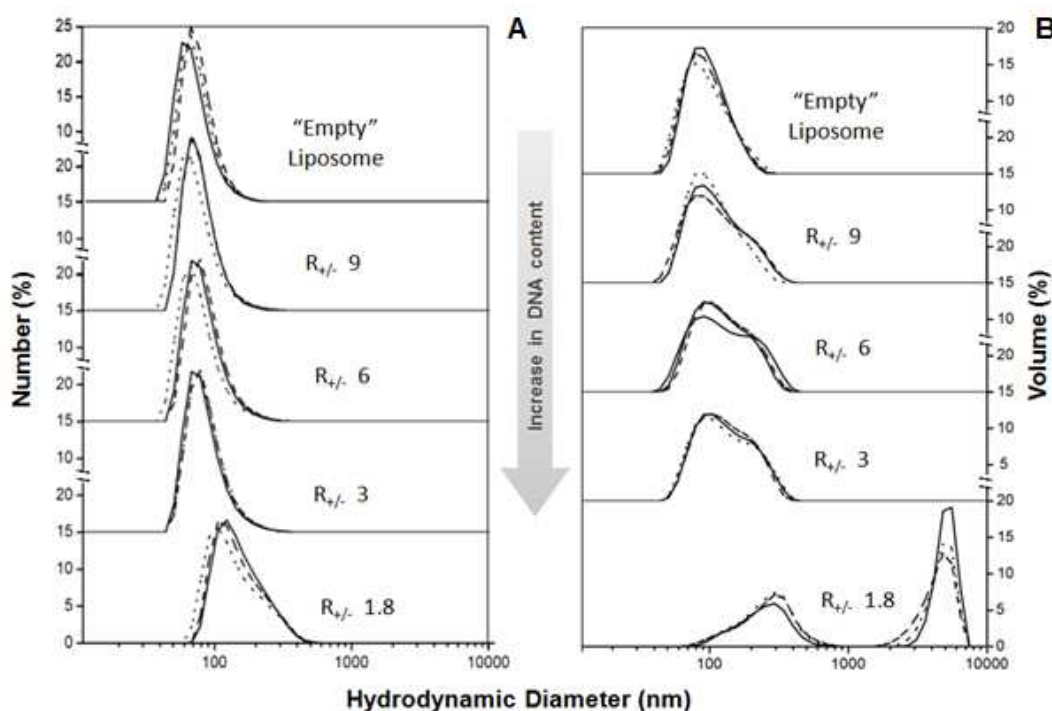


**Figure 2.** Number (A) and volume-weighted (B) size distribution of pDNA/CL complexes at  $R_{+/-}$  values of 1.8, 3, 6 and 9. “Empty” cationic liposomes are presented for comparison. The lines in each size distribution represent the profile of three independent pDNA/CL complexes.

The volume-weighted size distribution (Figure 2B) shows that with increasing amounts of DNA (decreasing  $R_{+/-}$ ), there is a slight increase in the width of the size distribution, and at  $R_{+/-}=1.8$ , a second population arises with a diameter of approx. 5  $\mu\text{m}$ . However, when the number-weighted size distribution is analyzed (Figure 2A), only one population is found at  $R_{+/-}=1.8$  (being the most abundant). These nuances in the size range may suggest structural changes induced by the proportion of DNA in cationic liposomes and the presence of groups with different structural organizations.

The ability of cationic liposomes to incorporate pDNA into their structure was evaluated *via* a gel retardation assay at different  $R_{+/-}$  values (Figure 3). Free pDNA migrates out of the well towards the positive pole, giving rise to two bands: the high-mobility band represents the most compact (super-coiled) form, while the less-intense

band is considered to represent the non-super-coiled form. The pDNA/CL molar charge ratio ( $R_{+/-}$ ) that results in complete retention of the DNA in the lipid structure is 1.5 (Figure 3).

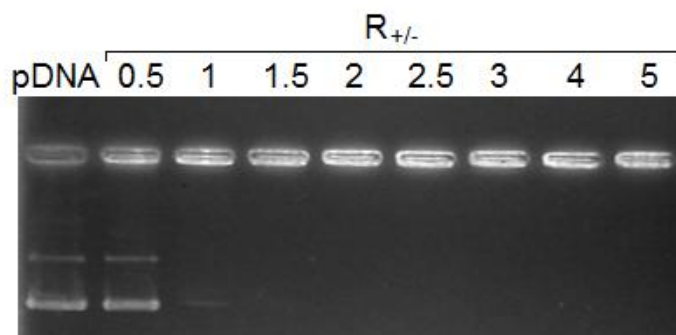


**Figure 3.** Gel retardation assay. One microgram of pDNA was complexed with CL at different positive/negative molar charge ratios ( $R_{+/-}$ ) in PBS.

The morphology of “empty” CL and pDNA/CL complexes at  $R_{+/-}=3$  were evaluated by transmission electron microscopy (TEM) using a negative staining technique (Figure 4). The “empty” CL (Figure 4A and B) has a rather spherical shape with a diameter of ~130 nm (Figure 4B). Isolated liposomes can be observed without evidence of aggregation and/or fusion. As summarized in Figure 4 C and D, aggregates are observed in the presence of DNA. Due to this phenomenon, the pDNA/CL complexes (Figure 4C and D) exhibit polymorphic characteristics and a different volume-weighted size distribution (Figure 2B) when compared to empty liposomes (Figure 4A and B). It is also possible to identify some deformation in the spheroidal shape of the complexes and aggregation of vesicles.

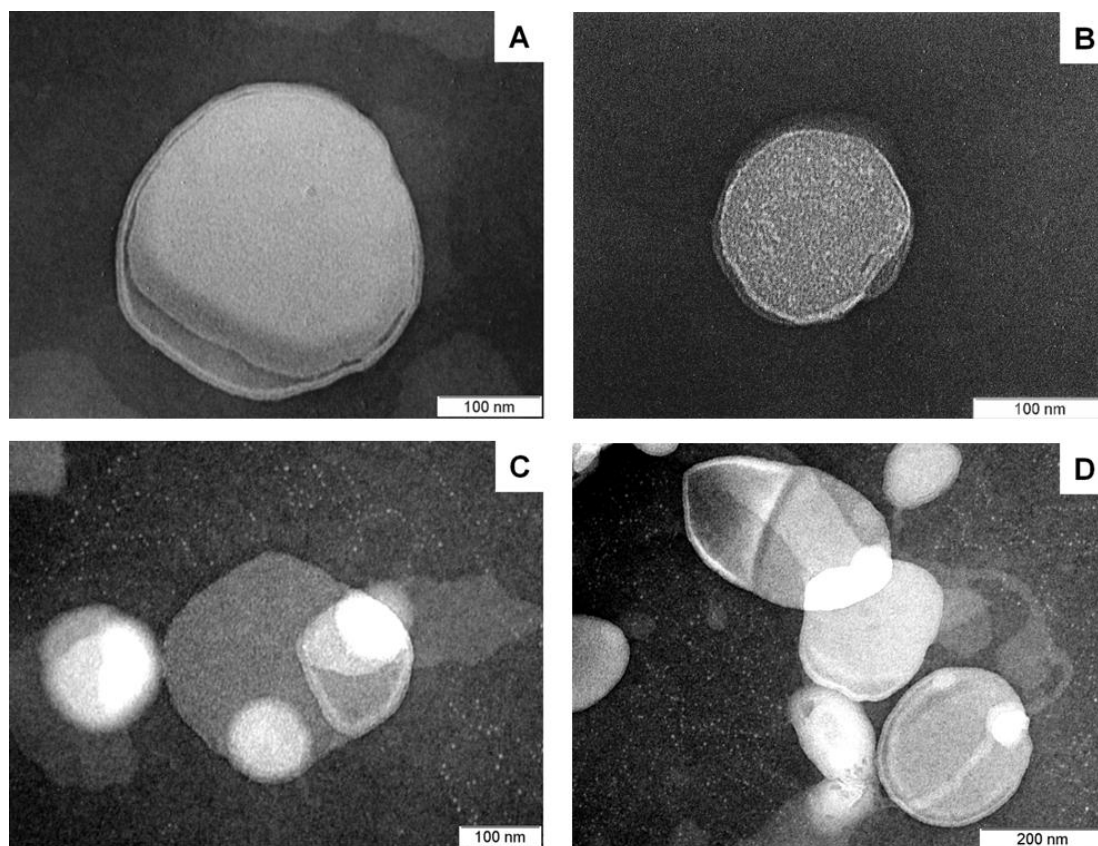


**Figure 4.** Negative staining electron micrographs of “empty” cationic liposomes (CL) (A and B) and pDNA/CL complexes at a molar charge ratio of  $R_{+/-}=3$  (C and D). Scale bars indicate 100 nm in (A, B and C) and 200 nm in (D).

### 3.2. *In vitro* transfection of HeLa cells

The ability of EPC/DOPE/DOTAP liposomes complexed with DNA to transfect HeLa cells *in vitro* was examined based on the previous physicochemical characterization (Figure 5). It can be observed that when  $R_{+/-}$  decreases from 10.2 to 3, there is an increase in luciferase activity, indicating an increase in the transfection level. However, the transfection level decreases at an  $R_{+/-}$  value of 1.8. In this context,  $R_{+/-}=3 - 6$  is the best range for *in vitro* transfection of HeLa cell using the lipids EPC/DOTAP/DOPE (50:25:25% molar ratio).

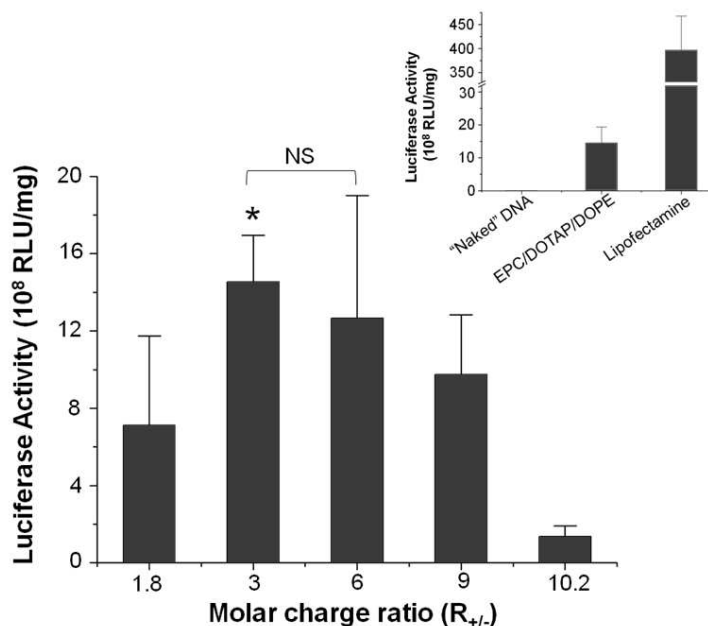


**Figure 5.** *In vitro* efficacy of HeLa cell transfection using pDNA/CL complexes at different molar charge ratios (R<sub>+/-</sub>); the plasmid pVAXLUC contains a luciferase reporter gene under the control of the CMV promoter. Luciferase activity was expressed in RLU/mg protein. “Naked” pDNA and Lipofectamine (negative and positive controls) are shown in the inset graph. The error bars represent the standard error of triplicates. \*  $p < 0.05$  was considered statistically different compared to other samples, except at R<sub>+/-</sub>=6. NS, not significant.

We used the commercial transfection reagent Lipofectamine® as a positive control and naked plasmid DNA as a negative control. Figure 5 (inset graph) shows that when naked DNA was used, there was no (or very low) transfection. When the positive control (Lipofectamine®) was used, higher transfection levels were achieved compared to those obtained with pDNA/LC at R<sub>+/-</sub>=3.

### 3.3. *In vitro* cytotoxicity

To determine whether the CL comprised of the investigated lipids have an effect on HeLa cell death, we assessed cell viability after treatment with pDNA/CL complexes, the commercial transfection reagent Lipofectamine® and “naked” pDNA (Figure 6). Free pVAX-LUC did not show any effects on cell viability. Similar results were found for the pDNA/CL complexes at all of the examined molar charge ratios (R<sub>+/-</sub>). However, the Lipofectamine transfection reagent significantly decreased cell viability by approx. 30%, indicating a higher cytotoxicity level.

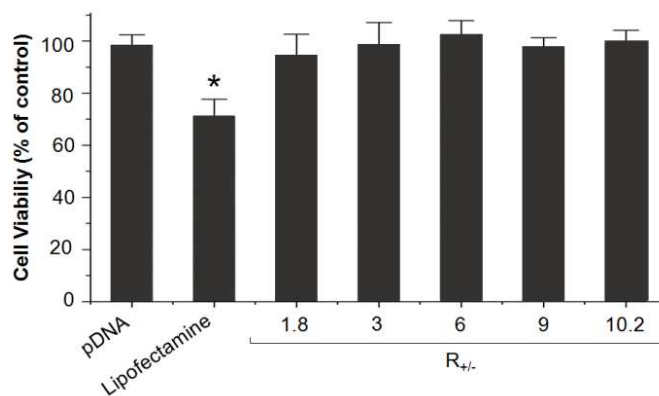


**Figure 6.** Cell viability assay of pDNA/CL complexes in HeLa cells. Lipofectamine and pDNA were used as controls. Data are presented as the mean  $\pm$  SD of six experiments. \*  $p < 0.05$  was considered statistically different.

### 3.4. Structural characterization of the pDNA/CL complexes using Synchrotron SAXS

The small angle x-ray scattering intensities of four molar charge ratios ( $R_{+/-}=1.8, 3, 6$  and  $9$ ), previously studied in *in vitro* transfections, were measured for comparison with the reference “empty” liposome. Figure 8 shows the scattering curves for all 5 systems. The “empty liposome” presents a typical scattering profile for a unilamellar vesicle system. It can be observed that the scattering curves for all of the pDNA/CL complexes show correlation peaks, which we will later associate with a fraction of the system exhibiting multilamellar order. As the molar charge ratio ( $R_{+/-}$ ) decreases (increased pDNA amounts), the correlation peaks become more pronounced, showing the great contribution of the structure factor for large amounts of DNA into the system.

The scattering vector range achieved in our SAXS experiment is able to provide reasonable information about the membrane bilayer and long range ordering. This information can be obtained from a proper modeling of the scattering data using two terms: (1) the form factor, which carries information about the shape of the bilayer and its electronic contrast, and (2) the structure factor, which provides information about system periodicity, membrane rigidity, fluctuation and the average number of correlated layers. We described the form factor as a sum of equally spaced Gaussian functions, which simulates the electronic density profile (EDP) across the lipid bilayer, and we used the Modified Caillé structure factor to simulate bilayer stacking [32, 33].

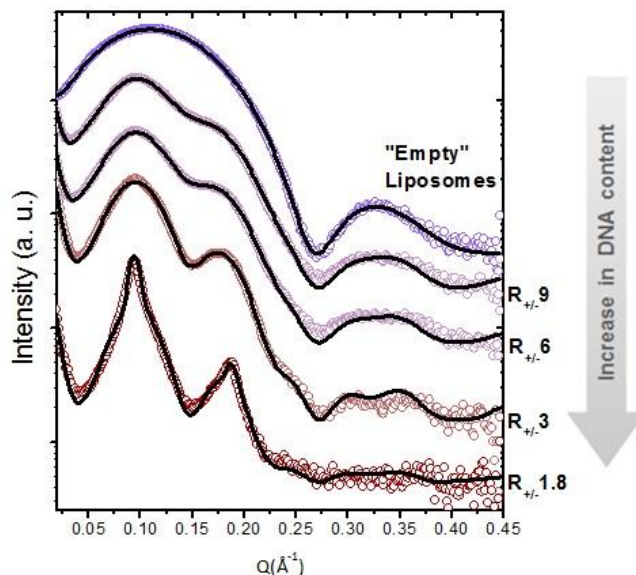


**Figure 7.** Small angle x-ray scattering intensity for “empty” liposomes and pDNA/CL complexes at four different molar charge ratios ( $R_{+/-}$ ) with the respective fitting curves.

We proposed two different models to fit the scattered intensity. As a first attempt, the scattering curves were fitted using a single form factor for each of four different molar charge ratio ( $R_{+/-}$ ) systems. Additionally, it was assumed that the system can be composed of two phases: a fraction of unilamellar vesicles and a fraction of multilamellar vesicles. In this approach, the scattered intensity  $I(q)$  is written as

$$I(q) = P(q)S_{eff}(q) \quad (\text{Equation 2})$$

where  $S_{eff}(q) = f_{sb} + f_m S_{MCT}(q)$ , in which  $f_{sb}$  is a constant related to the fraction of single bilayers;  $f_m$  gives the relative fraction of multilayers; and  $S_{MCT}(q)$  is the Modified Caillé structure factor. This model fits the data reasonably well for  $R_{+/-} = 9, 6$  and  $3$  but gives a poor fit for the  $R_{+/-} = 1.8$  scattering curve (data not shown). An interesting result from this first step was that the average number of correlated bilayers,  $N$ , was always  $\sim 2$  when  $R_{+/-}$  was  $9, 6$  or  $3$ . This finding strongly indicates the formation of double bilayers (rather than triple or other multiples), which may suggest the existence of domains such as juxtaposed neighbor unilamellar liposomes. These domains were previously observed using electron microscopy [38, 39], where it was found that juxtaposed double bilayers could even exist in large aggregates composed of several liposomes. Another interesting result was that the convergence of the fitting was only achieved after allowing superposition between the last Gaussian function of the bilayer EDP in the double

bilayer phase model. Although on first glance, this superposition may oddly suggest an overlap of head groups, it can actually represent the average electronic density of the DNA inserted between consecutive bilayers.

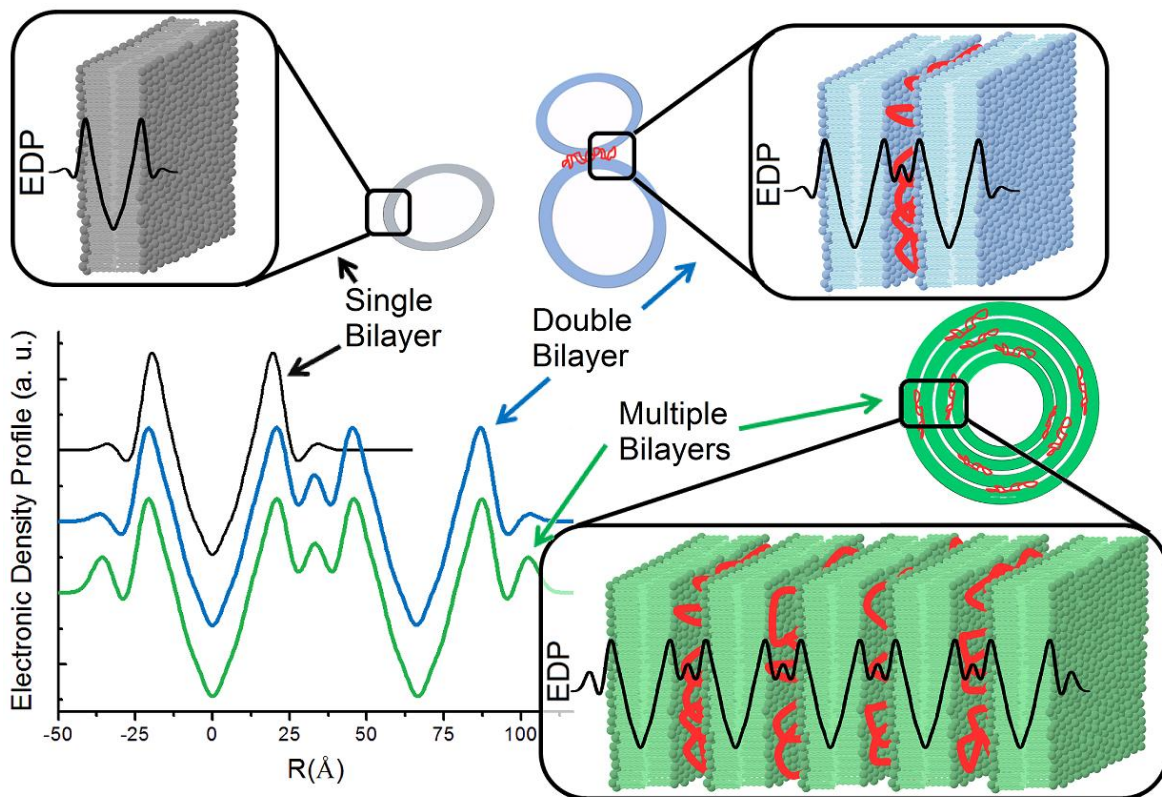
The main limitation of this first approach was the use of a single bilayer profile to describe the system. Therefore, a more sophisticated model was proposed enabling the use of multiple bilayer sizes and shapes. In this new approach, the system is composed of two phases: (1) a single bilayer and (2) a double bilayer bounded by DNA between two consecutive bilayers. In this model, we fit all of the curves presented in Figure 8 simultaneously. This model enabled better fitting of the scattering data because it allows differences among the electron density profiles for a single bilayer and a double bilayer (where the DNA is inserted). As will be discussed below, several assumptions were made to decrease the number of fitting parameters. This model was supported by the results of the complementary techniques that we used previously: (1) the Zeta potential assured that there would be no DNA on the external surface of the liposome, as shown in Figure 1C; (2) the gel retardation assay ensured that we would not observe free DNA on the water, as seen in Figure 3; (3) the TEM images suggested the existence of agglomerates such as juxtaposed liposomes with a double bilayer at the interface; and (4) the DLS results demonstrated a slight distortion of the volume-weighted size distribution, suggesting larger aggregates associated with increases in DNA, as seen in Figure 2B. Moreover, the TEM images shown in the works of Huebner *et al.*, [38] and Angelov *et al.* [40] indicate that the pDNA/CL lipoplexes are composed mainly of single and double bilayers, despite the fact that multibilayers can still be found.

Figure 8 shows that the  $R_{+/-}=1.8$  scattering curve presents sharp correlation peaks, characteristic of a periodic structure, in addition to the scattering from double and single bilayer phases. Therefore, a new phase composed of several bilayers was added to the model. This effect could be a contribution of aggregates formed by liposomes that might have been fragmented and stacked, as proposed by Barrileiro *et al.*, [41, 42] and Hueber *et al.* [38].

The scattered intensity using this model was given as follows:

$$I(q) = N_{SC} \{ f_s P_s(q) + f_d P_d(q) S_d(q) + f_m P_m(q) S_m(q) \} \quad (\text{Equation 3})$$

where the subscripts  $s$ ,  $d$  and  $m$  indicate the single, double and multiple bilayer phases, respectively;  $f$  represents the relative phase fraction of each system ( $f_m$  is zero for  $R_{+/-}=9$ , 6 and 3);  $P(q)$  is the form factor;  $S(q)$  is the Modified Caillé structure factor; and  $N_{sc}$  is an overall scaling constant. To decrease the number of fit parameters and permit convergence of the fitting procedure, a number of assumptions were made: The form factor for the double and multiple bilayers were considered to be the same ( $P_d(q)=P_m(q)$ ), but they could be different from the single bilayer form factor. As suggested by the first model step, the changes in the form factor were obtained through the inclusion of an extra Gaussian function between consecutive bilayers to represent the DNA electronic density. This change was sufficient to represent both the double bilayer and the multiple bilayer phases. The electronic density profile obtained for the three phases is shown in Figure 8.



**Figure 8.** Electronic density profile across the lipid membrane for three different phases resulting from modeling and fitting of SAXS data.

Certain parameters related to the Structure factor also had to be fixed to permit model convergence after studying the influence of each parameter in the scattering intensity. The Caillé parameter, for example, had a small influence on the scattering intensities for the double bilayer phase and was fixed at zero. It was possible to observe that when this parameter is greater than 0.05, the peak in the simulated curve for all  $R_{+/-}$  values located at  $Q \sim 0.37 \text{ \AA}^{-1}$  disappears, which indicates that this parameter should be lower than that value. For the multiple bilayer phase, there is greater precision in the determination of the Caillé parameter. The value obtained was  $0.08 \pm 0.02$ , indicating a decrease in membrane rigidity in comparison with the double bilayer, which is probably induced by the fragmentation and stacking of bilayers above a critical concentration of pDNA. In all cases, the periodicity, which is the size of bilayer plus water layer between two consecutive bilayers, was close to  $66 \text{ \AA}$ . The number of bilayers,  $N$ , was let as a free parameter only in the multiple bilayer phase, when it was found to be around  $N=5.2$ . The fitting parameters are shown in Table 1.

**Table 1.** Parameters obtained from simultaneous fitting of all scattering curves.

Parameters	Phases		
	single bilayer	double bilayer	multiple bilayer
fraction of $R_{+/-}$ 1.8	$0.28 \pm 0.05$	$0.51 \pm 0.05$	$0.20 \pm 0.02$
fraction of $R_{+/-}$ 3	$0.69 \pm 0.04$	$0.31 \pm 0.04$	na**
fraction of $R_{+/-}$ 6	$0.87 \pm 0.01$	$0.13 \pm 0.01$	na**
fraction of $R_{+/-}$ 9	$0.92 \pm 0.01$	$0.08 \pm 0.01$	na**
Number of bilayers (N)	1*	2*	$5.2 \pm 0.5$
Caillé parameter ( $\eta$ )	na**	$< 0.05$	$0.08 \pm 0.02$
Periodicity (D, in $\text{\AA}$ )	na**	$66.2 \pm 0.2$	$66.6 \pm 0.2$

\*fixed parameter; \*\*not applied.

Summarizing the results from the SAXS experiments, we found three independent phases: the single, double and multiple bilayer phases. These phases can be understood to correspond to empty unilamellar liposomes, juxtaposed neighbor liposomes bounded by a pDNA layer and large aggregates formed by stacked bilayers, also bounded by pDNA layers.

The  $f_s$ ,  $f_b$  and  $f_m$  fractions were obtained from the model results. The form factor of each phase is normalized to 1 and the fractions satisfy the constraint  $f_s + f_b + f_m = 1$ .

Although there are several other procedures for normalization and fraction estimation, this procedure at least provides the relative trend of each contribution. The results, as shown in Figure 9, are an indication of the evolution of the phases, suggesting an increase in the double bilayer phase as a function of pDNA complexation. We also observe a saturation point between the molar ratios  $1.8 < R_{+/-} < 3$ , where the aggregates with multiple bilayers start to appear.

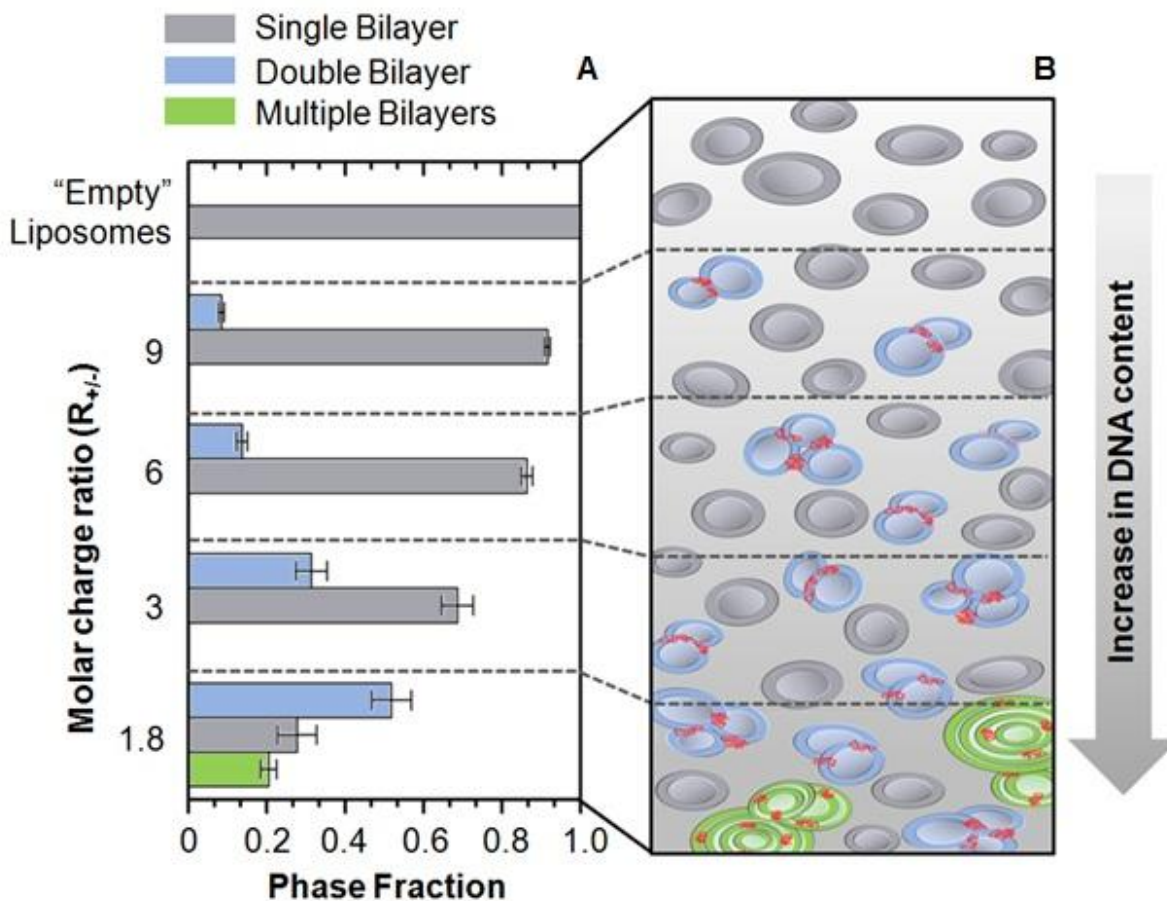


**Figure 9.** Phase partitioning for all of the studied systems. The largest amount of pDNA added to the system generates a ternary phase system with single, double and multiple bilayers.

#### 4. Discussion

Cationic liposomes composed of EPC/DOTAP/DOPE were initially studied as dehydrated-rehydrated vesicles (DRVs) for conventional encapsulation of pRc/CMV HBS DNA (encoding the small region of the hepatitis B surface antigen) [27]. Later, the viability of EPC/DOTAP/DOPE-DRVs surface complexed with DNAhsp65 for the

administration of a single dose tuberculosis vaccine [25, 26], and tuberculosis treatment [2] was demonstrated *in vivo*. Different researchers have evaluated the use of cationic liposomes containing the same lipid composition focusing on different production methods [43] and on *in vitro* cell viability [44].

Considering the previous successful *in vivo* studies, the current work was focused on the *in vitro* evaluation of EPC/DOTAP/DOPE liposomes with the same lipid composition studied earlier. Because DRV structures present a complex size distribution [25, 26], the behavior of these liposomes was investigated at a controlled size to obtain a proper understanding of the pDNA/CL association. The conventional protocol based on the hydration of dried film method followed by extrusion was employed. Using this procedure, it was possible to produce CLs with a diameter of 100 nm, polydispersity index of 0.1 and zeta potential of 60 mV (Figure 1). The plasmid DNA model used, pVAX-Luc, encode a luciferase reporter gene, enabling easy assessment of transfection efficiency.

The initial step in the investigation of the pDNA/CL complexes focused on conventional physicochemical characterization, aimed at identification of the proper conditions for *in vitro* transfection analyses. Here, the mean hydrodynamic diameter (number-weighted), polydispersity index (Pdl) and zeta potential profiles were evaluated as a function of the cationic/anionic molar charge ratio between cationic lipids and DNA ( $R_{+/-}$ ). It was observed that  $R_{+/-}$  values higher than 1.5 represent the ideal range for the investigation of *in vitro* transfection, as the mean diameter and Pdl are less than 200 nm and 0.25, respectively, and the zeta potential assumes positive values (Figure 1). At  $R_{+/-}$  =3 or higher, the average diameter and Pdl tend to stabilize near the values of “empty” CL (Figures 1A and B). The gel retardation assay confirmed the physicochemical characterization, showing that at  $R_{+/-}$  values higher than 1.5, all of the pDNA is retained (Figure 3) as a consequence of DNA condensation into the lipid structure. These results are in good agreement with those of previous studies involving DNAhsp65/DOTAP/DOPE liposomes [25].

Based on the physicochemical characterization, we strategically selected some pDNA/CL complexes at  $R_{+/-}$  values ranging from 1.8 to 10.2 to evaluate variations in the size distribution (Figure 2) and the level of transfection (Figure 5) and to study liposome

structural modification as a function of  $R_{+/-}$  (Figure 7), with the aim of determining the correlation between these properties.

In the *in vitro* studies, we observed a significant influence of  $R_{+/-}$  on the transfection level (Figure 5). An  $R_{+/-}$  value of 10.2 was associated with the lowest transfection level; when  $R_{+/-}$  was 3 or 6, the transfection levels were statistically equal, and these values represented the best conditions for achieving higher luciferase expression (Figure 5), confirming that  $R_{+/-}$  is an important parameter to be considered in the development of pDNA/CL complexes. These results are in agreement with those of other published studies. Candiani and co-workers [45] found that maximum transfection levels were achieved at a molar charge ratio of 5, and the transfection levels decreased when  $R_{+/-}$  was decreased until reaching 1.25 and increased until  $R_{+/-}$  reached 15. The lipid composition investigated by Candiani *et al.* [45] (DOPC/DOPE with different surfactants) was also shown to be more susceptible to size and polydispersity variations in the presence of pDNA compared to our lipid composition. Similar trends were observed by Masotti and co-workers [46], who investigated several commercially available transfection agents at various  $R_{+/-}$  values.

To understand the variation in the transfection results as a function of different  $R_{+/-}$  values, our initial approach was comparison of the physicochemical properties of these complexes. All of the tested pDNA/CL complexes exhibited a positive zeta potential (Figure 1A), and all of the pDNA was incorporated into the lipid structure (Figure 3). When we examined the number and volume-weighted size distribution (Figure 2) and Pdl, it was found that  $R_{+/-}$  values ranging from 3 to 9 resulted in similar profiles. Differences can be observed at  $R_{+/-}=1.8$ , which is a pDNA/CL ratio close to the isoneutrality region. However,  $R_{+/-}=10.2$  was associated with a controllable diameter, Pdl and zeta potential close to the values for “empty” liposomes (Figure 1). Considering only the physicochemical results, we concluded that there was not sufficient information to elucidate the influence of the pDNA/CL complexes on *in vitro* HeLa cell transfection.

The cationic liposomes examined in the present study were composed of three different lipids. Most of the reported studies have used cationic liposomes composed of only two lipids: one with cationic characteristics (e.g., DC-Chol, DOTMA or DOTAP) and another with neutral characteristics (e.g., DOPE or DOPC). Stegmann & Legendre [47],

who employed lipid compositions of DOTAP/DOPE and DOTMA/DOPE, and Congiu and co-workers [22], who employed the lipid composition DC-Chol/DOPE, reported no correlations between the obtained transfection results and physicochemical properties such as size, zeta potential and lipid mixing. Another study examining the lipid compositions DOTAP/DOPE and DOTAP/DOPC reported an influence of lamellarity and the pDNA/CL preparation method on transfection efficiency [48].

Thus, the presence of the third EPC in the present work reflects a difference compared to previously reported studies. To improve our understanding of the pDNA/CL complexes, we carried out SAXS experiments to examine the structural properties of the complexes (Figure 7). For the selected  $R_{+/-}$  values, ranging from 1.8 to 9, we observed that complexation with DNA contributes to increasing the number of double bilayers in the system, as if the pDNA plays the role of an electrostatic adhesive between two unilamellar neighbor liposomes, which corroborates the TEM image analysis (Figure 4), providing further evidence supporting the formation of aggregates of juxtaposed unilamellar liposomes. If more than two vesicles are juxtaposed, the final volume of the aggregate will be very large, but the number of correlated bilayers,  $N$ , is still approximately 2 because of the double bilayer in the interface between neighboring vesicles. According to the results presented herein, double bilayers appear to provide the ideal structure for DNA storage for later efficient transfection.

Close to the isoneutrality region, at  $R_{+/-} \sim 1.8$ , it was determined that a considerable fraction of the system had an average of 5 bilayer domains. These domains, together with the liposome stacking promoted by the pDNA, significantly increase the size of the aggregates, as confirmed by DLS measurements weighted by volume (Figure 2).

This event was also confirmed by TEM images (Figure 4) showing a significant change in the morphology of the complex compared to liposomes without pDNA. Huebner *et al.* [38] employed the lipid composition DMPC/DC-Chol and reported morphological changes in the liposomes in contact with DNA. They also observed the formation of clusters of DNA-coated unilamellar vesicles and flattening of the bilayers at the contact regions of adjacent vesicles, forming particle aggregates.

This rapid structural change close to the isoneutrality region is supported by the ability of the lipid EPC to maintain the liposomal structure in the presence of pDNA, as we did not observe an inverse hexagonal phase ( $H_{II}^C$ ) at any of the studied  $R_{+/-}$  values. This behavior is a consequence of the presence of EPC at a 50% molar ratio in the liposome composition [49]. Additionally, the complexation process was carried out under a controlled temperature (ice bath), which decreases the velocity of the electrostatic reaction, allowing the formation of more organized structures [50, 51]. Close to the isoneutrality region, an excess of pDNA may induce saturation of the vesicles regarding retaining pDNA in their bilayers, generating new structures showing greater numbers of bilayers and fusion of aggregates of particles, which does not appear to be efficient for later release processes or transfection.

Considering the characteristics presented above, the pDNA/CL complexes present two different types of structural configuration, dependent on  $R_{+/-}$ . The first type presents only controllable structures with double bilayers, which are increased with increases in the amount of DNA (or decreasing values of  $R_{+/-}$ ). This finding explains the transfection differences observed for  $R_{+/-}=9$  compared with  $R_{+/-}=3$  or 6. All of the wells were transfected with amounts of pDNA per well that were statistically equal, which means that different amount of lipids were used. Taking previous findings into account, the electrostatic complexation between pDNA and CL was controlled, and the difference between these complexes is the proportion of double bilayers formed based on the presence of pDNA and the lipid content, which can be related to the number of vesicles. This suggests that in the case of  $R_{+/-}=10.2$ , there will be an excess of “empty” liposomes, which will compete with the pDNA/CL complexes for cell internalization, resulting in a lower level of transfection (Figure 5). When  $R_{+/-}$  is decreased from 9 to 3, the proportion of bilayers is increased, and the number of “empty” liposomes is decreased (lower competition for cell incorporation). In this case, the transfection level is increased with decreases in  $R_{+/-}$ , reaching a maximum level at  $R_{+/-}=3$  (Figure 5). When  $R_{+/-}$  is 1.8, there is an excess of DNA, allowing the formation of aggregates with multiple bilayers. The elevated number of bilayers probably provides additional resistance to the release of pDNA inside the cells and adds to the effect of the increase in the size of the complex,

explaining the decrease in the transfection level. Figure 9B is a schematic diagram demonstrating the relationship between  $R_{+/-}$  and the described complexation process.

Additionally, comparison of this lipid composition with Lipofectamine and “naked” pDNA regarding the transfection of HeLa cells confirmed the viability of these lipids for gene delivery applications (Figure 6). Despite presenting a better transfection efficiency compared to other cationic lipids, Lipofectamine is much more cytotoxic. It is well-known that the cell death induced by cationic lipids is mainly caused through apoptosis [52], and multivalent cationic lipids (i.e., DOSPA, present in lipofectamine) are more toxic than monovalent cationic lipids (i.e., DOTAP) [53]. The ~30% decrease in cell viability shows the non-feasibility of using this commercial transfection reagent for *in vivo* applications. Reza *et al.* [54] also reported a reduction of 30% in cell viability induced by lipofectamine in Chinese hamster ovary cells. Furthermore, de la Torre *et al.* [25] showed that by using EPC in the liposomal composition, the cytotoxicity to the J744 macrophage cell line was significantly decreased, which also supports the potential applications of this formulation.

## 5. Conclusions

In conclusion, in this study, it was possible to verify that different molar charge ratios had a significant impact on the numbers of lamellae and, consequently, on the structural conformation of the complexes. These structural changes in the pDNA/CL complexes resulted in different transfection levels. Despite this relationship, at  $R_{+/-}$  values from 1.5 up to 9, the physicochemical properties of the complexes were nearly unaffected in terms of the number-weighted particle size, polydispersity and zeta potential. However, as the present SAXS analyses showed structural changes in the complexes at  $R_{+/-}=1.8$ , we could investigate these changes by screening the DLS measurements weighted by volume. We believe that the results presented here contribute to the understanding and correlation of the physicochemical and structural properties of pDNA/cationic liposome complexes with the associated transfection phenomenon, aimed at rational design of future nonviral gene vectors.

## 6. Acknowledgements

The authors gratefully acknowledge the financial support of the Fundação de Amparo à Pesquisa do Estado de São Paulo – FAPESP (São Paulo, Brazil) and the Universidade Estadual de Campinas (Campinas, Brazil). The SAXS experiments were performed at the Laboratório Nacional de Luz Síncrotron (LNLS) and the TEM analyses were performed at Instituto Butantan (São Paulo, Brazil).

## 7. References

1. Jeong, J.H., S.W. Kim, and T.G. Park, *Molecular design of functional polymers for gene therapy*. Progress in Polymer Science, 2007. 32(11): p. 1239-1274.
2. Rosada, R.S., *et al.*, *Effectiveness, against tuberculosis, of pseudo-ternary complexes: Peptide-DNA-cationic liposome*. Journal of Colloid and Interface Science, 2012. 373: p. 102-109.
3. Torchilin, V.P., *Recent advances with liposomes as pharmaceutical carriers*. Nature Reviews Drug Discovery, 2005. 4(2): p. 145-160.
4. Kim, T.-i. and S.W. Kim, *Bioreducible polymers for gene delivery*. Reactive & Functional Polymers, 2011. 71(3): p. 344-349.
5. Corsi, K., *et al.*, *Mesenchymal stem cells, MG63 and HEK293 transfection using chitosan-DNA nanoparticles*. Biomaterials, 2003. 24(7): p. 1255-1264.
6. Lasic, D.D., *Liposomes : from physics to applications*. 1993, Amsterdam; New York: Elsevier.
7. Balmayor, E.R., H.S. Azevedo, and R.L. Reis, *Controlled Delivery Systems: From Pharmaceuticals to Cells and Genes*. Pharmaceutical Research, 2011. 28(6): p. 1241-1258.
8. Rogers, M.-L. and R.A. Rush, *Non-viral gene therapy for neurological diseases, with an emphasis on targeted gene delivery*. Journal of Controlled Release, 2012. 157(2): p. 183-189.
9. Shan, Y., *et al.*, *Gene delivery using dendrimer-entrapped gold nanoparticles as nonviral vectors*. Biomaterials, 2012. 33(10): p. 3025-3035.
10. Ma, B., *et al.*, *Lipoplex morphologies and their influences on transfection efficiency in gene delivery*. Journal of Controlled Release, 2007. 123(3): p. 184-194.
11. Nikcevic, G., N. Kovacevic-Grujicic, and M. Stevanovic, *Improved transfection efficiency of cultured human cells*. Cell Biology International, 2003. 27(9): p. 735-737.
12. Rejman, J., *et al.*, *Size-dependent internalization of particles via the pathways of clathrin- and caveolae-mediated endocytosis*. Biochemical Journal, 2004. 377: p. 159-169.

13. Felgner, J.H., *et al.*, *ENHANCED GENE DELIVERY AND MECHANISM STUDIES WITH A NOVEL SERIES OF CATIONIC LIPID FORMULATIONS*. *Journal of Biological Chemistry*, 1994. 269(4): p. 2550-2561.
14. Farkas, N., *et al.*, *Combined scanning probe and light scattering characterization of multi-stage self-assembly of targeted liposome-based delivery systems*. *Measurement Science & Technology*, 2011. 22(2).
15. Munoz-Ubeda, M., *et al.*, *Gene vectors based on DOEPC/DOPE mixed cationic liposomes: a physicochemical study*. *Soft Matter*, 2011. 7(13): p. 5991-6004.
16. Penacho, N., *et al.*, *Physicochemical properties of transferrin-associated lipopolyplexes and their role in biological activity*. *Colloids and Surfaces B-Biointerfaces*, 2010. 76(1): p. 207-214.
17. Shim, G., *et al.*, *Trilysinoyl oleylamide-based cationic liposomes for systemic co-delivery of siRNA and an anticancer drug*. *Journal of Controlled Release*, 2011. 155(1): p. 60-66.
18. Hwang, S.H., *et al.*, *Tumor-targeting nanodelivery enhances the anticancer activity of a novel quinazolinone analogue*. *Molecular Cancer Therapeutics*, 2008. 7(3): p. 559-568.
19. Karkada, M., *et al.*, *A liposome-based platform, VacciMax (R), and its modified water-free platform DepoVax (TM) enhance efficacy of in vivo nucleic acid delivery*. *Vaccine*, 2010. 28(38): p. 6176-6182.
20. Sugano, M., *et al.*, *Gene delivery system involving Bubble liposomes and ultrasound for the efficient in vivo delivery of genes into mouse tongue tissue*. *International Journal of Pharmaceutics*, 2012. 422(1-2): p. 332-337.
21. Adler, A.F. and K.W. Leong, *Emerging links between surface nanotechnology and endocytosis: Impact on nonviral gene delivery*. *Nano Today*, 2010. 5(6): p. 553-569.
22. Congiu, A., *et al.*, *Correlation between structure and transfection efficiency: a study of DC-Chol-DOPE/DNA complexes*. *Colloids and Surfaces B-Biointerfaces*, 2004. 36(1): p. 43-48.
23. Savva, M., *et al.*, *Correlation of the physicochemical properties of symmetric 1,3-dialkoylamidopropane-based cationic lipids containing single primary and tertiary amine polar head groups with in vitro transfection activity*. *Colloids and Surfaces B-Biointerfaces*, 2005. 43(1): p. 43-56.
24. Neves Silva, J.P., *et al.*, *DODAB:monoolein-based lipoplexes as non-viral vectors for transfection of mammalian cells*. *Biochimica Et Biophysica Acta-Biomembranes*, 2011. 1808(10): p. 2440-2449.
25. de la Torre, L.G., *et al.*, *The synergy between structural stability and DNA-binding controls the antibody production in EPC/DOTAP/DOPE liposomes and DOTAP/DOPE lipoplexes*. *Colloids and Surfaces B-Biointerfaces*, 2009. 73(2): p. 175-184.
26. Rosada, R.S., *et al.*, *Protection against tuberculosis by a single intranasal administration of DNA-hsp65 vaccine complexed with cationic liposomes*. *Bmc Immunology*, 2008. 9.

27. Perrie, Y., P.M. Frederik, and G. Gregoriadis, *Liposome-mediated DNA vaccination: the effect of vesicle composition*. *Vaccine*, 2001. 19(23-24): p. 3301-3310.
28. Toledo, M.A.S., *et al.*, *Development of a recombinant fusion protein based on the dynein light chain LC8 for non-viral gene delivery*. *Journal of Controlled Release*, 2012. 159(2): p. 222-231.
29. Radler, J.O., *et al.*, *Structure and interfacial aspects of self-assembled cationic lipid-DNA gene carrier complexes*. *Langmuir*, 1998. 14(15): p. 4272-4283.
30. Bangham, A.D., M.M. Standish, and J.C. Watkins, *DIFFUSION OF UNIVALENT IONS ACROSS LAMELLAE OF SWOLLEN PHOSPHOLIPIDS*. *Journal of Molecular Biology*, 1965. 13(1): p. 238-&.
31. Montgomery, D.C., *Design and Analysis of Experiments*. 4th ed. 1997.
32. Trevisan, J.E., *et al.*, *Technological Aspects of Scalable Processes for the Production of Functional Liposomes for Gene Therapy*, in *Non-Viral Gene Therapy*. 2011, InTech.
33. C. L. P. Oliveira, B.B.G., E. R. T. Silva, F. Nallet, L. Navailles, E. A.Oliveira, J. S. Pedersen, *submitted*. 2012.
34. Amenitsch, H., *et al.*, *Existence of hybrid structures in cationic liposome/DNA complexes revealed by their interaction with plasma proteins*. *Colloids and Surfaces B-Biointerfaces*, 2011. 82(1): p. 141-146.
35. Rodriguez-Pulido, A., *et al.*, *A physicochemical characterization of the interaction between DC-Chol/DOPE cationic liposomes and DNA*. *Journal of Physical Chemistry B*, 2008. 112(39): p. 12555-12565.
36. Chesnoy, S. and L. Huang, *Structure and function of lipid-DNA complexes for gene delivery*. *Annual Review of Biophysics and Biomolecular Structure*, 2000. 29: p. 27-47.
37. Egelhaaf, S.U., *et al.*, *Determination of the size distribution of lecithin liposomes: A comparative study using freeze fracture, cryoelectron microscopy and dynamic light scattering*. *Journal of Microscopy-Oxford*, 1996. 184: p. 214-228.
38. Huebner, S., *et al.*, *Lipid-DNA complex formation: Reorganization and rupture of lipid vesicles in the presence of DNA as observed by cryoelectron microscopy*. *Biophysical Journal*, 1999. 76(6): p. 3158-3166.
39. Alfredsson, V., *Cryo-TEM studies of DNA and DNA-lipid structures*. *Current Opinion in Colloid & Interface Science*, 2005. 10(5-6): p. 269-273.
40. Angelov, B., *et al.*, *Topology and internal structure of PEGylated lipid nanocarriers for neuronal transfection: synchrotron radiation SAXS and cryo-TEM studies*. *Soft Matter*, 2011. 7(20): p. 9714-9720.
41. Barreleiro, P.C.A. and B. Lindman, *The kinetics of DNA-cationic vesicle complex formation*. *Journal of Physical Chemistry B*, 2003. 107(25): p. 6208-6213.
42. Barreleiro, P.C.A., R.P. May, and B. Lindman, *Mechanism of formation of DNA-cationic vesicle complexes*. *Faraday Discussions*, 2003. 122: p. 191-201.

43. Pupo, E., *et al.*, *Preparation of plasmid DNA-containing liposomes using a high-pressure homogenization-extrusion technique*. *Journal of Controlled Release*, 2005. 104(2): p. 379-396.
44. Chiaramoni, N.S., *et al.*, *Liposome/DNA systems: correlation between association, hydrophobicity and cell viability*. *Biotechnology Letters*, 2007. 29(11): p. 1637-1644.
45. Candiani, G., *et al.*, *Bioreducible Liposomes for Gene Delivery: From the Formulation to the Mechanism of Action*. *Plos One*, 2010. 5(10).
46. Masotti, A., *et al.*, *Comparison of different commercially available cationic liposome-DNA lipoplexes: Parameters influencing toxicity and transfection efficiency*. *Colloids and Surfaces B-Biointerfaces*, 2009. 68(2): p. 136-144.
47. Stegmann, T. and J.Y. Legendre, *Gene transfer mediated by cationic lipids: Lack of a correlation between lipid mixing and transfection*. *Biochimica Et Biophysica Acta-Biomembranes*, 1997. 1325(1): p. 71-79.
48. Zuidam, N.J., *et al.*, *Lamellarity of cationic liposomes and mode of preparation of lipoplexes affect transfection efficiency*. *Biochimica Et Biophysica Acta-Biomembranes*, 1999. 1419(2): p. 207-220.
49. Koltover, I., *et al.*, *An inverted hexagonal phase of cationic liposome-DNA complexes related to DNA release and delivery*. *Science*, 1998. 281(5373): p. 78-81.
50. Pozzi, D., *et al.*, *How lipid hydration and temperature affect the structure of DC-Chol-DOPE/DNA lipoplexes*. *Chemical Physics Letters*, 2006. 422(4-6): p. 439-445.
51. Wasan, E.K., *et al.*, *A multi-step lipid mixing assay to model structural changes in cationic lipoplexes used for in vitro transfection*. *Biochimica Et Biophysica Acta-Biomembranes*, 1999. 1461(1): p. 27-46.
52. Kongkaneramt, L., *et al.*, *Dependence of reactive oxygen species and FLICE inhibitory protein on lipofectamine-induced apoptosis in human lung epithelial cells*. *Journal of Pharmacology and Experimental Therapeutics*, 2008. 325(3): p. 969-977.
53. Dokka, S., *et al.*, *Oxygen radical-mediated pulmonary toxicity induced by some cationic liposomes*. *Pharmaceutical Research*, 2000. 17(5): p. 521-525.
54. Samadikhah, H.R., *et al.*, *Preparation, characterization, and efficient transfection of cationic liposomes and nanomagnetic cationic liposomes*. *International Journal of Nanomedicine*, 2011. 6: p. 2275-2283.



---

## CAPÍTULO 4 – CONTINUOUS FLOW PRODUCTION OF CATIONIC LIPOSOMES AT HIGH LIPID CONTENT IN MICROFLUIDIC DEVICES FOR GENE AND VACCINE THERAPY

---

Tiago A. Balbino<sup>1</sup>, Nayla T. Aoki<sup>1</sup>, Antônio Gasperini<sup>2</sup>, Cristiano L. P. Oliveira<sup>3</sup>,  
Leide P. Cavalcanti<sup>2</sup>, Adriano R. Azzoni<sup>1,3</sup>, Lucimara G. de La Torre<sup>1\*</sup>

<sup>1</sup>University of Campinas, Brazil;

<sup>2</sup>Synchrotron Light National Lab, Brazil;

<sup>3</sup>University of São Paulo, Brazil.

\*Corresponding author: [latorre@feg.unicamp.br](mailto:latorre@feg.unicamp.br)

To be submitted to *Langmuir*

### Abstract

Microfluidics is a powerful technology that allows the production of cationic liposomes by the hydrodynamic focusing method. We first studied a single hydrodynamic focusing (SHF) device, which uses a central stream in which lipids dispersed in ethanol are injected and hydrodynamically compressed by the two aqueous streams. The ethanol diffusion from the inner stream to the aqueous stream encourages the formation of the liposomes. To intensify the mass diffusion and increase the surface area between the two fluids, a second device was designed with double hydrodynamic focusing (DHF). We investigated the influence of Fluid Flow Velocity ( $V_f$ ), Flow Rate Ratio (FRR) and Total Lipid Concentration ( $C_{lip}$ ) on the particle size of the CLs produced. The DHF microfluidic device had the ability of using higher  $V_f$  values than the SHF device, which resulted in a higher productivity level. Small Angle X-ray Scattering (SAXS) experiments were performed to structurally characterize the cationic liposomes produced by both microfluidic devices. The SAXS results revealed that both devices produce unilamellar cationic liposomes with a very small fraction of multilamellar liposomes;

this finding is in agreement with the observations made in the analysis of the liposomes using Transmission Electron Microscopy (TEM). The biological efficacies of the cationic liposomes produced by both microfluidic devices were examined *in vitro* in HeLa cells, which confirmed their potential for gene delivery and vaccine therapy applications.

## 1. Introduction

Liposomes are amphiphilic lipid systems that, in aqueous media, self-assemble into spherical bilayers with an aqueous interior lumen. They are generally formed because the lipid association yields entropically favorable states of low free energy in an energetically favorable manner [1]. Their biochemical structure is very similar to that of human cell membranes. Cationic lipids can form an electrostatic complex with DNA, which can then be efficiently delivered to the cell nucleus [2]. This feature makes cationic liposomes (CL) a promising gene delivery system for medical applications in the fields of vaccine and gene therapy [3].

Despite the longstanding interest in liposomes, especially cationic liposomes, only a small number of liposomal products have been approved for human application. This may be due to the lack of techniques that can produce liposomes efficiently and with a relatively low cost on an industrial scale. Furthermore, it is necessary to meet the requirements of the pharmaceutical industry, such as sterilization, when producing products for human use [4]. The majority of the current techniques used for liposome production require a unit operation step for the size reduction and homogenization of the particles. The most common post-processing methods are sonication [5, 6], extrusion [7] and high pressure homogenization [8]. Recent approaches in the field of liposome production aim to develop techniques that decrease the number of steps and time-consuming processes involved in the current production protocols [9].

The use of microfluidic systems in liposome production might overcome these major challenges. Microfluidics is a powerful technology that manipulates minute volumes of fluids ( $10^{-9}$  to  $10^{-18}$  liters) inside channels with dimensions in the

order of micrometers. Therefore, microfluidic systems are able to control concentrations of molecules in space and time [10]. A number of different microfluidic approaches have been employed in liposome production. The sequential infusion of water, oil that contains lipids and water into the main channel results in the formation of bilayer lipid membranes on chambers that are located on the walls of the main channel. These chambers, which were pneumatically driven by valves, allowed the formation of liposomes [11]. In addition, a microfluidic 3D flow focusing device with a modified surface was shown to control the immiscible flows, in which, after solvent extraction, double emulsion templates could be transformed into liposomes [12].

Another simple microfluidic strategy for liposome production, which was developed by Jahn and co-workers [13-15], used a hydrodynamic focusing (MHF) method to control the liposome formation with particle sizes ranging from 50 to 500 nm by improving the classical alcohol injection. The liposomes were composed of dimyristoylphosphatidylcholine, cholesterol and dihexadecyl phosphate. This technique uses a microfluidic device with a four-microchannel intersection geometry and an organic solvent (isopropanol) with dispersed lipids. The lipid-dispersed solution is injected into the middle stream, where it is hydrodynamically compressed by two aqueous (or buffered) streams. The control of the Flow Rate Ratio (FRR) between the aqueous and organic streams and the Total Volumetric Flow Rate ( $Q_t$ ) in the outlet stream allows the ethanol and aqueous streams to mix through molecular diffusion influenced by convection, resulting in the self-assembly of phospholipids into liposomes. In the reported studies, the lipid content of the liposomal formulations obtained by the microfluidic devices ranged between 0.1 and 0.4 mM. Therefore, the size particle homogenization post-processing step is not required, which results in a simpler liposome production protocol that can be used for personalized medicine applications, such as gene and vaccine therapy. Furthermore, the potential on-chip liposome production at the point of care would facilitate the therapeutic treatment, minimizing the amount of lipid oxidation and degradation.

Recently, our research group developed a cationic liposome formulation (EPC/DOTAP/DOPE 50:25:25% molar) that complexes with DNA<sub>hsp65</sub> for use in the tuberculosis vaccine and treatment. The liposome was produced using the conventional method at the laboratory scale and exhibited a high lipid content with a concentration of extruded liposomes of 16 mM [7, 16-18]. The necessity of liposome production methods that can yield liposomes with high lipid contents that can be further tested *in vivo* and *in vitro* has led our group to search for new production strategies.

The potential of microfluidics and the lack of studies that use microfluidic devices for the production of cationic liposomes led us to study the production of CL, which is useful for gene delivery at the same lipid composition that we achieved in the tuberculosis gene vaccine and therapy, through two methodologies: (i) single hydrodynamic focusing (SHF), which is based on the work of Jahn and co-workers [13-15], and (ii) double hydrodynamic focusing (DHF), which was designed to intensify the mass diffusion by increasing the diffusion surface area and thus the productivity of the CL formulations. We optimized the production of CL by both microfluidic devices using Central Composite Rotatable Designs. We also studied the effect of the following parameters: Flow Rate Ratio (FRR), Average Fluid Flow Velocities ( $V_f$ ) and Total Lipid Content ( $C_{lip}$ ). In addition, to evaluate the biological viability of the CL formulations produced, we assayed their transfection ability in human epithelial carcinoma (HeLa) cells *in vitro*. In this manuscript, we show the feasibility of using these two microfluidic devices for the high yield production of CLs with suitable characteristics for gene delivery and vaccine therapy.

## 2. Materials and Methods

### 2.1. Materials

The lipids were composed of egg phosphatidylcholine (EPC), 1,2-dioleoyl-sn-glycero-3-phosphoethanolamine (DOPE) and 1,2-dioleoyl-3-trimethylammonium-propane (DOTAP) (50/25/25% molar). All the lipids were

obtained from Lipoid and were not purified further. We used absolute ethanol from Sigma Chemical Co.

## 2.2. Cationic Liposome Production

The CL production was carried out in two hydrodynamic flow focusing microfluidic devices, which are illustrated in Figure 1. The lipids, which were dispersed in ethanol in the proportion that was previously described [16-18], were loaded into a 1 mL glass syringe. Deionized water was loaded into two 3 mL glass syringes. Infusion syringe pumps (Kd Scientific, model 200, USA) were used to control the flow of each solution into the inlet channels. In the Single Hydrodynamic Focusing (SHF) microfluidic device (Figure 1A), the lipid dispersion in ethanol flows through the center inlet channel and the deionized water flows through the two side inlet channels and hydrodynamically compresses the middle stream. The Double Hydrodynamic Focusing (DHF) microfluidic device (Figure 1B) had two consecutive flow focusing regions, which increase the diffusion surface area between the organic and the aqueous streams. Both devices were designed in AutoCAD (Autodesk). All channels, which had a rectangular cross section with a depth of 100  $\mu\text{m}$  and a width of 140  $\mu\text{m}$ , were constructed using soft lithography in polydimethylsiloxane (PDMS) and bounded to glass through  $\text{O}_2$  plasma surface activation, as described elsewhere [19]. The flow rates of the streams were adjusted to control the degree of hydrodynamic focusing and the width of the center stream, thus controlling the liposome formation.

The Flow Rate Ratio (FRR) is defined as the ratio of the volumetric aqueous flow rate to the volumetric flow rate of the lipid dispersion in ethanol. The microfluidic production of CL by both devices was examined at various FRRs, Average Fluid Flow Velocities at the device outlet ( $V_f$ ) and Total Lipid Concentrations ( $C_{lip}$ ) in the lipid dispersion. The stability of the focusing region was observed at 40x magnification under a trinocular stereo microscope (Bell Engineering, Italy). The liposome samples were collected at the microfluidic device outlet for subsequent analysis.

The CLs used in the *in vitro* assays were produced under sterilized conditions prior to experimentation by using sterile syringes and collected in sterile conical centrifuge tubes. The microfluidic devices were carefully washed with ethanol (70% v/v) and dried with nitrogen pressure prior to use.

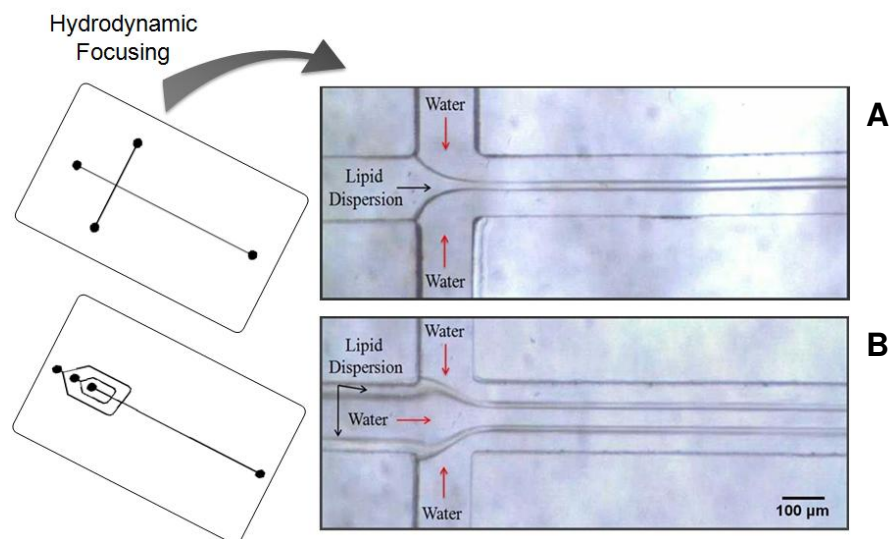


**Figure 1.** Microfluidic devices with single (**A**) and double (**B**) hydrodynamic focusing with a Total Lipid Concentration of 25 mM dispersed in ethanol, a Fluid Flow Velocity of 143 mm/s and a Flow Rate Ratio of 10.

To evaluate the biological applications of the liposomes produced by the microfluidic methods, the CLs were also prepared using a bulk method described elsewhere [20] under sterile conditions. This method, which is called the thin film method, required that all lipids be dispersed in chloroform and the required amounts of the stock solutions (EPC/DOPE/DOTAP 50/25/25% molar) were mixed and dried to produce a thin film using a rotary evaporator in a 650 mmHg vacuum for 1 hour. The dried lipid film was then hydrated with water to a final lipid concentration of 16 mM. The prepared liposomes were extruded through double polycarbonate membranes with a 100 nm nominal diameter under a nitrogen pressure of 12 kgf/cm<sup>2</sup>; this extrusion step was repeated 15 times.

## **2.3. Physicochemical and structural characterization**

### **2.3.1. Average hydrodynamic diameter and Polydispersity**

The dynamic light scattering (DLS) technique was used to measure the size distribution, polydispersity and the average hydrodynamic diameter using a Zetasizer Nano ZS (Malvern) with a backscattering detection angle of 173°, a He/Ne laser that emits at 633 nm, and a 4.0 mW power source. The average hydrodynamic diameter, or Z-average size, was weighted by the intensity of the scattering in the DLS. The mean particle size was obtained from the results of three experiments. The size distribution was evaluated with the polydispersity index. This index ranges from 0 to 1; the lower values indicate more a homogeneous distribution of the particle sizes. In addition, the polydispersity index was calculated from analysis of the cumulants of the DLS-measured intensity autocorrelation function. The CONTIN algorithm, which is based on an inverse Laplace transform in the autocorrelation function, was used to estimate the average diameter and polydispersity index of the particle sizes. All the samples were diluted to 0.2 mM prior to the analysis.

### **2.3.2. Zeta Potential Measurement**

The zeta potential of the samples was measured by applying an electric field across the samples, and the zeta potential value was obtained by measuring the electrophoretic mobility of the particles using the Laser Doppler Anemometry technique. The measurements for each sample were performed in triplicate in water at 25 °C using a Malvern Zetasizer 3000 (Malvern).

### **2.3.3. Morphology**

The liposomes produced by the two microfluidic devices were imaged to verify their morphology by means of Transmission Electron Microscopy (TEM) and the negative staining method. A drop of the samples (~5  $\mu$ L) was placed on a copper grid coated with a carbon film. The excess liquid was removed with blotting paper, leaving a thin film stretched over the grid. The negative staining was performed with a 2% solution of ammonium molybdate for ~10 s and then blotted

dry. The electron microscopy was performed using a LEO 906E microscope (Zeiss, Germany) at 80 kV, the MEGA VIEW III/Olympus camera and the ITEM E 23082007/Olympus Soft Imaging Solutions GmbH software.

### 2.3.4. Structural characterization using Synchrotron SAXS

The structural information of the produced CLs, such as the fraction of multilayer vesicles in relation to SUVs and the bilayer size, was obtained through Small Angle X-ray Scattering (SAXS) analysis. The SAXS experiments were performed on the beamline SAXS1 at the Brazilian Synchrotron Light National Lab (LNLS) using a beam energy of 8 keV ( $\lambda=1.55 \text{ \AA}$ ) and a sample to detector distance of 561 mm. The measured intensity is displayed as a function of the reciprocal space momentum transfer modulus  $q=4\pi \sin(\theta) / \lambda$ , where  $2\theta$  is the scattering angle and  $\lambda$  is the radiation wavelength. The typical range of  $q$  values was  $0.017 \text{ \AA}^{-1}$  to  $0.45 \text{ \AA}^{-1}$ .

The analyses were performed using the models described in our previous work [20]. We assumed that the system was composed of two phases: a fraction of unilamellar vesicles and a fraction of multilamellar vesicles. Therefore, the scattering intensity  $I(q)$  can be written as follows:

$$I(q) = P(q)S_{\text{eff}}(q) \quad (\text{Equation 1})$$

where  $P(q)$  is the bilayer form factor. In addition, the effective structural factor  $S_{\text{eff}}(q)=f_{\text{sb}}+f_{\text{m}}S_{\text{MCT}}(q)$ , where  $f_{\text{sb}}$  is a constant related to the fraction of single bilayers,  $f_{\text{m}}$  represents the relative fraction of multilayers, and  $S_{\text{MCT}}(q)$  is the Modified Caillé structure factor.

### 2.4. Process productivity

To verify the feasibility of our microfluidic setup system for gene delivery and vaccine therapy applications, the molar productivity of the produced CL was calculated from Equation 2 as follows:

$$P = 6.0 \times 10^{-5} \frac{Q_T \cdot C_{Lip}}{FRR + 1} \quad (\text{Equation 2})$$

where  $P$  is the molar productivity of the CL produced by the microfluidic devices in mmol/s,  $Q_T$  is the total volumetric flow in the outlet channel in  $\mu\text{L}/\text{min}$ , and  $C_{\text{lip}}$  is the lipid concentration of the dispersion in ethanol in mM.

## 2.5. Culture and transfection of mammalian cells

We used the vector model pVAX-LUC as the plasmid DNA (pDNA) and luciferase as the reporter gene [21]. The pDNA was amplified in *Escherichia coli* bacteria and purified using the PureLink™ HiPure Plasmid DNA Purification Kit-Maxiprep K2100-07. The extruded CLs that were used as the control were prepared by the thin film method that was previously described [20]. The pDNA/CL complexes were prepared by adding the pDNA to the CLs at a molar charge ratio of 6, which balances the positive charges from the cationic lipid (DOTAP) and the negative charges from the pDNA phosphate group.

The cytotoxicity and the ability to transfect human epithelial carcinoma (HeLa) cells *in vitro* of the complexes were tested using a previously described protocol [21]. The cells were maintained in an F-12 (Ham) nutrient mixture (Gibco, UK), which contained 10% (v/v) fetal bovine serum (FBS) (Gibco, UK) and was supplemented with non-essential amino acids (Gibco, UK), gentamicin (Gibco, UK), sodium pyruvate (Gibco, UK), and antibiotic–antimycotic (Gibco, UK). The cultures were incubated under standard conditions (37°C, 5% CO<sub>2</sub> in a humid atmosphere), allowed to grow to near confluency and harvested with trypsin. After reaching confluence, the cells were seeded into 24-well culture plates ( $5 \times 10^4$  cells per well), incubated for 48 h and transfected with 0.8  $\mu\text{g}$  of pVAX-Luc per well. The luciferase activity was determined using the Luciferase assay kit from Promega according to the manufacturer's protocol. The relative light units (RLUs) were measured with a chemiluminometer (Lumat LB9507, EG&G Berthold, Germany) and the luciferase activity was expressed as RLU/mg protein. The total protein was measured using a BCA protein assay kit (Pierce).

To simulate the ethanolic residual of the CLs produced by the microfluidic method, 10 % (v/v) ethanol was added to the extruded CLs obtained by the thin film method prior to measuring their *in vitro* cytotoxicity. We used the cell

proliferation reagent WST-1 from Roche Molecular Biochemicals (Mannheim, Germany). The cells were seeded onto 96-well microplates (7,000 cells per well) in 100  $\mu$ L of culture medium and incubated for 48 h under the same conditions described above, at which point the pDNA/CLs complexes were added. At the end of the treatment, 10  $\mu$ L of the cell proliferation reagent WST-1 was added to each well; the cells were then incubated for 2 h. The results of the WST-1 assay were then measured using a scanning multiwell spectrophotometer (ELISA-Reader MRX, Dynex Technologies) at wavelengths of 440 and 650 nm.

## 2.6. Experimental design for response surface methodology

The CL production conditions were examined by the Response Surface Methodology [22] to determine the particle size as a function of the microfluidic parameters FRR and  $V_f$ , and the system parameter  $C_{lip}$ . A total of 17 experimental trials were carried out, which were designed on a Central Composite Rotatable Design (CCRD) with six axial and three central points. All the experiments were randomized. The statistical significance of the results of the experimental design data was determined using the STATISTICA 5.5 software (Statsoft Inc.).

## 3. Results and Discussion

The development of microfluidic devices for liposome production has been extensively explored by different researchers, and the potential of using these devices has already been proven. However, most of the processes used a lipid content ( $C_{lip}$ ) lower than 5 mM [13-15, 23, 24], which is the approximate solubility of lipids in ethanol and isopropanol. Thus, the liposomal formulations obtained were at concentrations of  $\sim$ 0.5 mM, which have limited use. In the field of gene therapy and vaccine, for example, a low lipid content in the liposomal formulation is inadequate. Systematic studies on the use of microfluidic systems for the production of cationic liposomes have yet not been presented in the scientific literature.

We used the hydrodynamic focusing technique to find the operating conditions that would produce liposomes with the highest lipid concentration and

productivity. In addition to using a single hydrodynamic focusing (SHF) system (Figure 1A), we developed a double hydrodynamic focusing (DHF) system (Figure 1B) to produce liposomes with two flow focusing regions, which increases the surface area involved in the organic-aqueous diffusion phenomenon.

In both cases, the three lipids (EPC/DOTAP/DOPE 50:25:25% molar) were dispersed in ethanol at specified lipid contents ( $C_{lip}$ ) prior to processing. A previous Langmuir Monolayer study on these lipids demonstrated that a uniform dispersion of the lipids in ethanol can be attained because there are attractive forces that maintain the lipids balanced at their molar proportion [25]. In addition, we designed experiments (CCRD -  $2^3$ ) to evaluate the influence of FRR,  $V_f$  and  $C_{lip}$  on the resultant particle size and polydispersity.

### **3.1 Cationic liposome production using the single hydrodynamic focusing (SHF) microfluidic device**

We studied the SHF device using the CCRD experimental matrix. The resulting particle size and polydispersity index are shown in Table 1 for each experimental condition tested. As shown in Table 1, we obtain cationic liposomes with lipid concentrations ranging from  $\sim 0.6$  to 7 mM by varying the  $C_{lip}$  from 9 to 92 mM, the surface velocity from 0.08 to 0.16 and the FRR from 8 to 18.

The highest lipid concentrations of the liposomal formulations ( $\sim 7$  mM) were obtained in the third and fourth runs (high  $C_{lip}$  and low FRR), whereas the lowest concentration ( $\sim 0.6$  mM) was produced in the eleventh run (low  $C_{lip}$  and high FRR) (Table 1).

The differences between the different runs were analyzed by determining the variance using ANOVA to determine the statistical significance of the differences, as summarized in Table 2. The analysis of the  $F$ -test results reveals that the model of the SHF device is only predictive for the particle size because the calculated  $F$ -value (2.745) was slightly higher than the listed  $F$  (2.72), and the obtained R-squared (0.78) was considered satisfactory. Therefore, all the factors ( $C_{lip}$ ,  $V_f$  and FRR) significantly influenced the resulting particle size with a confidence level of 90%. The polydispersity response, however, did not show any significant variation.

**Table 1.** CCRD matrix with the real and coded values (in parenthesis) for the factors (Average Flow Velocity ( $V_f$ ), Lipid Concentration dispersed in ethanol ( $C_{lip}$ ), and Flow Rate Ratio (FRR)) tested and the responses (Particle Size and Polydispersity (Pdl)) obtained using the SHF device in the production of cationic liposomes.

Run	Factors			Responses	
	$V_f$ (mm/s)	$C_{lip}$ (mM)	FRR	Pdl $\pm$ SD	Particle Size <sup>(i)</sup> (nm $\pm$ SD)
1	95 (-1)	25 (-1)	10 (-1)	0.34	99.3
2	143 (+1)	25 (-1)	10 (-1)	0.31	85.8
3	95 (-1)	75 (+1)	10 (-1)	0.28	233.9
4	143 (+1)	75 (+1)	10 (-1)	0.20	145.2
5	95 (-1)	25 (-1)	16 (+1)	0.27	264.2
6	143 (+1)	25 (-1)	16 (+1)	0.21	172.2
7	95 (-1)	75 (+1)	16 (+1)	0.23	173.1
8	143 (+1)	75 (+1)	16 (+1)	0.29	241.0
9	80 (-1.68)	50 (0)	13 (0)	0.29	240.5
10	160 (+1.68)	50 (0)	13 (0)	0.32	198.7
11	120 (0)	8 (-1.68)	13 (0)	0.25	88.0
12	120 (0)	92 (+1.68)	13 (0)	0.25	202.4
13	120 (0)	50 (0)	8 (-1.68)	0.24	130.7
14	120 (0)	50 (0)	18 (+1.68)	0.50	508.6
15	120 (0)	50 (0)	13 (0)	0.31	254.6
16	120 (0)	50 (0)	13 (0)	0.33	260.9
17	120 (0)	50 (0)	13 (0)	0.32	257.9

<sup>(i)</sup>The average hydrodynamic diameter was weighed by the intensity.

**Table 2.** ANOVA for the Cationic Liposomes produced by the Single Hydrodynamic Focusing (SHF) device.

Source of Variation	Sum of squares		Degrees of freedom		Mean square		F-test	
	Pdl	Particle size	Pdl	Particle Size	Pdl	Particle Size	Pdl	Particle Size
Regression	0.03	122,706.7	9	9	0.004	13,634.1	0.654	2.75
Residual	0.04	34,723.5	7	7	0.006	4,960.5		
Total	0.07	157,430.2	16	16				

Pdl:  $F_{9;7;0.1} = 2.72$ ;  $R^2 = 0.457$

Particle size:  $F_{9;7;0.1} = 2.72$ ;  $R^2 = 0.779$

Based on the statistical analysis, we plotted the response surfaces (Figure 2) to verify the change in particle size behavior under the range of conditions studied; to visualize these surfaces, the independent variables were analyzed in pairs. The response surfaces for the particle size as a function of  $V_f$  and  $C_{lip}$ , (Figure 2A) and as a function of  $V_f$  and FRR (Figure 2B) show that the range of  $V_f$  values studied does not strongly influence the particle size. Jahn and co-workers [13-15] found a similar effect on liposomes assembled in similar microchannels at

lower  $C_{lip}$  values (5 mM). Huang and co-workers [24] reported a slight change in the particle size obtained with different  $V_f$  values. The low influence of this variable on the particle size has also been observed in the synthesis of niosomes using the SHF technique [26]. This low influence of  $V_f$  on the particle size might indicate that the microfluidic system can operate at higher total volumetric flow rates, which could increase the productivity.

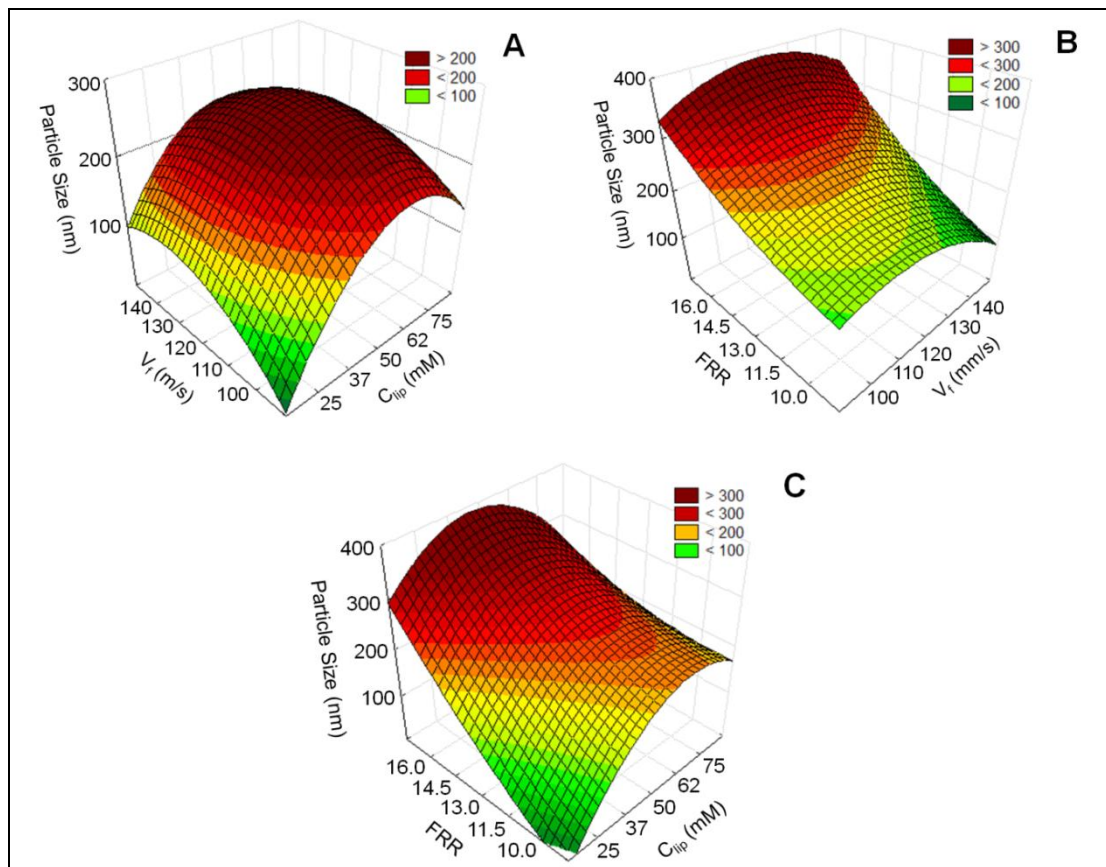


**Figure 2.** Response surfaces of the particle size of cationic liposomes produced by the single hydrodynamic focusing (SHF) microfluidic device as a function of the Lipid Concentration of the dispersion in ethanol ( $C_{lip}$ ), the Average Flow Velocity ( $V_f$ ) and the Flow Rate Ratio (FRR).

Additionally, the  $V_f$  is inversely proportional to the fluid residence time in the microreactor. Thus, in the explored ranges, the residence time was sufficient. At the axial minimum ( $V_f = 80$  mm/s) and maximum ( $V_f = 160$  mm/s) points, the residence times are 0.38 and 0.19 s, respectively.

The  $C_{lip}$  is another important parameter that contributes to the increase in the production of CL in microfluidic devices because an increase in this concentration directly results in an increase in the lipid concentration of the final liposomal formulation. The influence of this independent variable is illustrated in Figures 2A and C. As shown, the system produces smaller particles for lower values of  $C_{lip}$ . A similar behavior was reported by Pradhan and co-workers [27], who studied the effect of lipid flow concentration on liposome particle behavior. However, the authors used lower lipid concentrations in the organic phase and obtained a maximum lipid concentration in the liposomal solution of ~2 mM.

This influence of  $C_{lip}$  on particle size was expected based on the liposome formation theory [28]. For different liposome production methods that involve the diffusion of an organic solvent (e.g., ethanol injection method), phospholipid bilayers fragments (PBFs), which are highly unstable and take the formation of vesicles, form during the diffusion process. However, in the formation of liposomes using microfluidic devices, the aggregation process is controlled by the ordered ethanol and water mixing process. The lower polarity regions of the solvent make the lipids increasingly less soluble, which encourages them to self-assemble into PBFs. To minimize the hydrophobicity of the PBF edges, these PBFs form spherical vesicles with an aqueous interior core [23], as shown in the schematic in Figure 3.

This process occurs simultaneously with the ethanol/water diffusion. In fact, the formation of the PBFs might be an additional mass transfer resistance for the diffusion of the ethanol. If the ethanol/water diffusion is completed before all the lipid particles have formed vesicles (or at least PBFs), the remaining lipids will most likely aggregate in an uncontrolled manner, leading to the formation of liposomes with uncontrolled sizes. This happens, for example, when the proportion of ethanol to lipid is not adequate, such as at a high lipid content. Therefore, in the production of CLs in microfluidic devices using hydrodynamic focusing, the ethanol/lipid mass rate ( $C_{lip}$ ) that results in the maximal lipid concentration must be determined.

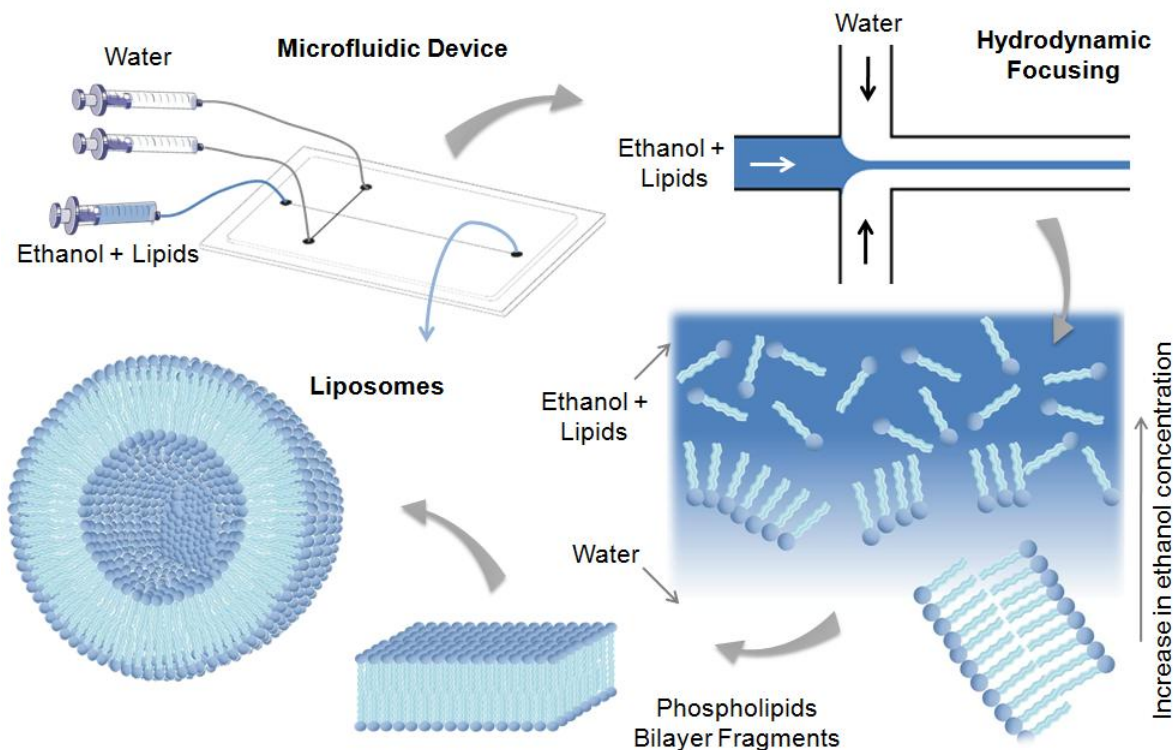


**Figure 3.** Schematic diagram of the hypothesized mechanism for liposome formation in a microfluidic hydrodynamic focusing device. The central stream is composed of the lipid dispersion in ethanol, which is hydrodynamic compressed by the two adjacent aqueous streams. The mixing of the water and ethanol through the main channel forms phospholipid bilayer fragments (PBF) that grow into vesicles to stabilize their hydrophobic PBF edges. The decrease in ethanol concentration destabilizes the PBFs, influencing then to close into vesicles and thus form liposomes.

This hypothesis was confirmed when we compared our results from Table 1 with a previous study that used a microfluidic device with a higher  $C_{lip}$  [29]. At the same lipid composition, using ethanol as the organic solvent, and with FRR values ranging from approximately 7 to 11 and  $V_f$  values ranging from 1.02 to 1.35 mm/s, a  $C_{lip}$  of 100 mM results in the formation of cationic liposomes with Pdl values of 0.44 to 0.62, which indicate that these particles were formed in an uncontrolled manner.

We can also observe that an increase in FRR also results in an increase in the particle size. However, our experimental data are not in agreement with Zook *et al.* [23] and Jahn *et al.* [14, 15]. These studies reported an increase in liposome size with a decrease in FRR using comparable systems, a similar FRR range and a lower  $C_{lip}$ . However, because these authors used isopropanol as the organic

solvent instead of ethanol, the differences in the influence of FRR could be a consequence of the molecular diffusivities of the different organic solvents into water. We decided to use ethanol because it is an acceptable solvent for *in vitro* experiments with human applications [30]. The molecular diffusivities ( $D_{AB}$ ) for isopropanol and ethanol in water at 25° C are  $0.87 \times 10^{-9}$  and  $1.132 \times 10^{-9}$  m<sup>2</sup>/s, respectively [31]. Therefore, the ethanol  $D_{AB}$  is 51.7% higher than the isopropanol  $D_{AB}$ . This difference will result in differences in the mass transfer rate and thus in the process of liposome formation. For a constant  $V_f$  and  $C_{lip}$ , an increase in the FRR means that the proportion of water to solvent in the microchannel increases. This decrease in the amount of ethanol means that the diffusion process will be faster and thus require a shorter distance, which compromises the balance between the ethanol diffusion and the PBF formation, causing a larger liposome to be produced. However, considering the lower molecular diffusivity of isopropanol, a decrease in the amount of isopropanol will contribute positively to the balance between the organic solvent mass transfer and the PBF formation, which results in better control of the liposome size.

### **3.2 Cationic liposome production using the double hydrodynamic focusing (DHF) microfluidic device**

The liposomes produced by the DHF device were explored using the same variable ranges that were used in the investigation of the SHF device. The matrix of experimental conditions (CCRD ( $2^3$ )) and the corresponding responses (particle size and polydispersity) obtained using the DHF device are shown in Table 3. The analysis of variance (ANOVA) of the model in the responses is shown in Table 4.

As shown in Table 4, the surface model is not predictive because the  $F$ -values for the polydispersity index and particle size are 0.781 and 0.745, respectively, which are lower than the listed  $F$ -value (2.72 for both cases, with  $\alpha = 0.10$ ). In addition, the R-squared values are 0.501 and 0.489 for the polydispersity index and particle size, respectively. These results suggest that the operational range for the DHF is different from the SHF.

**Table 3.** CCRD matrix with the real and coded values (in parenthesis) for the factors (Average Flow Velocity ( $V_f$ ), Lipid Concentration of the dispersion in ethanol ( $C_{lip}$ ) and Flow Rate Ratio (FRR)) tested and the responses (Particle Size and Polydispersity (Pdl)) obtained using the DHF device in the production of cationic liposomes.

Run	Factors			Responses	
	$V_f$ (mm/s)	$C_{lip}$ (mM)	FRR	Pdl $\pm$ SD	Particle Size (nm $\pm$ SD)
1	95 (-1)	25 (-1)	10 (-1)	0.30	298.2
2	143 (+1)	25 (-1)	10 (-1)	0.31	243.1
3	95 (-1)	75 (+1)	10 (-1)	0.36	384.2
4	143 (+1)	75 (+1)	10 (-1)	0.32	312
5	95 (-1)	25 (-1)	16 (+1)	0.31	285.6
6	143 (+1)	25 (-1)	16 (+1)	0.30	245.7
7	95 (-1)	75 (+1)	16 (+1)	0.64	659.2
8	143 (+1)	75 (+1)	16 (+1)	0.29	266.4
9	80 (-1.68)	50 (0)	13 (0)	0.31	243.8
10	160 (+1.68)	50 (0)	13 (0)	0.52	593.7
11	120 (0)	8 (-1.68)	13 (0)	0.28	262.9
12	120 (0)	92 (+1.68)	13 (0)	0.25	202.4
13	120 (0)	50 (0)	8 (-1.68)	0.87	1096
14	120 (0)	50 (0)	18 (+1.68)	0.36	353.3
15	120 (0)	50 (0)	13 (0)	0.57	612.3
16	120 (0)	50 (0)	13 (0)	0.35	344.9
17	120 (0)	50 (0)	13 (0)	0.49	530.1

**Table 4.** ANOVA for the Cationic Liposomes produced by the Double Hydrodynamic Focusing (DHF) device.

Source of Variation	Sum of squares		Degrees of freedom		Mean square		F-test	
	Pdl	Particle size	Pdl	Particle Size	Pdl	Particle Size	Pdl	Particle Size
Regression	0.22	408670.9	9	9	0.024	45407.9	0.781	0.745
Residual	0.21	426570.4	7	7	0.031	60938.6		
Total	0.43	835241.4	16	16				

Pdl:  $F_{9;7;0,1} = 2.72$ ;  $R^2 = 0.501$

Particle size:  $F_{9;7;0,1} = 2.72$ ;  $R^2 = 0,489$

The particle sizes obtained for the liposomes by the DHF microfluidic device ranged between 202.4 and 1096 nm and the Pdl values ranged from 0.25 to 0.87. A comparison of these particles to those produced using the SHF microfluidic device, which exhibited ranges of particle sizes and polydispersity indexes between 85.8 and 508.6 nm and between 0.20 and 0.50, respectively, reveals that the particles seem to be produced in an uncontrolled manner in the DHF.

### 3.3. Comparison of the effect of flow velocities on the particle size of the liposomes produced using the SHF and DHF microfluidic devices

The analysis of the experimental results shown in Tables 3 and 4 shows that the variable ranges studied in the production of liposomes using the DHF device were not optimized. Thus, it is probable that, as the interfacial area is increased, the DHF configuration allows the system to work at higher total volumetric flow rates, which would result in higher productivity. To confirm this hypothesis, we kept the FRR and  $C_{lip}$  constant at 10 and 25 mM, respectively, and performed a comparative analysis on the particle size obtained using both devices over different ranges of  $V_f$ ; the results of this study are presented in Figure 4.

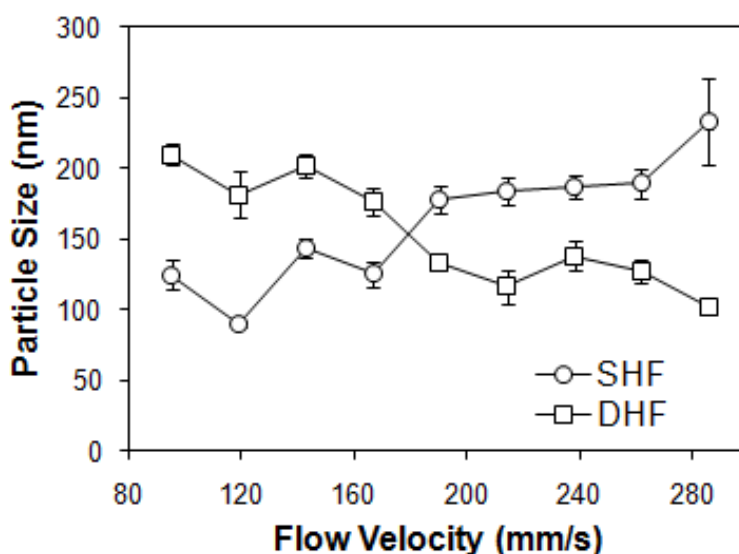


**Figure 4.** Effect of average flow velocity ( $V_f$ ) on particle size (intensity-weighted) for the production of cationic liposomes using the Single (SHF) and Double (DHF) Hydrodynamic Focusing devices. Production conditions: FRR of 10 and  $C_{lip}$  of 25 mM. The error bars represent the standard deviation of three independent experiments.

Figure 4 shows the effect on particle size of a large range of  $V_f$  values in the production of CLs using both devices. The CLs produced using the SHF device at higher flow rates exhibited larger particle sizes, which is contradictory with the previous experimental results for SHF (Table 1 and Figure 2) that identified the  $V_f$  does not strongly influence the particle size. However, the previous studies used a  $V_f$  range from 80 to 160 mm/s, whereas Figure 4 illustrates the influence of higher values of  $V_f$  and indicates that  $V_f$  values higher than 160 mm/s the SHF device

produce liposomes with increased size, from approximately 100 to 180 nm. It is possible that, for values of  $V_f$  higher than 160 mm/s, the convective contribution due to the increase in flow velocity disturbs the ethanol and water mixing, which modifies the lipid self-assembly into PBFs and thus produces liposomes of larger size.

The behavior observed with the DHF device was the opposite of that observed with the SHF. The DHF was able to produce CLs with an approximated size of 100 nm at  $V_f$  values higher than 160 mm/s (Figure 4), which implies a higher productivity level than that achieved with the SHF. It is possible that doubling the interfacial area in the DHF resulted in a decrease in the distance required to complete the ethanol diffusion leading to a compromised balance between the ethanol diffusion and the lipid formation. When  $V_f$  is increased to values higher than 160 mm/s, the residence time decreases and the distance required to complete the ethanol mass transfer increases. Consequently, it is possible that a longer microchannel distance in the microfluidic device will ensure controlled BPF and liposome formation.

The productivity of the DHF device is higher than the SHF device because it was possible to use higher fluid flow velocity, or total volumetric flow rate; these results are discussed in detail in Table 5.

### 3.4. Flow properties and mixing time

We calculated two dimensionless numbers to characterize and classify the flow properties of our system, which make it possible to compare it to other systems with different dimensions. Dimensionless numbers are widely used in various branches of chemical engineering because of their clear physical interpretation, which contributes to the physical comprehension of the phenomenon involved in the process under study [32]. The Reynolds number ( $Re$ ) represents the ratio of the inertial forces to the viscous forces. It is generally considered to be the most important dimensionless parameter in studies of transport phenomena in fluid flows and is expressed as follows [33]:

$$Re = \frac{\rho V_f D_h}{\mu} \quad (\text{Equation 3})$$

where  $D_h$  is the hydraulic diameter,  $\rho$  is the fluid density and  $\mu$  is the dynamic viscosity. The second dimensionless parameter that we used is the Peclet number ( $Pe$ ), which correlates the transport via hydrodynamic convection (flow of the medium,  $V_f$ ) and the molecular diffusion of mass (mass diffusivity  $D_{AB}$ ) [32].  $Pe$  therefore represents the ratio of convection and diffusion mass transports and is given by the following equation:

$$Pe = \frac{V_f L}{D_{AB}} \quad (\text{Equation 4})$$

where  $L$  is the microchannel length. The  $Re$  and  $Pe$  values for our system ranged from 11.1 to 33.2 and from  $2.52 \times 10^6$  to  $7.57 \times 10^6$ , respectively. These results are similar to those reported by other studies on liposome synthesis in microchannels. Zook and co-workers [23] worked at a similar  $Re$  value of 22.9 and a slightly higher  $Pe$  number of  $7.66 \times 10^6$  due to their longer channel length. Jahn and co-workers [15] operated at lower  $Re$  numbers ranging from 2 to 8 and at lower  $Pe$  values of  $0.25 \times 10^6$  to  $0.96 \times 10^6$ . As expected in microfluidic systems, the  $Re$  numbers under all operation conditions were much lower than 1,800, which is the onset of the transition of laminar to turbulent [34]. All the  $Pe$  values obtained indicate the predominance of advection over diffusion in the systems studied.

The mixing time is also an important parameter in microfluidic processes because it dictates whether the fluids will attain complete mixing through the length of the microchannel. The estimation of the time required for the complete diffusion of ethanol into the aqueous stream is based on the mass continuity equation [33, 35]. Considering that the mass transfer process occurs in laminar flow, without a chemical reaction and in two directions, the mean molar flux of ethanol ( $N_A$ ), or the molar diffusion rate along the microchannel, is given by the following equation:

$$N_A = \sqrt{\frac{4 D_{AB} v}{\pi L}} (C_{A0} - C_{A\infty}) \quad (\text{Equation 5})$$

where  $v$  is the velocity of the aqueous phase, which is calculated by the volumetric rate of water per the flow area of water,  $L$  is the microchannel length,  $C_{A0}$  corresponds to the concentration of ethanol at the ethanol stream and  $C_{A\infty}$  is the concentration of ethanol at the channel wall, which is considered to be zero at the

beginning of the process. According to the conditions shown in Figure 1, the corresponding values of  $v$  for the SHF and DHF devices are 0.033 and 0.095 m/s, respectively. Therefore, because  $C_{A0}$  is the concentration of pure ethanol, which is  $17.13 \text{ kmol/m}^3$ , the values of  $N_A$  for the SHF and DHF devices are  $7.0 \times 10^{-4}$  and  $11.8 \times 10^{-4} \text{ kmol/m}^2 \text{ s}$ , respectively. Thus, the mixing time required for the two fluids to be completely diffused can be calculated by Equation 6 as follows:

$$\tau = n/N_A \quad (\text{Equation 6})$$

where  $n$  is the total moles of ethanol diffused per square meter in both diffusion directions and is given by the following equation:

$$n = 2 \delta \rho/M \quad (\text{Equation 7})$$

where  $\delta$  is the thickness of the lipid phase in the direction of diffusion,  $\rho$  represents the density of ethanol and  $M$  is the molecular weight of ethanol. Therefore, the mixing times,  $\tau$ , required for the SHF and DHF devices are 3.34 and 1.29 ms, respectively. This  $\tau$  can be interpreted as the minimum residence time required to complete the liposome formation. These values are 100-fold lower than the residence time that was previously estimated, which ranged from 315 ms (95 mm/s) to 111 ms (286 mm/s), and thus justify the weak influence of the range of  $V_f$  values studied in the CCRD experiments on the size of the liposomes produced using both the SHF and DHF devices. At  $V_f$  values that are higher than 160 mm/s, however, the particle size is influenced by the  $V_f$ , as observed in Figure 3. In addition to the difference between the water-ethanol diffusion time and the residence time, the particle size variations are most likely due to the combined effects of the diffusion and convection phenomena reflected by the  $Pe$  numbers of both geometries, which are above  $5.05 \times 10^6$  for  $V_f$  values above 160 mm/s.

The proper formation of liposomes is dependent on the balance between the ethanol mass transfer and the PBF formation. This process occurs in a controlled manner until the ethanol and water streams are completely mixed. Therefore, the low mixing times indicate that the mixing process is completed close to the beginning of the microchannel, which results an uncontrolled formation of PBFs.

Consequently, to produce liposomes in a controlled manner, the maximum  $C_{lip}$  in the alcoholic stream will need to be limited.

### 3.4. Analysis of the Productivity and Physicochemical and Structural characterization of the Cationic Liposomes Produced by the SHF and DHF Devices

For each microfluidic device, the best condition that produced CLs with a particle size less than 150 nm was chosen; the respective molar productivities for these conditions were then estimated, as summarized in Table 5. The selected conditions for the SHF and DHF devices involved  $V_f$  values of 165 mm/s and 285 mm/s at a FRR of 10 and a  $C_{lip}$  of 25 mM. As shown, we obtained higher molar productivities (approximately 13-fold higher) compared to previous reports on liposome production in microfluidic systems, in which the maximum values were approximately 0.5 mmol/s [13] and 2.5 mmol/s [15]. Although the particle size and polydispersity index of the CL produced by both devices are significantly different, the values obtained are considered suitable for gene delivery and vaccine therapy.

**Table 5.** Physicochemical properties of cationic liposomes produced by the single and double hydrodynamic focusing microfluidic devices (SHF and DHF, respectively). Operating parameters: FRR of 10,  $C_{lip}$  of 25 mM and  $V_f$  of 165 and 285 mm/s for the SHF and DHF, respectively.

	Hydrodynamic Microfluidic Devices	
	SHF	DHF
Particle Size <sup>(i)</sup> (nm)	124.9 ± 8.9	101.9 ± 1.6*
Polydispersity Index	0.31 ± 0.05	0.34 ± 0.02
Zeta Potential (mV)	+57.4 ± 3.6	+65.0 ± 2.6*
Molar productivity (mmol/s)	19.1 ± 2.8 <sup>(ii)</sup>	32.7 ± 4.6 <sup>(ii)*</sup>

Results represent mean ± SD of three independent experiments

(i) Intensity-weighted averaged hydrodynamic diameter.

(ii) Standard deviation based on the Propagation Uncertainties Theory (Taylor, 1997)

\* Significantly different ( $p < 0.05$ ) when compared to the SHF.

The liposomes produced by both the SHF and DHF devices exhibited a positive zeta potential in water of 57.4 and 65 mV, respectively, which indicates that the liposomes are cationic and thus suitable for *in vitro* transfection experiments. The difference in the zeta potentials is most likely due to the

modifications in the physicochemical properties that occur when shear stress is applied during the liposome formation [36-38]. The difference in the flow velocity between the microfluidic devices generates differences in the shear rates that are applied in the liposome formation region, which is then reflected on the zeta potential of the vesicles that are produced.

The particle size distributions of the CLs produced by both the SHF and DHF microfluidic devices at  $C_{lip}$  values of 25 mM for both, FRR values of 10 for both and  $V_f$  values of 120 and 240 mm/s, respectively, are summarized in Figures 5A and 6A. The particle size of the CLs produced using the SHF device range from 60 to 400 nm, whereas the particle size distribution of the CLs produced by the DHF device show two populations, a major one that ranges in particle size from 20 to 400 nm and a second (smaller) population approximately 4,000 nm in size.

The morphology of the CLs produced by both the SHF and the DHF microfluidic devices were evaluated by transmission electron microscopy (TEM) using a negative staining technique (Figures 5B and 6B). As shown, the CLs obtained have rather spherical shapes with diameters in the order of 100 nm. The isolated vesicles can be observed without any evidence of aggregation and/or fusion. It is also possible to observe the presence of a well-defined region surrounding the particle, which is illustrated by the arrowheads in Figures 5B and 6B. The presence of this region suggests that the CLs produced by both devices are unilamellar with an estimated lamellar thickness of ~6 nm. This estimate is in agreement with Trevisan and co-workers [29], who applied small angle X-ray scattering techniques to determine a bilayer thickness of 5.9 nm in CLs with the same lipid composition produced by different methods.

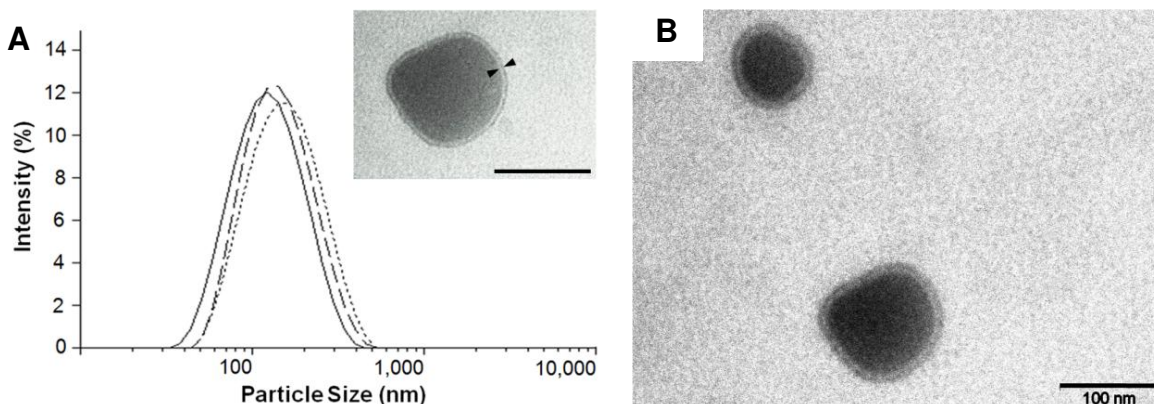


**Figure 5.** (A) Particle size distributions (intensity weighted) obtained by DLS and (B) Transmission electron micrographs of cationic liposomes produced by the Single Hydrodynamic Focusing microfluidic device at a  $C_{lip}$  of 25 mM,  $FRR$  of 10 and  $V_f$  of 143 mm/s. The bars represent 100 nm.

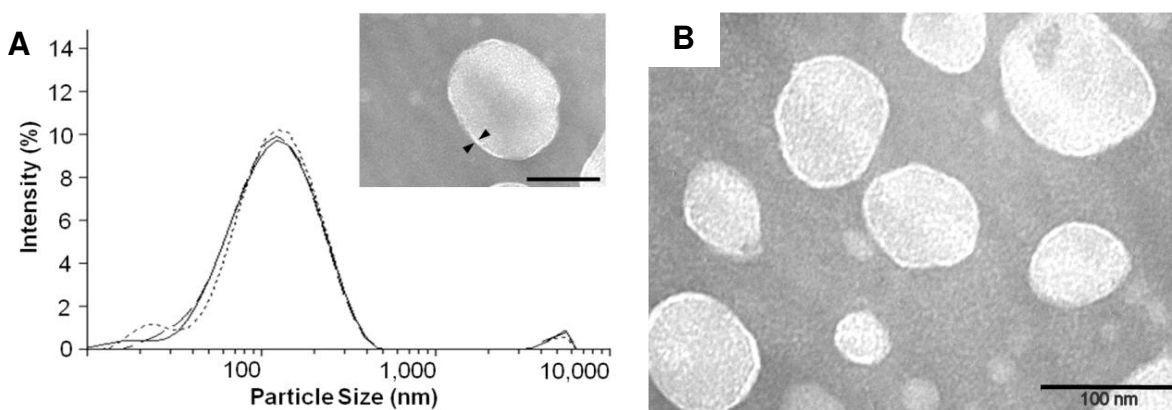


**Figure 6.** (A) Particle size distributions (intensity weighted) obtained by DLS and (B) Transmission electron micrographs of cationic liposomes produced by the Double Hydrodynamic Focusing microfluidic device at a  $C_{lip}$  of 25 mM,  $FRR$  of 10 and  $V_f$  of 285 mm/s. The bars represent 100 nm.

To confirm the unilamellar nature of the cationic liposomes produced by the SHF and DHF microfluidic devices, we performed SAXS experiments at a  $C_{lip}$  of 75 mM,  $FRR$  of 10 and  $V_f$  of 143 mm/s. Figure 7 shows the scattering intensity for two representative CLs produced by the SHF and DHF microfluidic devices. The fitting model that was used considered the presence of unilamellar and multilamellar vesicles [20]. The fraction of multilayers produced by both devices was approximately 4% and lower than 0.2% for the SHF and DHF devices, respectively; both of these values can be considered negligible. We therefore found that both

methods produce unilamellar cationic liposomes, which confirms the previous finding from the TEM analysis. This is the first report that characterizes the liposomes produced in microfluidic devices as unilamellar through SAXS.

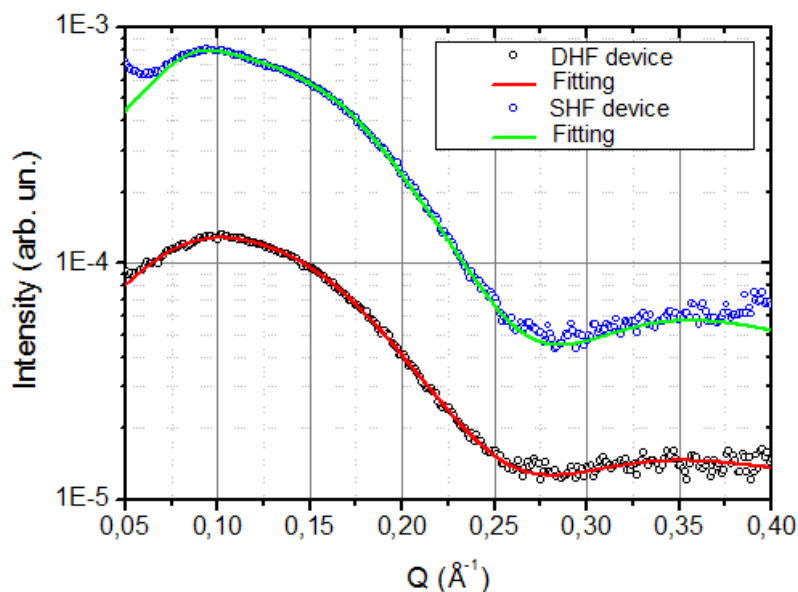


**Figure 7.** Small Angle X-ray Scattering intensity of cationic liposomes produced by the Single (SHF) and Double (DHF) Hydrodynamic Focusing devices with respective fitting curves. Production conditions:  $C_{lip}$  of 75 mM, FRR of 10 and  $V_f$  of 143 mm/s.

### 3.5. Biological evaluation of the Cationic Liposomes Produced by the SHF and DHF Devices

The cationic liposomes produced by the microfluidic methods contained residual organic solvent due to the lipid dispersion; therefore, we evaluated the effect of ethanol on the proliferation of HeLa cells by determining the percent of cell survival 24 h post treatment using the WST-1 assay. We added ~10% (v/v) of ethanol to liposomes that were prepared through the traditional bulk method; this addition of ethanol would better simulate the liposomal formulations obtained by the microfluidic methods at a FRR of 10. As shown in Figure 8 (inset graph), no cytotoxic effects were observed in any of the test samples, which indicates that the presence of ~10% of ethanol in the culture medium did not influence cell viability. Therefore, it is feasible to use the CLs produced by microfluidic devices in *in vitro* studies without any additional dialysis processing steps.

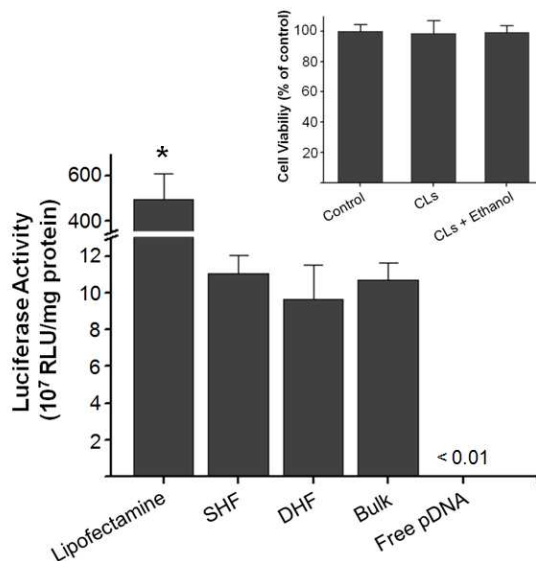


**Figure 8.** *In vitro* efficacy on the transfection of HeLa cells with DNA complexed with cationic liposomes produced by the SHF and DHF microfluidic devices and the typical bulk process. Activity was expressed in RLU/mg protein. Free pDNA and Lipofectamine were used as negative and positive controls, respectively. Inset: Cell viability assay of cationic liposomes produced by the bulk process complexed with pDNA in the presence of ~10% (v/v) residual ethanol. Cells without treatment were used as the control. The data represent the means  $\pm$  SD of six and three experiments in the inset and the main graph, respectively. \*  $p < 0.05$  was considered statistically significant.

The biological efficacies of the cationic liposomes produced by both microfluidic devices were examined *in vitro* in human epithelial carcinoma cells (HeLa) cells. The CLs were complexed with the plasmid DNA vector model pVAX-Luc, as described by Toledo *et al.* [21]. The transfection was quantified by determining the luciferase activity after an incubation time of 24 h. The results, which are summarized in Figure 8, show the viability in transfected HeLa cells of the CLs produced by both microfluidic devices studied and the liposomes produced by the conventional bulk method. As shown in Figure 8, there is no (or very low) transfection with the use of naked DNA. The positive control (Lipofectamine®, a commercial transfection reagent) exhibited higher transfection levels than those achieved by the transfection of the CLs produced by either of the microfluidic devices. However, even though it results in a higher amount of transfection, lipofectamine is more cytotoxic than our lipid composition [20], which may render it unsuitable for any *in vivo* applications.

## 4. Conclusions

In conclusion, we have demonstrated the potential of using microfluidic devices for the production of cationic liposomes at high yields; this was achieved with both single and double hydrodynamic focusing techniques. Both devices studied produced unilamellar CLs with average diameters of 100 to 130 nm and suitable characteristics for gene delivery and vaccine therapy at higher molar productivity than previous studies. The technology employed is particularly useful for CL production because of the advantages of using a continuous process, the reduced number of steps that are required, and the process intensification that is achieved.

## 5. References

1. Balazs, D.A. and W. Godbey, *Liposomes for Use in Gene Delivery*. Journal of Drug Delivery, 2011. **2011**.
2. Felgner, J.H., *et al.*, *ENHANCED GENE DELIVERY AND MECHANISM STUDIES WITH A NOVEL SERIES OF CATIONIC LIPID FORMULATIONS*. Journal of Biological Chemistry, 1994. **269**(4): p. 2550-2561.
3. Herweijer, H. and J.A. Wolff, *Gene therapy progress and prospects: Hydrodynamic gene delivery*. Gene Ther, 2006. **14**(2): p. 99-107.
4. Mozafari, M.R., *Liposomes: An overview of manufacturing techniques*. Cellular & Molecular Biology Letters, 2005. **10**(4): p. 711-719.
5. Maulucci, G., *et al.*, *Particle Size Distribution in DMPC Vesicles Solutions Undergoing Different Sonication Times*. Biophysical Journal, 2005. **88**(5): p. 3545-3550.
6. Lapinski, M.M., *et al.*, *Comparison of Liposomes Formed by Sonication and Extrusion: Rotational and Translational Diffusion of an Embedded Chromophore*. Langmuir, 2007. **23**(23): p. 11677-11683.
7. de Paula Rigoletto, T., *et al.*, *Effects of extrusion, lipid concentration and purity on physico-chemical and biological properties of cationic liposomes for gene vaccine applications*. Journal of Microencapsulation, 2012. **0**(0): p. 1-11.
8. Pupo, E., *et al.*, *Preparation of plasmid DNA-containing liposomes using a high-pressure homogenization-extrusion technique*. Journal of Controlled Release, 2005. **104**(2): p. 379-396.

9. Meure, L.A., N.R. Foster, and F. Dehghani, *Conventional and Dense Gas Techniques for the Production of Liposomes: A Review*. Aaps Pharmscitech, 2008. **9**(3): p. 798-809.
10. Whitesides, G.M., *The origins and the future of microfluidics*. Nature, 2006. **442**(7101): p. 368-373.
11. Kurakazu, T., S. Takeuchi, and leee, *GENERATION OF LIPID VESICLES USING MICROFLUIDIC T-JUNCTIONS WITH PNEUMATIC VALVES*, in *Mems 2010: 23rd leee International Conference on Micro Electro Mechanical Systems, Technical Digest*. 2010, leee: New York. p. 1115-1118.
12. Davies, R.T., D. Kim, and J. Park, *Formation of liposomes using a 3D flow focusing microfluidic device with spatially patterned wettability by corona discharge*. Journal of Micromechanics and Microengineering, 2012. **22**(5).
13. Jahn, A., et al., *Controlled vesicle self-assembly in microfluidic channels with hydrodynamic focusing*. Journal of the American Chemical Society, 2004. **126**(9): p. 2674-2675.
14. Jahn, A., et al., *Microfluidic directed formation of liposomes of controlled size*. Langmuir, 2007. **23**(11): p. 6289-6293.
15. Jahn, A., et al., *Microfluidic Mixing and the Formation of Nanoscale Lipid Vesicles*. Acs Nano, 2010. **4**(4): p. 2077-2087.
16. Rosada, R.S., et al., *Protection against tuberculosis by a single intranasal administration of DNA-hsp65 vaccine complexed with cationic liposomes*. Bmc Immunology, 2008. **9**.
17. Rosada, R.S., et al., *Effectiveness, against tuberculosis, of pseudo-ternary complexes: Peptide-DNA-cationic liposome*. Journal of Colloid and Interface Science, 2012. **373**: p. 102-109.
18. de la Torre, L.G., et al., *The synergy between structural stability and DNA-binding controls the antibody production in EPC/DOTAP/DOPE liposomes and DOTAP/DOPE lipoplexes*. Colloids and Surfaces B-Biointerfaces, 2009. **73**(2): p. 175-184.
19. Moreira, N.H., et al., *Fabrication of a multichannel PDMS/glass analytical microsystem with integrated electrodes for amperometric detection*. Lab on a Chip, 2009. **9**(1): p. 115-121.
20. Balbino, T.A., et al., *Correlation between Physicochemical and Structural Properties with In Vitro Transfection of pDNA/Cationic Liposomes Complexes*. Langmuir,
21. Toledo, M.A.S., et al., *Development of a recombinant fusion protein based on the dynein light chain LC8 for non-viral gene delivery*. Journal of Controlled Release, 2012. **159**(2): p. 222-231.
22. Montgomery, D.C., *Design and Analysis of Experiments*. 4th ed. 1997.

23. Zook, J.M. and W.N. Vreeland, *Effects of temperature, acyl chain length, and flow-rate ratio on liposome formation and size in a microfluidic hydrodynamic focusing device*. *Soft Matter*, 2010. **6**(6): p. 1352-1360.
24. Huang, X.M., *et al.*, *Ultrasound-enhanced Microfluidic Synthesis of Liposomes*. *Anticancer Research*, 2010. **30**(2): p. 463-466.
25. Rigoletto, T.d.P., *et al.*, *Surface miscibility of EPC/DOTAP/DOPE in binary and ternary mixed monolayers*. *Colloids and Surfaces B-Biointerfaces*, 2011. **83**(2): p. 260-269.
26. Lo, C.T., *et al.*, *Controlled Self-Assembly of Monodisperse Niosomes by Microfluidic Hydrodynamic Focusing*. *Langmuir*, 2010. **26**(11): p. 8559-8566.
27. Pradhan, P., *et al.*, *A facile microfluidic method for production of liposomes*. *Anticancer Research*, 2008. **28**(2A): p. 943-947.
28. Lasic, D.D., *Liposomes : from physics to applications*. 1993, Amsterdam; New York: Elsevier.
29. Trevisan, J.E., *et al.*, *Technological Aspects of Scalable Processes for the Production of Functional Liposomes for Gene Therapy*, in *Non-Viral Gene Therapy*. 2011, InTech.
30. Walia, A.S., *et al.*, *In vitro effect of ethanol on cell-mediated cytotoxicity by murine spleen cells*. *Immunopharmacology*, 1987. **13**(1): p. 11-24.
31. Cussler, E.L., *Diffusion: Mass transfer in fluid systems*. Vol. 31. 1984: Cambridge University Press. 523-523.
32. Ruzicka, M.C., *On dimensionless numbers*. *Chemical Engineering Research & Design*, 2008. **86**(8A): p. 835-868.
33. Bird, R.B., W.E. Stewart, and E.N. Lightfoot, *Transport Phenomena*. 2nd ed. 2007: John Wiley & Sons.
34. Sharp, K.V. and R.J. Adrian, *Transition from laminar to turbulent flow in liquid filled microtubes*. *Experiments in Fluids*, 2004. **36**(5): p. 741-747.
35. Zhang, S., *et al.*, *Formation of solid lipid nanoparticles in a microchannel system with a cross-shaped junction*. *Chemical Engineering Science*, 2008. **63**(23): p. 5600-5605.
36. Diat, O., D. Roux, and F. Nallet, *EFFECT OF SHEAR ON A LYOTROPIC LAMELLAR PHASE*. *Journal De Physique li*, 1993. **3**(9): p. 1427-1452.
37. Soubiran, L., *et al.*, *Effects of Shear on the Lamellar Phase of a Dialkyl Cationic Surfactant*. *Langmuir*, 2001. **17**(26): p. 7988-7994.
38. Alvarez, M.A., *et al.*, *Influence of the electrical interface properties on the rheological behavior of sonicated soy lecithin dispersions*. *Journal of Colloid and Interface Science*, 2007. **309**(2): p. 279-282.



---

## CAPÍTULO 5 – MICROFLUIDIC DEVICES FOR CONTINUOUS PRODUCTION OF DNA/CATIONIC LIPOSOMES COMPLEXES FOR GENE DELIVERY AND VACCINE THERAPY

---

Tiago A. Balbino<sup>1</sup>, Adriano R. Azzoni<sup>1,2</sup>, Lucimara G. de La Torre<sup>1\*</sup>

<sup>1</sup>University of Campinas, Brazil;

<sup>2</sup>University of São Paulo, Brazil.

\*Corresponding author: [latorre@feq.unicamp.br](mailto:latorre@feq.unicamp.br)

To be submitted to *Chemical Engineering and Processing: Process Intensification*

### Abstract

Aiming to evaluate the process parameters of the plasmid DNA/ cationic liposomes (pDNA/CL) complexes production in microfluidic systems, we studied two microfluidic devices: one with a simple straight hydrodynamic flow focusing (SMD) and a second one with barriers in the mixing microchannel (patterned walls, PMD). The conventional bulk mixing method was used as comparison. We complexed CL composed of egg phosphatidylcholine, 1,2-dioleoyl-sn-glycero-3-phosphoethanolamine and 1,2-dioleoyl-3-trimethylammonium-propane (50/25/25% molar) and the pDNA vector model with luciferase as reporter gene at the molar ratio between positive and negative charge of 6, identified before in the best range for *in vitro* transfection in Hela cells. The results showed that the incorporation of the DNA into the liposomal structures was different for both microfluidic devices; the temperature influenced the average size of complexes produced by the simple microfluidic device, while it did not influence in the patterned walls. The differences were also observed in DNA probe accessibility into the complexes. The SMD yielded similar quantity of non-electrostatic bound DNA to that of the bulk mixing

method. Interestingly, the complexes produced by the PMD presented DNA probe accessibility decreased in 40% and achieved lower *in vitro* transfection levels in HeLa cells than the bulk mixing and simple microfluidic complexation methods. These differences are probably consequence on different association between DNA and CL controlled by the microfluidic devices. This study contributes to the development of rational strategies in controlling the formation of pDNA/CL complexes for further applications in gene and vaccine therapy.

## 1. Introduction

Microfluidics is a multidisciplinary science and technology that process small amounts of fluids ( $10^{-9}$  to  $10^{-18}$  liters) and is essentially dedicated to miniaturized plumbing and fluidic manipulation [1, 2]. Besides the small dimensions, microfluidics explores hydrodynamic characteristics to control in space and time concentrations of different molecules [3-7]. Unique transport properties are observed when employing microfluidic systems, that result in laminar flows and vastly increased surface-to-volume ratios [8].

Unlike on the macroscale, where the mixing is generally made through turbulent flows, within microfluidic devices, the mixing occurs by molecular diffusion as influenced by convection, which is an inherently slow process. However, fast mixing time (in order of ms) in microfluidic devices can be achieved due to their small dimensions and thus a short diffusion length between the components [9, 10]. In this fashion, a large number of micromixers with clever geometries have been designed to enhance the mixing efficiency by increasing the contact area between the mixing species as they flow along the mixing channel [11-14]. One prospective application of microfluidic processes is in the field of gene and vaccine delivery [15].

Gene delivery is a potential method for treating of different diseases, including gene-related disorders, infectious diseases, AIDS, cancer etc [16]. It is based on the process of introducing into the cell nucleus an engineered DNA that encodes a functional, therapeutic gene to modulate cellular functions and responses [15, 17]. However, the efficient delivery needs DNA protection and the

DNA/Cationic liposome (CL) complexes are a promising strategy for nonviral gene therapy [18]. Liposomes are vesicles of colloidal dimensions formed when phospholipids self-assemble in aqueous media with an interior core, mimicking cell membranes. The use of cationic lipids allows the electrostatic complexation with DNA. Cationic liposomes (CL) effectively protect the DNA from extracellular matrix and shuttles it inside the cell [15, 18].

The production of liposomes using microfluidic hydrodynamic focusing devices has been extensively studied [19-23]. Recently, our research group investigated the production of cationic liposomes in microfluidic devices using a lipid composition previously studied for tuberculosis gene vaccination and treatment [24-27]. However, the final application for gene vaccine or therapy requires the electrostatic complexation with the therapeutic molecule, the plasmid DNA. The spontaneous complexation process between DNA and CL relies on DNA/CL packing. Depending on the lipid composition, molar charge ratio between positive (from cationic lipids) and negative charges (from the DNA phosphate group) ( $R_{+/-}$ ), temperature of complexation, concentration of the solutions, lipid and DNA mixture ratio and order of mixing of the solutions, complexes with different morphological and physicochemical characteristics can be obtained [18, 28-30]. These differences generate different biological results [31]. Currently, the conventional method of preparing nonviral complexes is the bulk mixing (BM) process in which the two solutions are mixed followed by hand shaking or brief vortexing [30, 32, 33]. Due to these several factors that influence on DNA/CL complexes formation, the conventional BM method for preparation of DNA/CL complexes may yield inconsistent and poor reproducible transfection efficiencies [33, 34], probably due to uncontrolled complexation process. Consequently, the development of different strategies that can produce DNA/CL complexes with narrow particle size distribution and polydispersity is essential for the reproducibility of gene transfection results, attending the requirements for applications in gene and vaccine therapy.

Another important fact is the future demand for higher quantities of DNA/CL complexes for clinical trials and considering the difficulties in controlling the

complexation between DNA and LC using bulk methods at higher volumes, microfluidics emerges as a promising strategy that can be explored to increase the productivity and the for the development of innovative processes.

The use of microfluidic devices for forming nonviral carriers and DNA complexes has been previously demonstrated, such as employing the hydrodynamic flow focusing technique with the central DNA stream being focused for the two adjacent streams with the nonviral carriers [35-38], as well as employing picolitre incubators, in which the lipid and DNA solutions are confined into droplets formed by emulsion water in oil with a centrifugation post-processing step for separating the organic solvent [34, 39]. However, as far as we know, there has been no systematic study on the production of DNA/CL complexes in microfluidic flow focusing devices exploring operational parameters.

In this research, we investigated the parameters involved in the continuous production of DNA/CL complexes employing two microfluidic devices, one with a simple hydrodynamic flow focusing microfluidic device (SMD) (Figure 1A) and a second one with barriers in mixing channel (patterned microfluidic device, PMD, Figure 1B) with contraction and expansion regions, using the complexes produced by the BM method as control, aiming at the development of processes for the formation of DNA/CL complexes in microfluidic devices, which is a continuous flow process, is able to achieve the process intensification by producing such complexes with desired physicochemical properties.

## **2. Materials and Methods**

### **2.1. Materials**

Lipid were Egg phosphatidylcholine (EPC), 1,2-dioleoyl-sn-glycero-3-phosphoethanolamine (DOPE) and 1,2-dioleoyl-3-trimethylammonium-propane (DOTAP) (50/25/25% molar) from Lipoid and used with no purification. Absolute ethanol was purchase from Sigma.

## 2.2. Microfluidic Devices Fabrication

The polydimethylsiloxane (PDMS)/glass microfluidic devices fabrication was carried out according to Moreira *et al.* [40] employing conventional UV photolithographic and soft-lithography methods. The design of the devices geometries were projected using AutoCAD (Autodesk). Basically, the mask layouts were photo-plotted with 8000 dpi resolution and the UV exposures made in a MJB-3 UV300 contact mask aligner (Karl-Suss, Garching, Germany). Sylgard 184 Silicone Elastomer Kit (Dow Corning, Midland, MI, USA) was used as material precursor of PDMS layers with a weight ratio of 1:10 of sylgard curing agent and prepolymer base, respectively. PDMS channels and glass were irreversible sealed by oxidizing PDMS surfaces and cleaning glass substrates which were placed for 20 s exposition in an oxygen plasma cleaner (Plasma Technology PLAB SE80 plasma cleaner, Wrington, England). Immediately after removal from plasma, the two pieces were put into contact, manually aligned and allowed to stand for two hours. All channels had a rectangular cross section with a depth of 100  $\mu\text{m}$  and a width of 140  $\mu\text{m}$ , as depicted in Figure 1.

The microfluidic hydrodynamic focusing geometry of the Figure 1A, named here as simple microfluidic device (SMD), has a single straight channel of 30 mm long. The second geometry, Figure 1B, has patterned walls with uniform barriers, or blocks, throughout the channel and is 130 mm long channel (PMD). The barriers are used to form swirling sections, accelerating the mixing time.

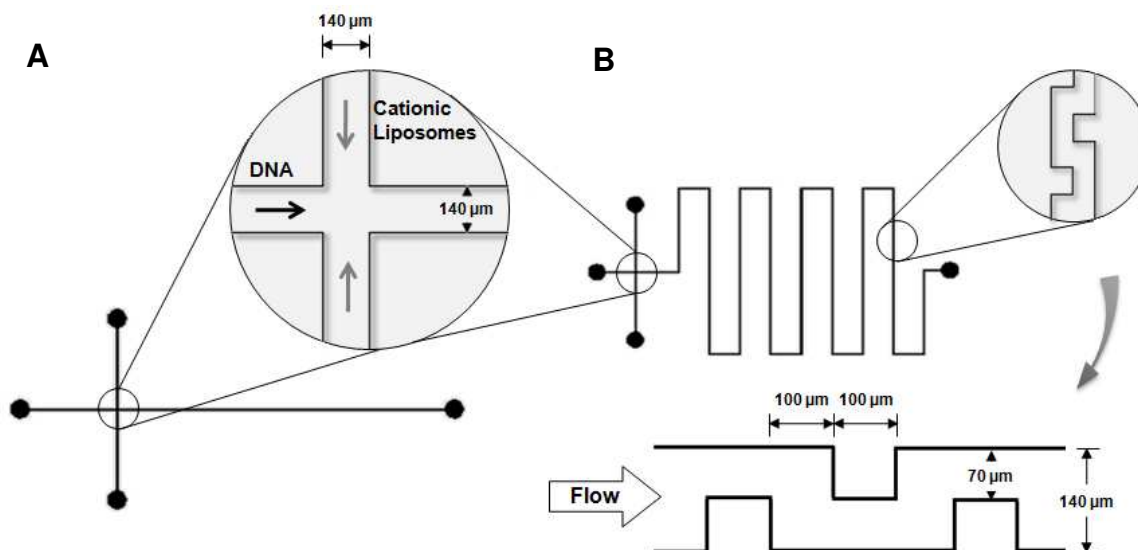


**Figure 1.** Schematic diagram of (A) simple microfluidic hydrodynamic focusing device with inset illustrating the hydrodynamic focusing (SMD). (B) Patterned microfluidic device and the inset illustrating the geometry and dimensions of the barriers (PMD). The microchannels are 140  $\mu\text{m}$  wide and 100  $\mu\text{m}$  deep.

### 2.3. Plasmid DNA purification

We used pVAX-Luc as plasmid DNA vector model with luciferase as reporter gene and the human cytomegalovirus (CMV) immediate-early promoter [41]. The plasmid DNA was amplified in *Escherichia coli* bacteria and purified using PureLink™ HiPure Plasmid DNA Purification Kit-Maxiprep K2100-07 (Invitrogen). The DNA quality and quantity were spectrophotometrically measured with an ND-1000 NanoDrop UV-Vis spectrophotometer (PeqLab, Erlangen, Germany).

### 2.4. Cationic Liposome Production

The CL production was carried out in a hydrodynamic flow focusing microfluidic device (Figure 1A), according to Balbino et al [42]. Briefly, the lipids EPC, DOTAP and DOPE (50:25:25% molar) dispersed in ethanol at a lipid concentration of 25 mM and deionized water were loaded into an 1mL and into two 3mL glass syringes, respectively, at room temperature. The syringes were mounted on an infusion syringe pump (Kd Scientific, model 200, USA) that controls in a programmable manner the flow of each solution into the inlet channels. The lipid dispersion in ethanol flows through the center inlet channel, and the deionized

water flows through the two side inlet channels that hydrodynamically compressed the central stream.

The Flow Rate Ratio (FRR) is the ratio of the volumetric flow rate of the central stream to the total volumetric flow rate of the side streams. In the present study, for producing cationic liposomes, we used FRR of 10, lipid concentration in the dispersion of ethanol in the central stream of 25 mM and an average fluid flow velocity ( $V_f$ ) of 143 mm/s, at room temperature.

## 2.5. Preparation of DNA/CL complexes

We carried out the preparation of the complexes in the continuous microfluidic methods and in bulk mixing method. DNA/CL complexes obtained by both methods were prepared at cationic lipid/DNA molar charge rate ( $R_{+/-}$ ) of 6, once it was in the best range of DNA/LC molar charge ratio ( $R_{+/-}$ ) for *in vitro* transfection in HeLa cells [27]. In the microfluidic method, we compared two microfluidic flow focusing devices (Figure 1) to verify the geometries effects on physicochemical and biological properties of the complexes. The DNA and liposomal solutions were loaded into sterile 1 and 3 mL glass syringes, respectively. The syringes containing the DNA and the cationic liposomes were placed in two separate infusion syringe pumps (Kd Scientific, model 200, USA) which were programmable adjusted to the desired volumetric flow rate ratio between the DNA and CL. The DNA solution was injected in the central stream and hydrodynamically compressed by two liposomal streams, as illustrated in the inset of Figure 1. The FRR of the liposomal solution stream to the DNA solution stream in all experiments was 5. To control the temperature, a Peltier thermoelectric system (Watronix, Inc) was employed, the temperature was maintained at approximately 4 °C and the cooling platform was placed under the microfluidic devices. In the bulk mixing methods, the complexes were prepared by adding the appropriate amount of plasmid DNA to CL under vortex [25, 26].

## **2.7. Physicochemical characterization**

### **2.7.1. Average hydrodynamic diameter and Polydispersity**

To measure the size distribution, polydispersity and the average hydrodynamic diameter of the complexes we employed the Dynamic Light Scattering (DLS) technique, using Zetasizer Nano ZS (Malvern) with a backscattering configuration with detection at a scattering angle of  $173^\circ$  with a He/Ne laser emitting at 633 nm and a 4.0 mW power source. The average hydrodynamic diameter, or Z-average size, was weighted by intensity of scattering in DLS. The size distribution is evaluated with the polydispersity index, which has a range from 0 up to 1, indicating more and less homogeneous distribution of the particle size, respectively. It is calculated from Cumulants analysis of the DLS measured intensity autocorrelation function. All the analyzed samples were diluted at a lipid concentration of  $\sim 0.2$  mM before analysis.

### **2.7.2. Zeta Potential Measurement**

The zeta potential of the samples was measured by applying an electric field across the samples and the zeta potential value was obtained by measuring the velocity of the electrophoretic mobility of the particles using the technique of laser Doppler anemometry. The measurements were performed in triplicate for each sample at  $25^\circ\text{C}$ , in water, using Malvern Zetasizer 3000 (Malvern) equipped with a standard 633 nm laser. The viscosity was assumed to be the same as that of water.

### **2.7.3. Morphology**

The DNA/CL complexes obtained by two microfluidic devices were observed to verify the morphology by means of Transmission Electron Microscopy (TEM) and the negative staining method. Approximately  $5\ \mu\text{L}$  of each sample were put on a copper grid coated with a carbon film. The excess of the liquid was removed with blotting paper. Negative staining was done with a 2% solution of ammonium molybdate for  $\sim 10$  s and then blotted dry. The electron microscopic model was LEO 906E (Zeiss, Germany) at 80 kV, together the camera MEGA VIEW III

/Olympus and the software ITEM E 23082007/ Olympus Soft Imaging Solutions GmbH.

#### **2.7.4. Gel retardation assay**

We used agarose gel electrophoresis technique to verify whether the DNA/CL complexes by bulk and microfluidic methods are able to compact the DNA into the liposomal structures. The DNA/CL complexes at molar charge ratio of 6 (containing 1  $\mu\text{g}$  of DNA) were electrophoresed in 0.8% agarose gel in 40mM TRIS-acetate buffer solution, 1mM EDTA (TAE 1X) at 60V during ~3 h and stained for 30 min in a 0.5  $\mu\text{g}/\text{mL}$  ethidium bromide solution. The location of the DNA was then visualized and photographed using an ultraviolet image acquisition system.

#### **2.7.5. Plasmid DNA accessibility**

We evaluated the plasmid DNA accessibility to the fluorescence probe using the double-stranded DNA quantification kit (Quant-iT PicoGreen dsDNA assay, Invitrogen) in accordance with manufacturer's instructions. Briefly, the working solution was prepared by diluting the Pico Green stock solution 200 times in TE buffer (10 mM Tris-HCl/1 mM EDTA, pH 7.5). One hundred microliters of the working solution was added to the same volume of complexes and then incubated for 3 min. The intensity of the fluorescence was measured using a plate fluorimeter (Gemini XS, Molecular Device) using excitation and emission wavelengths of 485 and 525 nm, respectively. The fluorescence intensity was expressed as relative fluorescence intensity using free DNA as the positive control and taken as 100% fluorescence level.

### **2.8. Culture and transfection of mammalian cells**

The biological evaluation of the complexes obtained by the different methods was assessed by the *in vitro* transfection in human epithelial carcinoma (HeLa) cells. Cells were cultivated in F-12 (Ham) nutrient mixture (Gibco, UK), containing 10% (v/v) fetal bovine serum (FBS) (Gibco, UK) and supplemented with non-essential amino acids (Gibco, UK), gentamicin (Gibco, UK), sodium pyruvate (Gibco, UK), and antibiotic-antimycotic (Gibco, UK). Cultures were incubated

under 37 °C and 5% CO<sub>2</sub> for 24 h in a humid atmosphere and allowed to grow near confluency and harvested with trypsin. After reaching confluence, cells were seeded into 24-well culture plates (5×10<sup>4</sup> cells per well). The cells were then incubated for 48 h and transfected with 0.8 μg of pVAX-Luc per well and the medium was replaced 6 h after the transfection to remove plasmids not internalized by cells. The medium was removed, the cells were washed using PBS, lysed, and the luciferase activity was determined according to the Promega Luciferase Assay protocol. The Relative Light Units (RLUs) were measured with chemiluminometer (Lumat LB9507, EG&G Berthold, Germany). The total protein was measured according to a BCA protein assay kit (Pierce) and luciferase activity was expressed as RLU/mg protein.

## 2.9. Statistical analysis

The data were expressed as the mean of triplicates ± standard deviation (SD). When indicated, the standard deviation was obtained based on the Propagation Uncertainties Theory [43]. Statistical significance was determined using two-tailed Student's *t*-test with the level of confidence being  $p < 0.05$ .

## 3. Results and Discussion

The primary motivation for our work was the investigation of continuous process in microfluidic devices for production of pDNA/CL complexes for gene delivery and vaccine therapy. We used two different microfluidic devices: one with a simple straight channel with a hydrodynamic focusing, as showed in Figure 1A (SMD), and another with a patterned channel (Figure 1B, PMD), which has contraction and expansion regions through regular blocks in the microchannel walls, involving the generation of turbulence or eddies and the mixing occurs through chaotic advection [44, 45]. As a comparison, we formed the complexes in the bulk mixing method.

Considering the comparative study, we investigated the previous pDNA/CL bulk complexation using vortexing, but at the same molar charge ratio ( $R_{+/-}$ ) of 6 between cationic charges from the cationic lipid and the negative charges from the

phosphate in the DNA molecule. This  $R_{+/-}$  was previously identified in the best range for *in vitro* HeLa transfection of EPC/DOTAP/DOPE liposomes complexed with DNA, using bulk method [27]. Since the pDNA/CL charge molar proportion was previously established, the volumetric flow ratio between DNA and CL streams were constant. The investigated parameters were the complexation temperature and the total fluid flow velocity.

Additionally, since  $R_{+/-}$  used was 6, it means that there is an excess of cationic charge in comparison to negative charge from DNA, we introduced the pDNA stream at the central inlet in both devices and it is hydrodynamic compressed by the two aqueous streams (Figure 1). This central inlet of pDNA stream was evaluated before by Jellema et al [38] and Otten *et al.* [35].

### **3.1. Effect of temperature control on complexation process between CLs and plasmid DNA in microfluidic devices**

Due to the spontaneous, fast and irreversible electrostatic interactions between positively charged lipids and negatively charged plasmid DNA, we hypothesized that the processing temperature in the microchannel can influence the process of complexation and affect the formation of the complexes. Thereby, we assessed the effect of temperature (at 25°C and 4 °C) on particle size and polydispersity of the complexes (Figure 2).

As observed in Figure 2, the temperature control was significant only for the simple microfluidic device, on both investigated parameters (particle size and polydispersity index). No statistical difference was observed when we changed the process temperature for production of DNA/CL complexes using the BM and the PMD, which the last one has a longer microchannel and thus the complexes go through a longer mixing time through the microfluidic device. We can separate the explored complexation methods in two groups: (i) group I with high average diameter and polydispersity (BM at 4/25°C and SMD at 25°C) and (ii) group II with the low average diameter and polydispersity (SMD at 4°C and PMD 4/25°C).

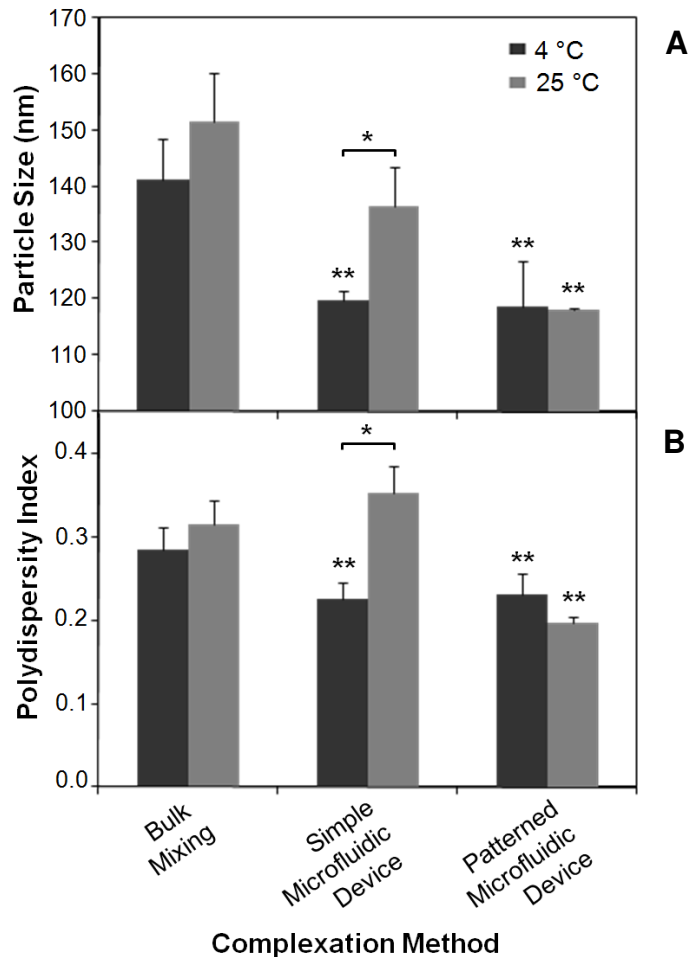


**Figure 2.** Effect of temperature on (A) Particle size and (B) Polydispersity Index of the complexation process between CLs and plasmid DNA for different methods. Average fluid flow velocity of the microfluidic devices of 140 mm/s. The flow rate ratio was maintained at 5. Error bars correspond to SD of three independent experiments. \*Statistically different ( $p < 0.05$ ) when compared between the pairs. \*\*Statistically different ( $p < 0.05$ ) when compared to the bulk mixing method at 4 or 25°C.

The influence of the temperature during the complexation process between DNA and cationic liposomes was reported by Wasan and co-workers [29] using a repeated slow mixing pipetting of equivolumetric suspensions and usually for a total volume of less than 1 mL. These authors showed that, by equilibrating the solutions of CL and DNA prior to mixing to temperatures of about 2 °C to about 7 °C, size control of the formed complexes was achieved. Considering pipetting mixing as an inefficient and usually poor reproducible mixing method, probably the

complexation temperature begins to exert great influence on the size of the aggregates, since it probably decreases the velocity of complexation reaction.

As well as pipetting mixing, vortex system mixing method is generally disadvantageous, since in this circular flow method the liquid moves in a streamline fashion and there is little mixing between fluid at different heights in the tank [46]. As consequence, the average diameter and polydispersity index of complexes obtained at 4 and 25°C were high and classified in the group I. Besides the high level of average diameter, we could not identify differences in process temperature for BM, probably due to the low lipid and DNA concentration. In addition, vortex is a laboratorial procedure that cannot be used in case of increasing the volumetric production.

Similar temperature behavior described by Wasan and co-workers [29] was identified for the SMD. Since the mixture in the hydrodynamic focusing depends basically on diffusive gradients and convective flow, the temperature has to be decreased for proper size control. When the DNA/CL complexation was carried out in the PMD, there is an enhancement in mixing performance as previous described in simulation studies, based on the Computational Fluid Dynamics using numerical methods and algorithms to investigate the behavior of the fluid flow throughout similar microchannels [44, 45]. In this last case, the channel geometry with obstacles allows the formation of swirling vortexes or eddies, increasing the contact area between the two fluids and reducing the diffusion distance to achieve uniform concentration. Thus, with higher mixing quality, the temperature exerts no significant influence as identified in Figure 2.

According to these results, the complexation between CL and DNA depends on a balance between mixing pattern and temperature. Considering the microfluidic devices, cases of poor mixing requires decrease in the process temperature in the same manner as previously described by Wasan *et al.*, [29], as identified in the SMD. However, when the PMD is used, the mixing is enhanced and there is no necessity in temperature control. As consequence this last process becomes more robust than the first one.

### 3.2. Effect of Average Fluid Flow Velocity ( $V_f$ ) on Complexes Size Distribution

Considering the differences on the process with the temperature control for simple and patterned microfluidic devices, we investigated the effects of the average fluid flow velocity ( $V_f$ ), or total volumetric flow rate, on complex size and polydispersity over five different conditions. In this case, all experiments were carried out at 4°C. As can be seen in Figure 3, the particle size and the polydispersity remain approximately unaffected by the fluid flow velocity at the studied ranges. Previous reports have also indicated that the  $V_f$  has little impact on particle formation [19-21, 42, 47, 48]. This event suggests that the fluid residence time in the microchannel for forming the complexes was sufficient even for higher  $V_f$ . The explored ranges of  $V_f$  had residence times of 0.3 and 0.06 s, for maximum and minimum  $V_f$ , respectively.

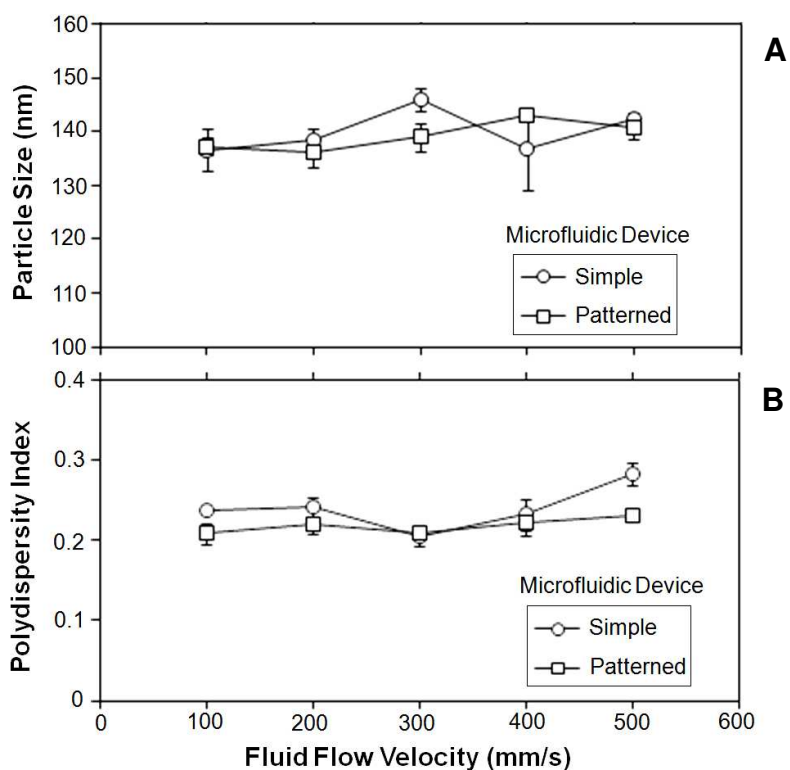


**Figure 3.** Particle size and polydispersity index of the complexes formed in simple and patterned microfluidic devices as function of mean fluid flow velocity in the center outlet channel (the combined flow velocities of all inlets) at 4°C. The flow rate ratio was maintained at 5. The error bars represent the standard error of independent triplicates.

The fluid flow velocity is a microfluidic parameter directly proportional to the Reynolds number ( $Re$ ).  $Re$  is generally considered the most important dimensionless parameter in the field of fluid mechanics, which represents the ratio of inertial forces to viscous forces and consequently quantifies the influence of these forces for a given flow conditions [49, 50]. We evaluated the Reynolds number ( $Re$ ) (Equation 1), that is a dimensionless parameter which represents the ratio of the inertial forces to viscous forces [49].

$$Re = \frac{\rho V_f D_h}{\mu} \quad (\text{Equation 1})$$

where  $D_h$  is the hydraulic diameter,  $\rho$  is the fluid density and  $\mu$  is the dynamic viscosity. The  $Re$  values are presented in Table 1. Despite having distinct dimensions when compared to macroscale equipments, the transition from laminar to turbulent flow in microchannels is similar. It is well known that the onset of this transition at the macroscale has a minimum lower critical Reynolds number between 1,800 and 2,300 and so have the channels with diameters between 50 and 247  $\mu\text{m}$  [51]. Thus, as summarized in Table 1, in our microfluidic system, the variation in  $Re$  did not undergo the transition range of the characteristic flow, i. e., in all studied ranges of  $V_f$  the fluid flow is in laminar flow conditions.

In addition, the influence of the walls in microfluidic devices has a strong impact on the particle motion [52], and as a consequence, the wall shear rate ( $S$ ). The wall shear rate between parallel plates is given by the following equation:

$$S = \frac{Q_T}{40 W d^2} \quad (\text{Equation 2})$$

where  $Q_T$  is the total volumetric flow rate in terms of mL/min,  $W$  is the microchannel width in terms of cm, and  $d$  is the half-microchannel depth in terms of cm [49]. The shear rate is presented in Table 1. Considering the patterned microfluidic device have two distinct regions (one with 140 and a second one with 70  $\mu\text{m}$ ), we calculated the maximum and minimum shear rate. We can observe that the PMD has regions with double shear rate than SMD. This is an additional information that can also justify the better mixing and no influence on temperature for DNA/CL complexes production.

**Table 1.** Flow properties of continuous formation of DNA/CL complexes in simple and patterned microfluidic devices at  $V_f$  of 140 mm/s and temperature control. The maximum and minimum for the patterned microfluidic device indicates the flow through compression regions (in the blocks) and expansion regions.

Microfluidic Device		Reynolds Number	Wall Shear Rate ( $10^4 \text{ s}^{-1}$ )
Simple		16.3	$0.9 \pm 0.1^{(i)}$
Patterned	Minimum	16.3	$0.9 \pm 0.1^{(i)}$
	Maximum	23.5	$1.7 \pm 0.3^{(i)}$

<sup>(i)</sup> Standard deviation based on the Propagation Uncertainties Theory [43].

### 3.3. Physicochemical properties and Morphology of DNA/CL complexes

To characterize the differences of DNA/CL complexes produced by simple and patterned microfluidic devices, we selected the process condition of  $V_f$  of 140 mm/s, FRR 5 and process temperature of 4°C. The DNA/CL complexes were obtained and characterized according particle size, polydispersity index and zeta potential (Table 2). The bulk method was evaluated for comparison.

**Table 2.** Physicochemical properties of DNA/CL complexes obtained by the bulk mixing and microfluidic methods with  $V_f$  of 140 mm/s and at 4 °C.

	Complexation method		
	Bulk Mixing	Simple Microfluidic Device	Patterned Microfluidic Device
Particle Size <sup>(i)</sup> (nm)	$141.4 \pm 7.2$	$119.8 \pm 1.6^*$	$118.8 \pm 7.9^*$
Polydispersity Index	$0.29 \pm 0.03$	$0.22 \pm 0.02^*$	$0.23 \pm 0.03$
Zeta Potential (mV)	$52.7 \pm 0.7$	$53.6 \pm 1.7$	$64.5 \pm 1.4^*$

Results represent mean  $\pm$  SD of three independent experiments

<sup>(i)</sup> Intensity-weighted averaged hydrodynamic diameter.

\* Statistically different ( $p < 0.05$ ) when compared to the bulk mixing method

DNA/CL complexes produced by both microfluidic device and also by the bulk method presented positive zeta potential in water as summarized Table 2, which indicates the complexes produced by both devices and by bulk method are cationic and considered suitable for *in vitro* transfection experiments. The difference in zeta potential is probably due to the modifications of physicochemical properties when shear is applied due the complexation process between DNA and CL [53-55], such as zeta potential [55]. Thus, the difference in Zeta Potential is probably due to the different shear rates applied, and as observed by Balbino *et al.*

[42], the higher shear rates applied the higher zeta potential values are for production of cationic liposomes.

Morphological characterization of the complexes formed by the microfluidic complexation method, performed by transmission electron microscopy (TEM) using negative staining technique, is presented in Figure 4. Complexes formed by both microfluidic devices had relatively small and homogeneous particle sizes, which is in good agreement with the DLS results (Figure 3).

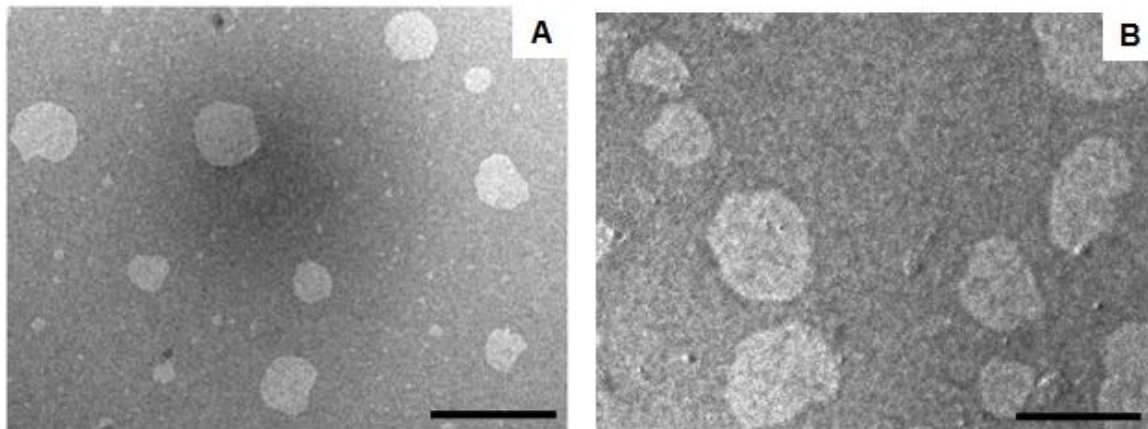


**Figure 4.** TEM images of DNA/cationic liposomes complexes produced by (A) simple microfluidic device and (B) patterned microfluidic device at flow rate ratio of 5, at 4 °C and  $V_f$  of 140 mm/s. Scale bars indicate 500 nm.

The complexation process between DNA and cationic liposomes for the different methods were evaluated by gel retardation assay (Figure 5). All samples were prepared at the molar charge ratio of 6. It is possible to see in lane 1 that the free pDNA migrated out of the well towards the cathode and presented two bands: the less-intense one is considered to be the DNA non-super-coiled, and the most intense band with high-mobility represents the DNA super-coiled form. As no running band of pDNA is observed in lanes 2 to 4, we can conclude that all the complexation methods were able to complex completely DNA into the cationic liposomes, indicating that all processes did not affect the stability and intactness of the structures. Such results are in good agreement with Balbino *et al.* [27], who studied the same lipid composition with extruded cationic liposomes produced by thin film method and complexed with plasmid pVAX-Luc also in bulk method. This

comparison shows that these methods for CL production and complexation with DNA did not alter the capacity in carrying the DNA.

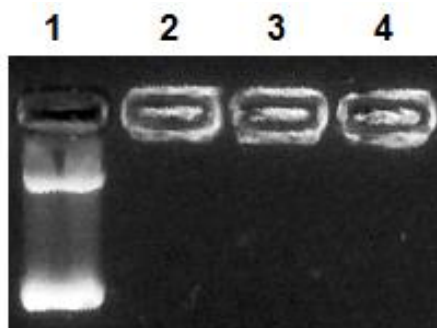


**Figure 5.** Electrophoretic mobility retardation assay of DNA complexed with cationic liposomes in different methods. Lanes: (1) free DNA; complexation processes: (2) bulk mixing; (3) simple microfluidic device; and (4) patterned microfluidic device. Average fluid flow velocity of the microfluidic devices of 140 mm/s, at 4°C and FRR 5.

To increase knowledge about the influence of the microfluidic device in the formation of DNA/CL complexes we evaluate the DNA accessibility to fluorescent probe (Figure 6). The fluorescent probe specifically binds to double-strand DNA, and its fluorescence increases proportionality to the quantity of non-electrostatically bound DNA into the liposomal structures [56]. The fluorescent probe can strongly interact not only to highly polymeric DNA but also to very small amounts.

We can observe that DNA/CL complexes produced by bulk and simple microfluidic mixing methods presented similar relative fluorescence of  $25.2 \pm 1.1$  and  $24.5 \pm 5.0\%$ , respectively. However, when we used the patterned microfluidic device the relative fluorescence was decreased in 44% (Figure 6). Considering we processed the DNA/CL at the same conditions and all DNA is incorporated into the cationic liposomes (Figure 5), the lower relative fluorescence for patterned microfluidic device indicates that lower quantity of non-electrostatically bound DNA into the liposomal structures. This pointed out that the patterned microfluidic device can increase the association between the cationic liposomes and electrostatically bound DNA, modifying the structural organization of the nucleic acid into the liposomal structures. The higher shear and intense mixing applied in the patterned microfluidic device are probably the reasons for different structural DNA organization into the liposomes.

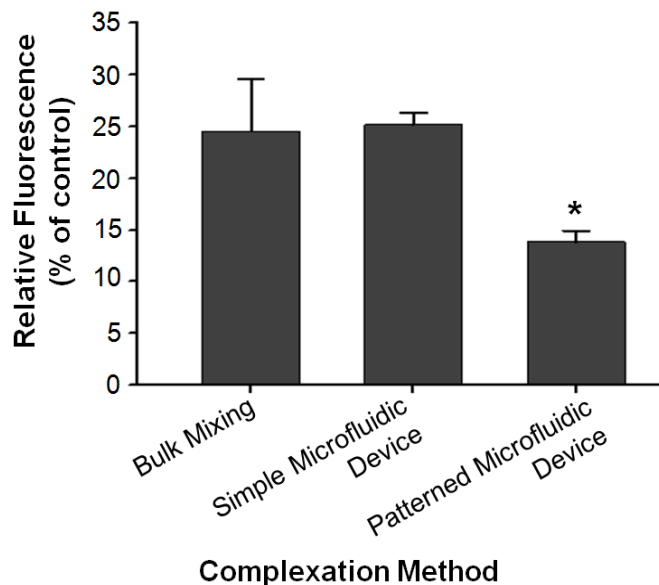


**Figure 6.** Relative fluorescence obtained by the probe in ultra pure water. Results with free DNA used as control for complexes DNA/cationic liposomes formed by three different methods: bulk, in the simple and in the patterned microfluidic devices. The operational conditions of the microfluidic process were average fluid flow velocity of 140 mm/s at 4°C and FRR 5. Error bars correspond to SD of three independent experiments (n = 3). \*  $p < 0.05$  was considered statistically different when compared to other samples.

Differences in relative fluorescence were previously reported using DOTAP/DOPE and dehydrated-hydrated vesicles (DRV-EPC/DOTAP/DOPE). DOTAP/DOPE liposomes presented lower relative fluorescence than DRV-EPC/DOTAP/DOPE [24]. In this reported case the lipid composition and probably the production method influenced on the quantity of non-electrostatically bound DNA into the liposomal structures. DNA-DOTAP/DOPE complexes presented 10% of relative fluorescence. In our case, the patterned microfluidic device presented relative fluorescence of  $13.8 \pm 1.1\%$ , similar to DNA/DOTAP/DOPE complexes. As far as our knowledge, there is no related studies regarding differences in association with DNA and cationic liposomes using different microfluidic devices.

### 3.6. *In vitro* HeLa transfection

The ability of pDNA/CL complexes obtained by BM and microfluidic methods to transfect HeLa cells *in vitro* was assessed (Figure 7) based on the previous physicochemical characterization and the established process conditions.

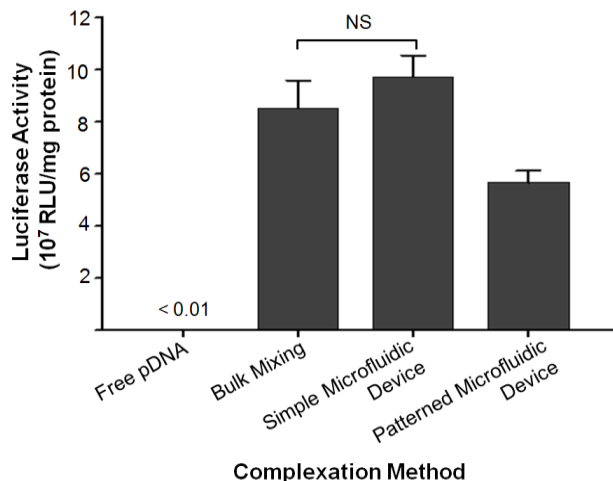


**Figure 7.** *In vitro* efficacy on HeLa cells transfection of DNA/CL complexes formed by bulk mixing and microfluidic methods. Activity was expressed in RLU/mg protein. The DNA/CL complexes were obtained applying average fluid flow velocity of the microfluidic devices of 140 mm/s at 4°C and FRR of 5. Each data represents SD of three experiments, \*  $p < 0.05$  was considered statistically different. NS, no significant ( $p < 0.05$ ).

As observed in Figure 7, the biological efficacies of complexes obtained by both microfluidic devices were *in vitro* proved in human epithelial carcinoma cells (HeLa) cells. It is possible to see that free DNA did not transfect cells (or very low) and the complexes prepared by the PMD presented the lower transfection efficacy for the period of time the transfection was conducted. This is possibly due to the low DNA accessibility to the probe in the fluorescence study for these complexes. The high quantity of electrostatically bound DNA into the liposomal structures yielded in the PMD (Figure 6) probably influenced in the DNA release to cell, impairing the transfection process for the evaluated transfection time. The complexes formed in the simple microfluidic device yielded in similar transfection levels than the complexes formed in the bulk mixing complexation methods, suggesting the same DNA/lipid organization, in accordance to the same level of DNA accessibility to the probe in the fluorescence study.

#### 4. Conclusion

In conclusion, we have demonstrated the feasibility of employing two different microfluidic devices with hydrodynamic focusing in producing DNA/cationic liposomes complexes in nanometric scale. It was demonstrated that

the microfluidic complexation methods provided better control in particle size than the bulk mixing complexation method. The process temperature is a factor that must be investigated according the type of microfluidic device is employed. In addiciton, the use of different microdevices can control the mode of association between DNA and CL reflecting in different biological results and the higher the shear rate and better mixing the higher is the association between DNA and CLs.

## 5. Acknowledgements

The authors gratefully acknowledge the financial support of the Fundação de Amparo à Pesquisa do Estado de São Paulo – FAPESP (São Paulo, Brazil) and Universidade Estadual de Campinas – Unicamp (Campinas, Brazil). The TEM analyses were performed at Instituto Butantan (São Paulo, Brazil) and the microfluidic devices were constructed at Laboratório de Microfabricação (LMF) of Laboratório Nacional de Luz Síncrotron (LNLS).

## 6. References

1. Whitesides, G.M., *The origins and the future of microfluidics*. Nature, 2006. **442**(7101): p. 368-373.
2. Squires, T.M. and S.R. Quake, *Microfluidics: Fluid physics at the nanoliter scale*. Reviews of Modern Physics, 2005. **77**(3): p. 977-1026.
3. Draghiciu, L., *et al.*, *Manipulation of nanoparticles within a microfluidic system based on SU-8 polymer for bio-applications*. Materials Science and Engineering B-Advanced Functional Solid-State Materials, 2010. **169**(1-3): p. 186-192.
4. Baek, J., *et al.*, *Investigation of Indium Phosphide Nanocrystal Synthesis Using a High-Temperature and High-Pressure Continuous Flow Microreactor*. Angewandte Chemie-International Edition, 2011. **50**(3): p. 627-630.
5. Yamashita, T., *et al.*, *Cultivation and recovery of vascular endothelial cells in microchannels of a separable micro-chemical chip*. Biomaterials, 2011. **32**(10): p. 2459-2465.
6. Reiner, J.E., *et al.*, *Accurate Optical Analysis of Single-Molecule Entrapment in Nanoscale Vesicles*. Analytical Chemistry, 2010. **82**(1): p. 180-188.
7. Kurita, H., *et al.* *Fluorescence observation and manipulation of individual DNA molecules in a microfluidic channel*. in *Micro-NanoMechatronics and Human Science (MHS), 2010 International Symposium on*. 2010.

8. Terray, A., J. Oakey, and D.W.M. Marr, *Microfluidic control using colloidal devices*. Science, 2002. **296**(5574): p. 1841-1844.
9. Lee, C.Y., et al., *Microfluidic Mixing: A Review*. International Journal of Molecular Sciences, 2011. **12**(5): p. 3263-3287.
10. Mengeaud, V., J. Josserand, and H.H. Girault, *Mixing processes in a zigzag microchannel: Finite element simulations and optical study*. Analytical Chemistry, 2002. **74**(16): p. 4279-4286.
11. Parvizian, F., M. Rahimi, and M. Faryadi, *Macro- and micromixing in a novel sonochemical reactor using high frequency ultrasound*. Chemical Engineering and Processing, 2011. **50**(8): p. 732-740.
12. Lim, C.Y. and Y.C. Lam, *Analysis on micro-mixing enhancement through a constriction under time periodic electroosmotic flow*. Microfluidics and Nanofluidics, 2012. **12**(1-4): p. 127-141.
13. Kuo, J.S. and D.T. Chiu, *Controlling Mass Transport in Microfluidic Devices*. Annual Review of Analytical Chemistry, Vol 4, 2011. **4**: p. 275-296.
14. Fan, Z., et al., *Evaluation of the performance of a constructal mixer with the iodide-iodate reaction system*. Chemical Engineering and Processing, 2010. **49**(6): p. 628-632.
15. Kim, T.-i. and S.W. Kim, *Bioreducible polymers for gene delivery*. Reactive & Functional Polymers, 2011. **71**(3): p. 344-349.
16. Ozbas-Turan, S., et al., *Co-encapsulation of two plasmids in chitosan microspheres as a non-viral gene delivery vehicle*. Journal of Pharmacy and Pharmaceutical Sciences, 2003. **6**(1): p. 27-32.
17. Corsi, K., et al., *Mesenchymal stem cells, MG63 and HEK293 transfection using chitosan-DNA nanoparticles*. Biomaterials, 2003. **24**(7): p. 1255-1264.
18. Lasic, D.D., *Liposomes : from physics to applications*. 1993, Amsterdam; New York: Elsevier.
19. Jahn, A., et al., *Microfluidic Mixing and the Formation of Nanoscale Lipid Vesicles*. Acs Nano, 2010. **4**(4): p. 2077-2087.
20. Jahn, A., et al., *Microfluidic directed formation of liposomes of controlled size*. Langmuir, 2007. **23**(11): p. 6289-6293.
21. Jahn, A., et al., *Controlled vesicle self-assembly in microfluidic channels with hydrodynamic focusing*. Journal of the American Chemical Society, 2004. **126**(9): p. 2674-2675.
22. Pradhan, P., et al., *A facile microfluidic method for production of liposomes*. Anticancer Research, 2008. **28**(2A): p. 943-947.

23. Zook, J.M. and W.N. Vreeland, *Effects of temperature, acyl chain length, and flow-rate ratio on liposome formation and size in a microfluidic hydrodynamic focusing device*. *Soft Matter*, 2010. **6**(6): p. 1352-1360.
24. de la Torre, L.G., *et al.*, *The synergy between structural stability and DNA-binding controls the antibody production in EPC/DOTAP/DOPE liposomes and DOTAP/DOPE lipoplexes*. *Colloids and Surfaces B-Biointerfaces*, 2009. **73**(2): p. 175-184.
25. Rosada, R.S., *et al.*, *Protection against tuberculosis by a single intranasal administration of DNA-hsp65 vaccine complexed with cationic liposomes*. *Bmc Immunology*, 2008. **9**.
26. Rosada, R.S., *et al.*, *Effectiveness, against tuberculosis, of pseudo-ternary complexes: Peptide-DNA-cationic liposome*. *Journal of Colloid and Interface Science*, 2012. **373**: p. 102-109.
27. Balbino, T.A., *et al.*, *submitted*.
28. Pozzi, D., *et al.*, *How lipid hydration and temperature affect the structure of DC-Chol-DOPE/DNA lipoplexes*. *Chemical Physics Letters*, 2006. **422**(4-6): p. 439-445.
29. Wasan, E.K., *et al.*, *A multi-step lipid mixing assay to model structural changes in cationic lipoplexes used for in vitro transfection*. *Biochimica Et Biophysica Acta-Biomembranes*, 1999. **1461**(1): p. 27-46.
30. De Smedt, S.C., J. Demeester, and W.E. Hennink, *Cationic polymer based gene delivery systems*. *Pharmaceutical Research*, 2000. **17**(2): p. 113-126.
31. Rejman, J., *et al.*, *Size-dependent internalization of particles via the pathways of clathrin-and caveolae-mediated endocytosis*. *Biochemical Journal*, 2004. **377**: p. 159-169.
32. Ma, B., *et al.*, *Lipoplex morphologies and their influences on transfection efficiency in gene delivery*. *Journal of Controlled Release*, 2007. **123**(3): p. 184-194.
33. Morille, M., *et al.*, *Progress in developing cationic vectors for non-viral systemic gene therapy against cancer*. *Biomaterials*, 2008. **29**(24-25): p. 3477-3496.
34. Hsieh, A.T.-H., *et al.*, *Nonviral gene vector formation in monodispersed picolitre incubator for consistent gene delivery*. *Lab on a Chip*, 2009. **9**(18): p. 2638-2643.
35. Otten, A., *et al.*, *Microfluidics of soft matter investigated by small-angle X-ray scattering*. *Journal of Synchrotron Radiation*, 2005. **12**: p. 745-750.
36. Koh, C.G., *et al.*, *Delivery of Polyethylenimine/DNA Complexes Assembled in a Microfluidics Device*. *Molecular Pharmaceutics*, 2009. **6**(5): p. 1333-1342.
37. Koh, C.G., *et al.*, *Delivery of antisense oligodeoxyribonucleotide lipopolyplex nanoparticles assembled by microfluidic hydrodynamic focusing*. *Journal of Controlled Release*, 2010. **141**(1): p. 62-69.

38. Jellema, R.K., *et al.*, *Transfection efficiency of lipoplexes for site-directed delivery*. Journal of Liposome Research, 2010. **20**(3): p. 258-267.
39. Ho, Y.-P., *et al.*, *Tuning Physical Properties of Nanocomplexes through Microfluidics-Assisted Confinement*. Nano Letters, 2011. **11**(5): p. 2178-2182.
40. Moreira, N.H., *et al.*, *Fabrication of a multichannel PDMS/glass analytical microsystem with integrated electrodes for amperometric detection*. Lab on a Chip, 2009. **9**(1): p. 115-121.
41. Toledo, M.A.S., *et al.*, *Development of a recombinant fusion protein based on the dynein light chain LC8 for non-viral gene delivery*. Journal of Controlled Release, 2012. **159**(2): p. 222-231.
42. Balbino, T.A., *et al.*, *submitted*.
43. Taylor, J.R., *An Introduction to Error Analysis: The Study of Uncertainties in Physical Measurements*. 2nd ed. 1997.
44. Wong, S.H., *et al.*, *Investigation of mixing in a cross-shaped micromixer with static mixing elements for reaction kinetics studies*. Sensors and Actuators B-Chemical, 2003. **95**(1-3): p. 414-424.
45. Naher, S., *et al.*, *Effect of micro-channel geometry on fluid flow and mixing*. Simulation Modelling Practice and Theory, 2011. **19**(4): p. 1088-1095.
46. Doran, P.M., *Bioprocess Engineering Principles*. 1995, London: Academic Press.
47. Huang, X.M., *et al.*, *Ultrasound-enhanced Microfluidic Synthesis of Liposomes*. Anticancer Research, 2010. **30**(2): p. 463-466.
48. Lo, C.T., *et al.*, *Controlled Self-Assembly of Monodisperse Niosomes by Microfluidic Hydrodynamic Focusing*. Langmuir, 2010. **26**(11): p. 8559-8566.
49. Bird, R.B., W.E. Stewart, and E.N. Lightfoot, *Transport Phenomena*. 2nd ed. 2007: John Wiley & Sons.
50. Ruzicka, M.C., *On dimensionless numbers*. Chemical Engineering Research & Design, 2008. **86**(8A): p. 835-868.
51. Sharp, K.V. and R.J. Adrian, *Transition from laminar to turbulent flow in liquid filled microtubes*. Experiments in Fluids, 2004. **36**(5): p. 741-747.
52. D'Avino, G., *et al.*, *Effects of confinement on the motion of a single sphere in a sheared viscoelastic liquid*. Journal of Non-Newtonian Fluid Mechanics, 2009. **157**(1-2): p. 101-107.
53. Diat, O., D. Roux, and F. Nallet, *EFFECT OF SHEAR ON A LYOTROPIC LAMELLAR PHASE*. Journal De Physique Ii, 1993. **3**(9): p. 1427-1452.
54. Soubiran, L., *et al.*, *Effects of Shear on the Lamellar Phase of a Dialkyl Cationic Surfactant*. Langmuir, 2001. **17**(26): p. 7988-7994.

55. Alvarez, M.A., *et al.*, *Influence of the electrical interface properties on the rheological behavior of sonicated soy lecithin dispersions*. Journal of Colloid and Interface Science, 2007. **309**(2): p. 279-282.
56. Ferrari, M.E., *et al.*, *Trends in lipoplex physical properties dependent on cationic lipid structure, vehicle and complexation procedure do not correlate with biological activity*. Nucleic Acids Research, 2001. **29**(7): p. 1539-1548.



---

## CAPÍTULO 6 – CONCLUSÕES GERAIS

---

Com o presente trabalho, que, prioritariamente, visou o desenvolvimento de processo microfluídico para incorporação de DNA plasmideal em lipossomas catiônicos destinados à terapia e à vacinação gênica, pôde-se concluir que:

- Os complexos formados por DNA plasmideal e por lipossomas catiônicos constituídos de EPC/DOTAP/DOPE são viáveis para aplicações *in vitro* quando produzidos com controle de tamanho e polidispersidade (processo “bulk”);
- A razão molar de cargas  $R_{+/-}$  entre 3 e 6 apresentaram melhores resultados (significativamente iguais) para transfecções em células humanas do tipo HeLa, além de não apresentarem níveis de citotoxicidade às células;
- As propriedades físico-químicas e estruturais dos complexos pDNA/lipossomas catiônicos se correlacionaram com o fenômeno de transfecção em células HeLa. Foi possível concluir que, conforme há um aumento da proporção de DNA nos complexos com lipossomas catiônicos, há um aumento na fração de nanopartículas com duplas bicamadas fosfolipídicas. Esse aumento ocorre até próximo à região de isoneutralidade de cargas, sendo que, nesse ponto, também se verificou com os estudos de SAXS a presença de uma população de complexos com uma média de cinco bicamadas;
- Foi possível produzir lipossomas catiônicos unilamelares em microcanais utilizando a focalização hidrodinâmica em altas concentrações com tamanho e polidispersidade controlados de aproximadamente 100 nm e 0,2, respectivamente. A viabilidade biológica dos lipossomas produzidos foi comprovada *in vitro* em células HeLa;

- Com a utilização do dispositivo microfluídico com dupla focalização hidrodinâmica foi possível operar com velocidades superficiais de escoamento mais altas que com o dispositivo de focalização única. Assim, foi possível aumentar a produtividade dos sistemas microfluídicos em até 13 vezes em relação aos reportados na literatura. Dessa forma, os lipossomas produzidos atendem aos requisitos industriais para aplicações das formulações lipossomais;
- Foi possível produzir complexos DNA/lipossomas catiônicos em dispositivos microfluídicos destinados à terapia e vacinação gênica. Os estudos mostraram a factibilidade desse processo para a formação de complexos com controle de tamanho e de polidispersidades já determinados inicialmente nesse estudo;
- A utilização de diferentes dispositivos mostrou que é possível se obter complexos entre DNA e lipossomas catiônicos com características diferentes. Os ensaios de acessibilidade à sonda de fluorescência ao DNA indicaram diferença na associação deste com as estruturas lipossomais, o que refletiu em diferentes níveis de transfecção para os complexos produzidos em ambos dispositivos.
- Concluiu-se que a organização do DNA aos lipossomas catiônicos formados no dispositivo microfluídico com blocos nas paredes possivelmente interferiu na liberação do DNA no processo de transfecção em células HeLa para o tempo estudado.

De modo geral, pode-se concluir que os sistemas microfluídicos empregados para a produção de lipossomas catiônicos e também para formação dos complexos DNA/lipossomas catiônicos em modo contínuo apresentaram-se promissores para aplicações em terapia e vacinação gênica.

---

## CAPÍTULO 7 – SUGESTÕES PARA TRABALHOS FUTUROS

---

Para a continuação de pesquisas futuras no que tange ao desenvolvimento de processos microfluídicos de formulações lipossomais destinadas à terapia e à vacinação gênica, sugere-se o seguinte:

- Estudar a cinética de transfecção *in vitro* para os lipossomas catiônicos constituídos pelos lipídeos EPC, DOTAP e DOPE.
- Explorar o dispositivo de focalização dupla para a produção de outros tipos de partículas. Adicionalmente, fazer um estudo através de Fluidodinâmica computacional quanto ao comportamento hidrodinâmico na dupla focalização.
- Desenvolver dispositivos com focalizações hidrodinâmicas múltiplas e estudar seu comportamento frente ao aumento do número de focalizações.
- Conduzir experimentos de complexação entre lipossomas catiônicos e DNA nos dispositivos microfluídicos em concentrações mais altas (lipossomas produzidos pelo método “bulk”), viabilizando análises de SAXS que detalhem a modificação estrutural causada pela diferente forma de empacotamento do DNA obtida em cada dispositivo.
- Estudar a influência da razão molar de cargas na complexação em microdispositivos. Também com o emprego de dispositivos com outras geometrias.
- Avaliar a potencialidade da formação de outros complexos em dispositivos microfluídicos e sua associação com outros materiais.